

DEVELOPMENT OF A NANOPARTICLE-BASED ELECTROCHEMICAL BIO-BARCODE
DNA BIOSENSOR FOR MULTIPLEXED PATHOGEN DETECTION ON SCREEN-
PRINTED CARBON ELECTRODES

By

Deng Zhang

A DISSERTATION

Submitted to
Michigan State University
in partial fulfillment of the requirements
for the degree of

DOCTOR OF PHILOSOPHY

Biosystems Engineering

2011

ABSTRACT

DEVELOPMENT OF A NANOPARTICLE-BASED ELECTROCHEMICAL BIO-BARCODE DNA BIOSENSOR FOR MULTIPLEXED PATHOGEN DETECTION ON SCREEN-PRINTED CARBON ELECTRODES

By

Deng Zhang

A highly amplified, nanoparticle-based, bio-barcoded electrochemical biosensor for the simultaneous multiplexed detection of the protective antigen A (*pagA*) gene (accession number = M22589) from *Bacillus anthracis* and the insertion element (*Iel*) gene (accession number = Z83734) from *Salmonella* Enteritidis was developed. The biosensor system is mainly composed of three nanoparticles: gold nanoparticles (AuNPs), magnetic nanoparticles (MNPs), and nanoparticle tracers (NTs), such as lead sulfide (PbS) and cadmium sulfide (CdS). The AuNPs are coated with the first target-specific DNA probe (1pDNA), which can recognize one end of the target DNA sequence (tDNA), and many NT-terminated bio-barcode ssDNA (bDNA-NT), which act as signal reporter and amplifier. The MNPs are coated with the second target-specific DNA probe (2pDNA) that can recognize the other end of the target gene. After binding the nanoparticles with the target DNA, the following sandwich structure is formed: MNP-2pDNA/tDNA/1pDNA-AuNP-bDNA-NTs. A magnetic field is applied to separate the sandwich structure from the unreacted materials. Because the AuNPs have a large number of nanoparticle tracers per DNA probe binding event, there is substantial amplification. After the nanoparticle tracer is dissolved in 1 mol/L nitric acid, the NT ions, such as Pb^{2+} and Cd^{2+} , show distinct non-overlapping stripping curves by square wave anodic stripping voltammetry (SWASV) on screen-printed carbon electrode (SPCE) chips. The oxidation potential of NT ions is unique for each nanoparticle tracer and the peak current is related to the target DNA concentration. The results

show that the biosensor has good specificity, and the sensitivity of single detection of *pagA* gene from *Bacillus anthracis* using PbS NTs is as low as 0.2 pg/mL. The detection limit of this multiplex bio-barcoded DNA sensor is 50 pg/mL using PbS or CdS NTs. The nanoparticle-based bio-barcoded DNA sensor has potential applications for multiple detections of bioterrorism threat agents, co-infection, and contaminants in the same sample.

ACKNOWLEDGMENTS

First, I would like to thank my wife, Yaling Liu, for her unconditional love and support during the most important period of my life. Her love and trust provide me the power to overcome all difficulties in the research and life.

I would like to express my sincere appreciation to Dr. Evangelyn Alocilja, for her constant support, guidance, encouragement, patience, and funding for the last five years. It is my great honor to have her as my mentor and friend. I am also grateful for the advice and resource provided by Dr. John Gerlach, Dr. Daniel Guyer, and Dr. Gary Blanchard.

I would like to thank my colleagues in the lab, Zarini Muhammad-Tahir, Sudeshna Pal, Yang Liu, Edith Torres-Chavolla, Yilun Luo, Michelle Packard, Shannon K. McGraw, Michael Anderson, and Yun Wang, for their help and motivation. I also want to thank those undergraduates and high school students who worked with me over the past years.

TABLE OF CONTENTS

LIST OF TABLES	viii
LIST OF FIGURES	ix
CHAPTER 1. INTRODUCTION	
1.1 Objective and Goals	1
1.2 Foodborne Disease and Bioterrorism	2
1.3 Current Detection Methods.....	4
1.4 Use of Biosensors.....	6
1.5 Novelty of Research.....	11
1.6 Hypothesis	12
1.7 Specific Aims.....	12
CHAPTER 2. LITERATURE REVIEW	
2.1 Overview of Nano-sensors	15
2.2 Electrochemical DNA Sensor	24
2.3 Bio-barcode Assay.....	29
2.4 Screen-printed Carbon Electrode	31
2.5 Square Wave Anodic Stripping Voltammetry.....	32
CHAPTER 3. MATERIALS AND METHODS	
3.1 Reagents and Materials	36
3.2 Facilities and Equipment	37
3.3 Synthesis of Nanoparticles	38
3.4 Bacteria Culture, DNA isolation, PCR and DNA Probes.....	39
3.5 Functionalization of Nanoparticles.....	40
3.6 Confirmation of Nanoparticle Functionalization	44
3.7 Validation and Optimization of the Biosensor	47
3.8 Electrochemical Analysis.....	47
CHAPTER 4. RESULTS AND DISCUSSION	
4.1 Characterization of Nanoparticles	49
4.2 Functionalization of Nanoparticles.....	51
4.3 Fluorescent Detection Using Bio-barcode Assay.....	54
4.4 Electrochemical Validation and Characterization of SPCE Chips.....	56
4.5 Detection of AuNPs on SPCE Chips.....	63
4.6 Biosensor Detection of Single Target DNA	67
4.7 Biosensor Detection of Multiple Target DNA	70
4.8 Conclusion and Summary.....	75
APPENDICES.....	78
Appendix I. DNA Extraction Procedure	79
Appendix II. PCR Amplification	81

Appendix III. Procedure of Bio-Barcode Assay-----	82
Appendix IV. Buffer Preparation -----	87
Appendix V. Conjugation of carboxylic group on NTs with amine group on bio-barcoded AuNPs -----	88
BIBLIOGRAPHY -----	89

LIST OF TABLES

Table 1.1 Foodborne diseases in the US by major foodborne pathogens in 2006 (CDC 2010).--- 2

Table 2.1. Electrochemical genosensors using AuNPs as label. GE: gold electrode; DPV: differential pulse voltammetry; ASV: anodic stripping voltammetry; SPMBE: sandwich-type screen-printed microband electrode; PSA: potentiometric stripping analysis; SPEs: screen-printed electrodes; M-GECE: magnetic graphite-epoxy composite electrode, GCE: glassy carbon electrode (Castada, Alegret et al. 2007). ----- 19

Table 2.2 Comparison of platforms for DNA electrochemical sensing (Drummond, Hill et al. 2003). -----26

Table 4.1. Fluorescence signal of supernatant solution for evaluation of conjugation efficiency between MNPs and 2pDNA. ----- 51

Table 4.2. The relationship between target DNA and the fluorescence signal of released bDNA.55

Table 5. Buffer preparation. -----87

LIST OF FIGURES

Figure 1.1. Schematic of a biosensor. (A) Biological reaction between biological sensing element and analytes; (B) Transduction from biological event to electrical output. For interpretation of the references to color in this and all other figures, the reader is referred to the electronic version of this dissertation. ----- 7

Figure 1.2. Schematic of a three-electrode electrochemical detection system. The system is composed of a potentiostat, working, reference, and auxiliary electrodes. (adapted from Bard and Faulkner 2001). ----- 9

Figure 1.3. Schematic of DNA base pairs.----- 10

Figure 2.1. The different strategies used for the integration of gold nanoparticles (AuNPs) into DNA-sensing systems: (A) previously dissolving AuNPs by using HBr/Br₂ mixture followed by Au(III)-ion detection; (B) direct detection of AuNPs anchored onto the surface of the genosensor; (C) conductometric detection; (D) enhancement with Ag or Au followed by detection; (E) AuNPs as carriers of other AuNPs; and, (F) AuNPs as carriers of other electroactive labels (adapted from Castada, Alegret et al. 2007). ----- 17

Figure 2.2. Magnetic beads (MBs) as versatile tools for bioassays. Beads modified with various recognition elements (examples of commercially available MBs shown on the gray background) can be used for specific bioaffinity capture of different molecules. For example, beads bearing covalently attached oligo(dT)₂₅ chains can bind nucleic acid involving (A)_n stretches, including natural eukaryotic mRNAs or tDNAs tagged with (A)_n adaptors. Streptavidin-coated beads are suitable for capturing any biotinylated molecules, including single strand or double strand nucleic acids, aptamers, peptides, proteins, etc. Antibodies can be attached to the beads either via a direct covalent linkage, or via specific antibody binding proteins such as protein A or protein G (beads functionalized with the latter proteins can be further modified with various antibodies on demand). Other affinity ligands attached to MBs are suitable for specific capture of tagged recombinant proteins (such as metal-affinity cobalt chelate for histidine tags). Biomolecules captured at the MB surface can serve as a biorecognition layer for interaction with other molecules. For example, a biotinylated single strand oligonucleotide (ssODN) immobilized at streptavidin-coated beads features a hybridization probe for complementary sequence, the dsDNA can represent a target for a DNA-binding protein, antibody can bind a specific antigen (including antigens exposed at surfaces of whole cells), immobilized protein (e.g., via antibody, his-tag or biotin–streptavidin linkage) can interact with a specific nucleic acid or another protein, etc. (adapted from Palecek and Fojta 2007). ----- 20

Figure 2.3. Schematic of an electrochemical DNA biosensor. (A) DNA probe immobilization; (B) hybridization between DNA probe and target DNA on the transducer; (C) signal processing by a biosensor system. ----- 25

Figure 2.4. Multi-target electrical DNA detection protocol based on different inorganic colloid nanoparticle tracers. (A) Introduction of probe-modified magnetic beads. (B) Hybridization with the DNA targets. (C) Second hybridization with the QD-labeled probes. (D) Dissolution of QDs and electrochemical detection (adapted from Wang, Liu et al. 2003). ----- 28

Figure 2.5. Schematic of bio-barcode DNA assay. (A) formation of MNP-2pDNA/tDNA/1pDNA-AuNP-bDNA sandwich structure; (B) probe separation and bDNA release. ---- 30

Figure 2.6. Waveform and measurement scheme for square wave voltammetry. Shown in bold is the actual potential waveform applied to the working electrode. The light intervening lines indicate the underlying staircase onto which the square wave can be regarded as having been superimposed. In each cycle, a forward current sample is taken at the time indicated by the solid dot, and a reverse current sample is taken at the time marked by the shaded dot (Adapted from Bard and Faulkner 2000). ----- 33

Figure 2.7. Principle of anodic stripping. Values shown are typical ones used; potentials and E_p are typical of Cu^{2+} analysis, (a) Preelectrolysis at E_d ; stirred solution, (b) Rest period; stirrer off. (c) Anodic scan ($v = 10\text{-}100$ mV/s) (Adapted from Bard and Faulkner 2000). ----- 34

Figure 3.1. Schematic of screen-printed carbon electrode: A) top view, B) cross-section view. It is composed of working electrode (carbon electrode) and auxiliary/reference electrode (Ag/AgCl) in an insulating well.----- 38

Figure 3.2. Schematic of the functionalization of AuNPs. A mixture of thiolated oligonucleotides (bDNA:1pDNA=100:1) form a self assembled monolayer on the surface of gold nanoparticles. ----- 41

Figure 3.3. Schematic of the functionalization of MNPs. (1) formation of maleimide-activated MNPs; (2) formation of MNP-2pDNA conjugate. ----- 42

Figure 3.4 Evaluation of conjugation efficiency: MNP- pDNA and AuNP-bDNA. ----- 43

Figure 3.5. Schematic of conjugation of bio-barcoded AuNP with NTs. (1) functionalization of gold nanoparticles with thiolated bDNA and thiolated 1pDNA; (2) formation of the 1pDNA-AuNP-bDNA-NTs complex by cross-linking amine group on bDNA and carboxylic group on NTs through 1-Ethyl-3-[3-dimethylaminopropyl] carbodiimide Hydrochloride (EDC) and N-hydroxysuccinimide (NHS).----- 44

Figure 3.6. Schematic of the bio-barcode assay: A) formation of MNP-2 pDNA/target DNA/1pDNA-AuNP-bDNA-fluorescein; B) bDNA-fluorescein separation and release. ----- 45

Figure 3.7. Schematics of electrochemical measurement of AuNPs. It is composed of 2 steps: AuNP dissolution on the SPCE and DPV measurement of Au^{3+} . ----- 46

Figure 3.8. The composition of the electrochemical detection system. ----- 48

Figure 4.1. Characterization of AuNPs: A) Transmission electron microscopy (TEM) image of AuNPs, showing an average of 15 nm in diameter; B) Absorbance spectrum of AuNPs at 519 nm. -----49

Figure 4.2. TEM images of NTs: A) CdS, showing an average diameter of 7 nm; B) PbS, showing an average diameter of 3 nm. -----50

Figure 4.3. Fluorescence signal of supernatant solution for evaluation of conjugation efficiency between AuNPs and bDNA. -----52

Figure 4.4. Confirmation of the conjugation of NTs and AuNPs. Three test tubes labeled A, B, C are under white light and UV light after centrifugation at 13,000 rpm for 30 min. (Tube A: bio-barcode AuNPs, NTs, EDC, and NHS; tube B: bio-barcode AuNPs and NTs; tube C: NTs only).-----53

Figure 4.5. The fluorescence signal of released bDNA with different concentrations of target DNA. -----55

Figure 4.6. Cyclic voltammogram of bare SPCE sensor in a 5mM $K_3Fe(CN)_6$ solution with 1M KCl. Scan rate is 50mV/s. -----56

Figure 4.7. The repeatability test of 1 mg/L of bismuth film-coated SPCE sensor and bare SPCE sensor. Deposition: -1.2 V for 10 min; SWASV scan from -1.2 V to 0.0 V, frequency 20 Hz, amplitude 25 mV, and potential step 5 mV, at room temperature and in nonstirred solution. ---57

Figure 4.8. Stripping voltammogram of 5 mg/L of lead(II) with various concentrations of bismuth on electrochemical sensor after 2 min deposition at -1.2 V. SWASV scan from -1.2 V to 0.0 V, frequency 20 Hz, amplitude 25 mV, and potential step 5 mV, at room temperature and in nonstirred solution. -----59

Figure 4.9. Stripping voltammogram on bismuth film-coated SPCE sensors with various deposition times. Deposition at -1.2 V; SWASV scan from -1.2 V to 0.0 V, frequency 20 Hz, amplitude 25 mV, and potential step 5 mV, at room temperature and in nonstirred solution. ---60

Figure 4.10. Stripping voltammogram of a mixture of lead(II) and cadmium(II) on bismuth film-coated SPCE sensors (a: 5 mg/L lead(II) and 5 mg/L cadmium(II); b: 2 mg/L lead(II) and 2 mg/L cadmium(II); c: 0.5 mg/L lead(II) and 0.5 mg/L cadmium(II)). Deposition: -1.2 V for 10 min; SWASV scan from -1.2 V to 0.0 V, frequency 20 Hz, amplitude 25 mV, and potential step 5 mV, with 1mg/mL bismuth, at room temperature and in nonstirred solution. -----61

Figure 4.11. Stripping voltammogram of a mixture of lead(II) and cadmium(II) on bare SPCE sensors. (a: 5 mg/L lead(II) and 5 mg/L cadmium(II); b: 2 mg/L lead(II) and 2 mg/L cadmium(II); c: 0.5 mg/L lead(II) and 0.5 mg/L cadmium(II)). Deposition: -1.2 V for 10 min; SWASV scan from -1.2 V to 0.0 V, frequency 20 Hz, amplitude 25 mV, and potential step 5 mV, with 1mg/mL bismuth, at room temperature and in nonstirred solution. -----62

Figure 4.12. The peak currents of stripping voltammogram with different concentrations of lead(II) and cadmium(II). ----- 63

Figure 4.13. Cyclic voltammogram of unmodified AuNPs (1.17×10^{-8} M) on SPCE : (A) AuNPs in 0.1M HCl; (B) 0.1 M HCl. CV scan from 1.4V to 0.0, scan rate 100 mV/s after 1.25 V electrooxidation for 2 min.----- 64

Figure 4.14. Cyclic voltammogram of probe-modified AuNPs in 0.1 M HCl on SPCE: (A) accumulation for 20 min; (B) accumulation for 10 min; (C) no accumulation; (D) control, no AuNPs and no accumulation. Conditions: electrooxidation potential, +1.25 V; electrooxidation time, 2 min, CV scan from +1.4 V to 0 V, scan rate 100 mV/s, nonstirred solution. ----- 66

Figure 4.15. DPV hybridization response of different concentrations of DNA targets on SPCE (a: 700 ng/mL; b: 70 ng/mL; c: 7 ng/mL; d: 0.7 ng/mL) and the calibration plot between peak current and the tDNA concentration (inset). DPV scan from +1.25 V to 0 V, step potential 10 mV, modulation amplitude 50 mV, scan rate 50 mV/s, and nonstirred solution.----- 67

Figure 4.16. Schematic of the bio-barcode assay. (A) formation of MNP-2pDNA /tDNA/1 pDNA-AuNP-bDNA/NTs sandwich structure; (B) tDNA separation and tracer dissolution. ---- 68

Figure 4.17. Single detection of various concentrations of *pagA* gene from *Bacillus anthracis* with the bio-barcode biosensor using PbS NTs. (A) stripping voltammogram of various concentrations of *pagA* gene from *Bacillus anthracis*; (B) the relationship of tDNA concentration and peak current. Conditions: deposition at -1.2 V for 10 min; SWASV scan from -1.2 V to 0.0 V, frequency 20 Hz, amplitude 25 mV, and potential step 5 mV, with 1mg/mL bismuth, at room temperature and in nonstirred solution. ----- 69

Figure 4.18. Schematic of the multiple bio-barcode biosensor: A) bio-barcode assay; B) SWASV measurement. ----- 71

Figure 4.19. Specificity test of the multiple bio-barcode biosensor using distilled water as control. (A) control and 0.05 $\mu\text{g/mL}$ of the insertion element (*Iel*) gene of *Salmonella* Enteritidis; (B) control and 0.05 $\mu\text{g/mL}$ of *pagA* gene from *Bacillus anthracis*; (C) control and a mixture of 0.05 $\mu\text{g/mL}$ of the insertion element (*Iel*) gene and 0.05 $\mu\text{g/mL}$ of *pagA* gene. Conditions: deposition at -1.2 V for 10 min; SWASV scan from -1.2 V to 0.0 V, frequency 20 Hz, amplitude 25 mV, and potential step 5 mV, with 1mg/mL bismuth, at room temperature and in nonstirred solution.72

Figure 4.20. The stripping signal of released NT ions (Pb^{2+} and Cd^{2+}) with different concentrations of tDNAs: A) stripping voltammogram of various concentrations of tDNA; B) the calibration plot between peak current and the tDNA concentration. ----- 74

Figure 4.21. Schematic of portable electrochemical biosensor. ----- 77

CHAPTER 1: INTRODUCTION

1.1 Objective and Goals

The long term goal of this research is to develop a handheld multiplex DNA sensor for a rapid, highly specific and sensitive, cost-effective detection of foodborne pathogens, especially in resource-limited settings or clinical facilities. This is to be accomplished by using a new biosensor architecture, which combines screen-printed carbon electrode (SPCE) chips, bio-barcode assay and a portable potentiostat. The model agents for this proof of concept research are *Salmonella* Enteritidis and *Bacillus anthracis*. The biosensor, designed to detect the protective antigen A (*pagA*) gene (accession number = M22589) from *Bacillus anthracis* and the insertion element (*Iel*) gene (accession number = Z83734) from *Salmonella* Enteritidis, is mainly composed of three nanoparticles: gold nanoparticles (AuNPs), magnetic nanoparticles (MNPs), and nanoparticle tracers (NTs, such as PbS and CdS). After hybridization, the nanoparticle tracer is dissolved in 1 M nitric acid. The NT ions show an attractive non-overlapping stripping behavior by square wave anodic stripping voltammetry (SWASV) on SPCE chips. Combined with a battery-powered, handheld potentiostat, the whole biosensor detection system can provide a rapid, on-site, cost-effective detection for health care professionals, food safety monitoring personnel, and anti-bioterrorism agents.

The short term goal of this research is to construct a prototype biosensor. The biosensor will be evaluated for its ability to detect the two target genes specifically and sensitively in the same liquid media. It represents an innovative approach to detect multiple pathogens with high sensitivity due to multiple NT ion detection capability with SWASV on SPCE chips, magnetic extraction and concentration, and inherently amplified signal from the bio-barcode assay.

1.2 Foodborne disease and Bioterrorism

Foodborne disease is caused by consuming contaminated foods or beverages. More than 250 different foodborne diseases have been described. Most of these diseases are infections, caused by a variety of bacteria, viruses, and parasites that can be foodborne. Centers for Disease Control and Prevention (CDC) reported each year an estimated 76 million cases of foodborne illness occur in the United States. Over 325,000 hospitalizations and 9,000 deaths are associated with foodborne diseases each year (CDC 2010).

The five food categories, excluding multi-ingredient foods, linked to the most foodborne illness outbreaks are seafood, produce, poultry, beef, and eggs. These five food categories were responsible for 59 % of all outbreaks and 54 % of the illnesses (CDC 2010). Bacterial pathogens are responsible for 60 % of outbreaks, while viruses cause 24 %, chemicals/toxins cause 15 %, and parasites cause 1 % (CDC 2010). Although anyone can develop a foodborne illness, the elderly, young children, the immuno-compromised, pregnant women and their fetuses are most at risk. Thousands of types of bacteria are naturally present in our environment. The most prominent bacterial pathogens in the outbreak data are *Salmonella*, *Clostridium*, and *Escherichia coli* (CDC 2010). Table 1.1 shows the foodborne disease in the US by major foodborne pathogens in 2006.

Table 1.1 Foodborne diseases in the US by major foodborne pathogens in 2006 (CDC 2010).

Etiology (confirmed or suspected)	Outbreaks	Illnesses
<i>Salmonella</i>	117	3296
<i>Clostridium perfringens</i>	34	1880
<i>Escherichia coli</i> , Shiga toxin--producing (STEC)	29	592
<i>Staphylococcus enterotoxin</i>	29	428

"*Salmonella*" bacteria are the most frequently reported cause of foodborne illness. CDC estimates that 1.4 million people in the United States are infected, and 1,000 people die each year with salmonellosis. A total of 40666 *Salmonella* isolates were reported from participating public health laboratories in 2005 (CDC 2005). The surveillance report from the Food Diseases Active Surveillance for 2004 identified *Salmonella* as the most common bacterial infection reported, accounting for 42 % of the foodborne illness cases in the United States (CDC 2005). There were 117 *Salmonella* outbreaks in 2006, causing greater than 3,300 illnesses reported to the CDC Foodborne Outbreak Reporting System. The most common outbreak serotypes is *Salmonella enterica* serovar Enteritidis (*Salmonella* Enteritidis) (CDC 2010). *Salmonella* Enteritidis is a major threat for food safety and public health. There is a widespread occurrence of *Salmonella* Enteritidis in animals, especially in poultry and swine. Environmental sources of the organism include water, soil, insects, factory surfaces, kitchen surfaces, animal feces, raw meats, raw poultry, and raw seafood. People infected with *Salmonella* Enteritidis develop diarrhea, fever, and abdominal cramps 12 to 72 hours after infection. In some patients, especially for infants and young children, pregnant women and their unborn babies, and older adults, *Salmonella* infection may spread from the intestines to the blood stream, and then to other body sites and can be life-threatening unless the person is treated promptly with antibiotics (CDC 2005).

Some foodborne pathogens could potentially be delivered by bioterrorists through foods, such as *Bacillus anthracis*. It is a spore forming rod-shaped bacterium and transmissible to humans through handling or consumption of contaminated animal products. *Bacillus anthracis* spores can resist harsh physical and chemical environment, and remain viable in soil for many years. Infection may also result from inhalation of *Bacillus anthracis* spores from contaminated animal products such as wool or the intentional release of spores during a bioterrorist attack.

Bacillus anthracis can enter the human body through the intestines (ingestion), lungs (inhalation), or skin (cutaneous) and causes distinct clinical symptoms based on its site of entry. In 2001, *Bacillus anthracis* spores were intentionally distributed through the postal system, causing 22 cases of anthrax, including 5 deaths, and forever changing the realm of public health (Hughes and Gerberding 2002). Since then, the prospect of bioterrorism in food, water, and agriculture has identified critical needs in prevention, protection, and mitigation for homeland security. Rapid, on-site detection or point-of-care diagnosis are one of such needs.

In addition to the health risk associated with contaminated foods, there is the often devastating economic impact to the food producer. Especially current wide distribution by these mega-processing plants puts potential outbreak risks on a national and international scale. Increasing automation in food processing facilities increases the risk of contamination by environmental sources following heat treatment. A recall of 21.7×10^6 lb of ground beef in 2007 owing to contamination with *E. coli* O157:H7 resulted in the Topps Meat Company going out of business after 67 years of operation. Therefore, monitoring of pathogen counts on processing surfaces is critical in maintaining low or zero counts in food products. The costs of warehousing along with the potential costs of product recalls have potentially made on-site pathogen testing economically advantageous.

1.3 Current Detection Methods

The market potential for food pathogen detection was estimated to be \$150 million per year. This study estimated that 144.3 million microbiological tests were conducted in the food industry in 1999. The majority of these tests came from processed-food plants, followed closely by dairy plants (Alocilja and Radke 2003).

The common detection methods for pathogens include microbiological, immunological and molecular biological techniques. Microbiological detection often relies on pathogen growth in culture media, followed by isolation, biochemical identification. For example, Laboratory procedures for the identification of *Bacillus anthracis* from CDC include incubation of purified specimens at 35-37 °C for 18-24 h, then the "Medusa head" colony shows the presumptive identification. For further confirmation, gram stain or india ink stain will be used (Weyant R.S 2001). The microbiological detection of *Salmonella* in food samples is also laborious and time-consuming. Several days are required to culture the bacteria from a sample followed by a final isolation and identification by biochemical and serological techniques. Although microbiological detection is sensitive and accurate, it is time-consuming and needs special reagents and facilities in the laboratory.

The immunological detection system, such as enzyme linked immunosorbent assay (ELISA), utilizes the specific binding reaction between antibody and antigen. For example, a commercial *Salmonella* ELISA Test Kit from Bioo Scientific Inc. provides a simple, rapid, sensitive and cost-effective screening method, which enables government agencies, seafood processors, as well as quality assurance organizations, to detect positive and negative *Salmonella* samples to as low as 10^5 cells/mL level. The ELISA technique is highly specific due to the specificity of monoclonal antibody. However, its sensitivity is relatively low and hard to satisfy the on-site detection.

Molecular polymerase chain reaction (PCR) utilizes a combination of reagents and temperature change schemes to anneal and denature nucleic acid sequences for exponential amplification of the gene of interest. Quantitative PCR (Q-PCR) is another primer-based molecular technique that combines the specificity of conventional PCR with the quantitative

measurement of fluorescence for determining the presence of specific types of nucleic acid in environmental samples. Both molecular biological techniques are very sensitive. However, PCR techniques are often criticized for their complex, expensive, time-consuming, and labor-intensive procedures and narrow target DNA (tDNA) quantification range after PCR amplification. The specialized labs staffed by highly trained personnel are also required.

In the meanwhile, some commercial rapid detection methods have been developed, which use a vast array of tests that include miniaturized biochemical kits, antibody- and DNA-based tests, and assays that are modifications of conventional tests to speed up analysis. Automation using traditional detection methods, such as microbiological and immunological methods, is also increasing in popularity. However, the detection systems are costly, require specialized training, have complex processing steps, need enrichment of bacteria in an enrichment medium before analysis. In addition, most of them are only for the detection of one agent. So a rapid, cost-effective, sensitive, multiple, user-friendly, on-site detection and valid identification of pathogenic agents, such as *Salmonella* Enteritidis and *Bacillus anthracis*, is vital within the overall context of food safety, anti-bioterrorism, and point-of-care diagnosis.

1.4 Use of Biosensors

A biosensor is an analytical device that integrates a biological sensing element with a transducer to quantify a biological event into an electrical output. Figure 1 shows the schematic of a biosensor. It consists of three components: 1) biological sensing element, which can bind the biological analytes specifically, such as antibody for antibody, DNA probe (pDNA) for DNA target (tDNA); 2) transducer, which can convert the biological event into an electrical output,

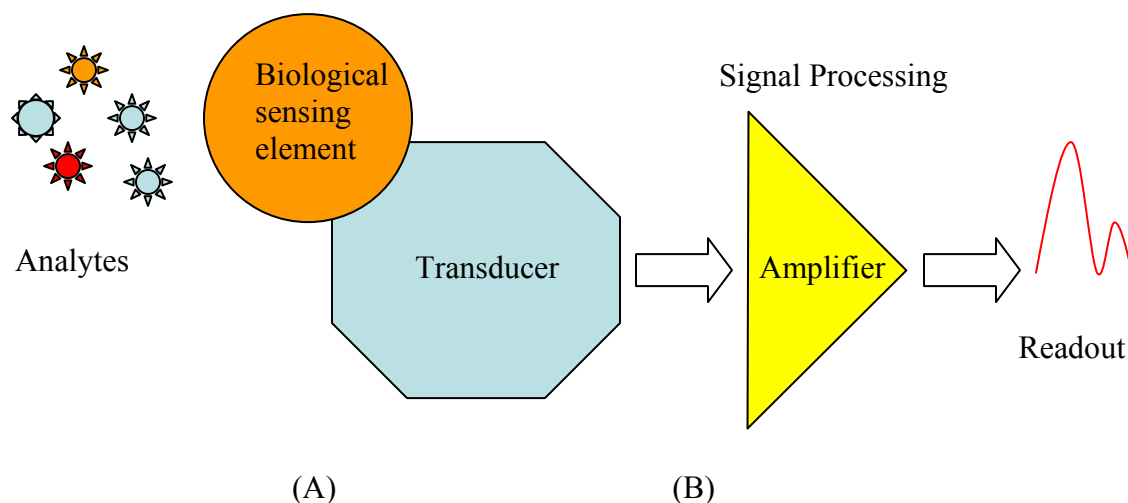


Figure 1.1. Schematic of biosensors. (A) Biological reaction between biological sensing element and analytes; (B) Transduction from biological event to electrical output. For interpretation of the references to color in this and all other figures, the reader is referred to the electronic version of this dissertation.

such as optical fibers and electrodes; 3) associated electronics or signal processors those are primarily responsible for the display of the results in a user-friendly way. Transduction of biological reaction is mainly measured electronically (Lee and Shim 2001), optically (Dubertret 2005; Pu, Pan et al. 2008; Sassolas, Leca-Bouvier et al. 2008) or electrochemically (Drummond, Hill et al. 2003; Weng, Zhang et al. 2008), or using mass-sensitive devices (Huang, Wang et al. 2006).

Optical methods are the most frequently used detection approach currently. The simplest detection units are spectrometers and fluorometers, which can be used for spectroscopic or fluorescence detection of target indicators, respectively. Another widely used option is flow cytometry (FCM), in which cells are physically analyzed based on characteristics such as natural fluorescence or light scattering. FCM is often paired with immunomagnetic capture to concentrate cells which are passed single file in a fluid stream with the light scatter from a laser defining cell count. Advanced flow cytometers can even sort target cells away from waste materials onto membranes or slides, for further verification methods. FCM systems have been

deployed in the field, but they are generally not portable or robust and require advanced training to operate. Although current optical sensing approaches are effective for high-density arrays, they are hard to miniaturize and use for in-field detection or point-of-care diagnosis.

Electrochemical systems for biomedical diagnostics can be miniaturized and integrated into micro-systems, including parts for signal processing, providing great deal of advantages over optical detection (Templin, Stoll et al. 2002). Because electrochemical reactions give an electronic signal directly, there is no need for expensive signal transduction equipment. Moreover, because immobilized biological sensing elements can be readily confined to a variety of electrode substrates, detection can be accomplished with an inexpensive electrochemical analyzer. Indeed, portable systems for clinical testing and on-site environmental monitoring are now being developed (Wang 2002). So in this study, an electrochemical method is employed as a transducer element in the biosensor design.

The fundamental process in an electrochemical method is the transfer of an electron between the electrode surface and the molecules in the solution adjacent to the electrode. An electrochemical detection system is composed of 2 major parts: 1) a potentiostat, which provides potential or current and collects the electrical signal; 2) an electrochemical cell, which consists of a certain volume of electrolytes and 3 electrodes, namely working, reference, and auxiliary electrodes.

Figure 1.2 shows a schematic of a three-electrode electrochemical detection system (Bard and Faulkner 2001). The working electrode is the one at which the reaction of electron transfer occurs; the reference electrode (commonly silver/silver chloride) provides a stable and well-known electrode potential against the working electrode; and the auxiliary electrode, coupled with working electrode, facilitates the electron transfer in the circuit.

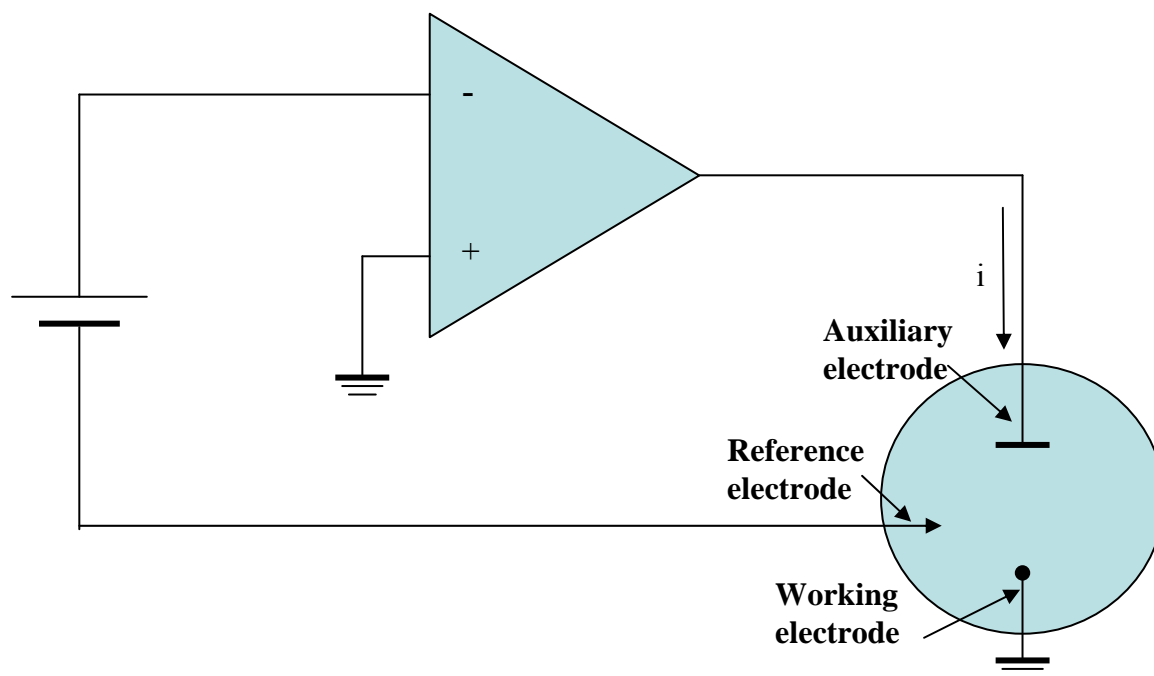


Figure 1.2 Schematic of a three-electrode electrochemical detection system. The system is composed of a potentiostat, working, reference, and auxiliary electrodes. (adapted from Bard and Faulkner 2001).

Electrochemical biosensors measure an electrochemical response of a biological event directly or indirectly, of which there are four basic types: 1) conductometric, which is a change in conductance of a bacterial cell between a pair of electrodes due to cell metabolism, such as conductive polymer (Pal, Alocilja et al. 2007); 2) potentiometric, which is the difference in electrical potential between a sample and a reference electrode (Karakus, Pekyardımcı et al. 2006); 3) amperometric, which is a response due to oxidation or reduction of a specific chemical at a constant applied potential (Hernandez-Santos, Diaz-Gonzalez et al. 2004; Karslan, Kayahan et al. 2009); 4) Impedimetric, which is the change in the capacitance layer between electrodes after biological binding (Kim, Park et al. 2009). All these electrochemical detection approaches are typically fast, sensitive and low-cost.

Based on different sensing elements, the biosensor can be divided into immunosensor, DNA sensor, cell-based biosensor, aptasensor, enzyme-based sensor, and other combinations. DNA

contains the genetic instructions used in the development and functioning of all known living organisms and some viruses. Chemically, DNA consists of two long polymers of simple units called nucleotides, with backbones made of sugars and phosphate groups. Attached to each sugar is one of four types of molecules called bases. It is the sequence of these four bases along the backbone that encodes information. Each type of base on one strand forms a bond with just one type of base on the other strand. This is called complementary base pairing. Purines form hydrogen bonds to pyrimidines, with adenine (A) bonding only to thymine (T), and cytosine (C) bonding only to guanine (G). This arrangement of two nucleotides binding together across the double helix is called a base pair.

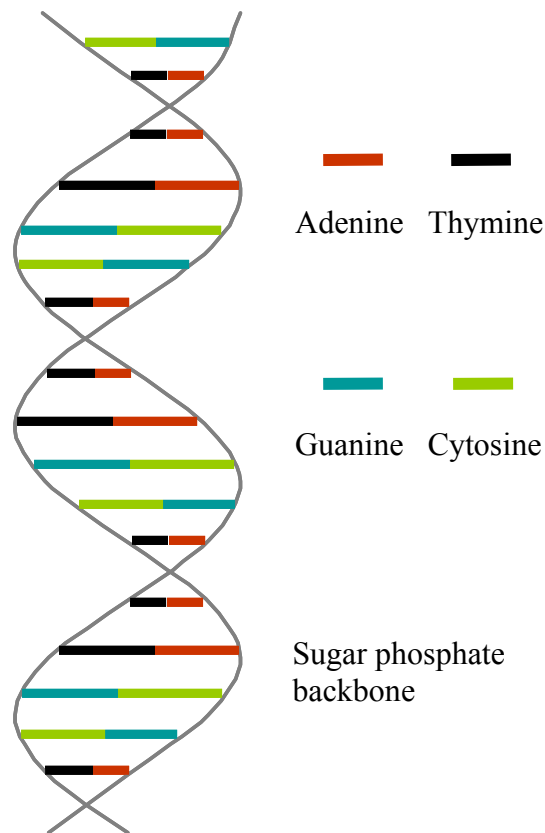


Figure 1.3. Schematic of DNA base pairs.

Figure 1.3 shows a schematic of DNA. The base pair coding mechanism make the DNA probe (pDNA) the most specific biological recognition molecules. The use of pDNA for isolating and identifying gene sequences through hybridization is the most common in DNA sensor research. Generally, a DNA sensor usually relies on the immobilization of a single-strand pDNA onto a surface to recognize its complementary DNA target (tDNA) sequence by hybridization. After specific hybridization between pDNA and tDNA, the transducer can convert the hybridization to an electrical signal. In recent years, the interest for DNA-based diagnostic tests has been growing. The development of systems allowing DNA detection is motivated by applications in many fields: DNA diagnostics, gene analysis, fast detection of biological warfare agents, and forensic applications (Sassolas, Leca-Bouvier et al. 2008). Moreover, these DNA sensors are able to distinguish closely related species which most antibody tests could not, which generate several other applications in the food industry. For example, with many countries refusing to accept the import of genetically modified organism (GMO) food products, there is an additional economic impact to their use. DNA sensors can be used to identify GMO products by detecting transgenic genes (Kalogianni, Koraki et al. 2006; Sun, Zhong et al. 2008). DNA biosensors have tremendous promise for obtaining sequence-specific information in a faster, simpler and more cost-effective manner compared to the traditional molecular techniques.

1.5 Novelty of Research

The multiplex DNA sensor developed here is the first design of nanoparticle-based electrochemical bio-barcode DNA detection based on a SPCE biosensor. The novelty is in the PCR-less DNA recognition coupled with rapid, multiplex detection of pathogens on a disposable SPCE biosensor. The bio-barcode DNA assay utilizes nanoparticle tracer (NT) terminated

oligonucleotides on gold nanoparticles (AuNPs) for signal amplification and magnetic nanoparticles (MNPs) for easy and clean separation from the sample. The detection system does not need PCR amplification due to its zeptomolar (10^{-21} M) sensitivity (Nam, Stoeva et al. 2004). The multiplex nanoparticle-based electrochemical bio-barcode DNA detection system provides a new, simple, fast, and field-ready technology as an alternative to the traditional PCR technique with comparable sensitivity. The biosensor design is very cost-effective to fabricate, is environmental-friendly when disposed of, has rapid detection time, no surface modification on the electrode surface, and is easy-to-miniaturize and integrate into micro-systems, and highly portable for field applications -- all these parameters lending well as an alternative device for bioterrorism and food safety countermeasure for prevention, protection, and mitigation.

1.6 Hypothesis

A nanoparticle-based electrochemical bio-barcode DNA sensor can simultaneously detect the protective antigen A (*pagA*) gene (accession number = M22589) from *Bacillus anthracis* and the insertion element (*Iel*) gene (accession number = Z83734) from *Salmonella* Enteritidis in the same sample.

1.7 Specific Aims

To demonstrate proof of concept, the specific aims of the research are:

- a) Synthesize and characterize gold nanoparticles and nanoparticle tracers (PbS and CdS);
- b) Functionalize gold nanoparticles and magnetic nanoparticles, and conjugate bio-barcode AuNPs with nanoparticle tracers (NTs);
- c) Evaluate and optimize SPCE chips for NT ion detection;

- d) Confirm bio-barcode assay;
- e) Evaluate biosensor sensitivity using a single purified PCR product from target organisms;
- f) Design multiplex detection of multiple targets in the same sample and evaluate its sensitivity and specificity.

CHAPTER 2: LITERATURE REVIEW

2.1 Overview of Nano-sensors

Nanotechnology is the engineering of functional systems at an atomic and molecular scale. The dimensional range of interest is approximately 1-100 nm. Because of effects such as the quantum size effect, mini size effect, surface effect and macro-quantum tunnel effect, nanomaterials or matrices with at least one of their dimensions ranging in scale from 1 to 100 nm, display unique physical and chemical features. Through the different physico-chemical phenomena taking place at nanodimensions, the integration of nanotechnology approaches into biosensors holds great promise for addressing the analytical needs of pathogen detection. Novel functional nanomaterials, such as porous silicon, nanowire, carbon nanotubes, and nanoparticles, biosensors are exerting a profound influence on food safety, environmental monitoring, and medical treatment (Staufer et al., 2007). Zhang and Alocilja (2008) reported a nano-scale porous silicon (PS)-based biosensor for DNA detection. Due to a lot of nano-scale pore formation on the silicon biosensor, much larger active surface area for hybridization was provided than planar silicon, which led to an increase in signal. A bigger electrochemical response was observed when hybridization occurred. When the concentration of tDNA increased, the charge transfer between the redox marker and porous silicon electrode was enforced so that the peak current rose with increasing DNA concentrations. The experiment result showed that the detection limit of the PS-based label-free DNA biosensor was 1 ng/mL (Zhang and Alocilja 2008). A nanowire labeled direct-charge transfer biosensor for detecting *Bacillus* species was reported (Pal, Alocilja et al. 2007). Testing of the biosensor showed that it had the ability to detect the presence of the target microorganism, *Bacillus cereus*, at concentrations as low as 10^1 CFU/ml, the detection

time being only 6 min (Pal, Alcocilja et al. 2007). Carbon nanotubes, the essential element of nanotechnology, have received considerable attention because of their inert properties, conducting behavior, and high-surface area. Particularly, their promotional ability for electron-transfer reactions with enzymes and other biomolecules has made carbon nanotubes the ideal supporting material for heterogeneous catalysts (Jianrong, Yuqing et al. 2004). A carbon multi-walled nanotubes (MWCNTs) based biosensor for direct and label-free detection of DNA of influenza virus (type A) was reported (Tam, Van Hieu et al. 2009). The hybridization was detected by changes in the conductance on the surface of sensors. The results showed that the DNA sensor could detect as low as 0.5 nM of the target DNA samples; the response time of DNA sensor was approximately 4 min (Tam, Van Hieu et al. 2009).

Besides porous silicon, conductive polymer, and carbon nanotubes, various nanoparticles have raised great expectations with respect to generating enhanced signal-to-noise ratios, reducing response times and using them in multiplexed systems (Khanna 2008). Nanoparticles play most important roles in the development of the nano biosensor because: 1) Nanoparticles exhibit higher ratios of surface area to volume than their bulk counterparts, so nanoparticle modified electrochemical interfaces will provide larger electrochemically active areas and therefore probably lead to higher detection sensitivity for target molecules; 2) some novel nanoparticles, particularly metal nanoparticles, can easily act as enhancing agents for effective acceleration of electron transfer between electrode and detection molecules, so leading to more rapid current response for target molecules; 3) nanoparticles can act as a supramolecular assembling unit with advanced functional properties for constructing a variety of architectures on the surface of electrodes and further tailoring of an electrochemical-sensing interface; 4) nanoparticles can be conjugated with some important biomolecules (e.g., redox enzyme) and also

act as nano-connectors that activate redox enzymes or electrical labels for bio-recognition events; and, 5) nanoparticle-modified electrochemical interfaces behave as nanoelectrode ensembles (Guo and Dong 2009). Inspired by these important features, literature already shows numerous examples of incorporating nanoparticles into biosensors. So far, there are nano-biosensors for the specific detection of biologically-relevant molecules (e.g., nucleic acids (Ting, Zhang et al. 2009; Zhang, Carr et al. 2009), proteins (Lin, Qu et al. 2007) and enzymes (Ren, Meng et al. 2005) and for the detection of infectious agents (Pal and Alocilja 2009).

Gold Nanoparticles (AuNPs)

Nanoparticles of noble metals, especially gold nanoparticles (AuNPs), have received great interest due to their attractive electronic, optical, and thermal properties as well as catalytic properties and potential applications in the fields of physics, chemistry, biology, medicine, and material science and their different interdisciplinary fields (Pingarr, Yez-Sede et al. 2008). In biosensor research, more attention has been paid to AuNPs because of their good biological compatibility, excellent conducting capability and high surface-to-volume ratio. The unique properties of gold nanoparticles to provide a suitable microenvironment for biomolecules immobilization retaining their biological activity, and to facilitate electron transfer between the immobilized proteins and electrode surfaces, have led to an intensive use of this nanoparticle for the construction of electrochemical biosensors with enhanced analytical performance with respect to other biosensor designs. Recent advances in the development of DNA biosensors using gold nanoparticles to improve DNA immobilization on electrode surfaces and as suitable labels to improve detection of hybridization events are considered.

Figure 2.1 shows the most important strategy used to integrate AuNPs in DNA-detection systems (Castada, Alegret et al. 2007), comprising: (A) the electrochemical detection of AuNP

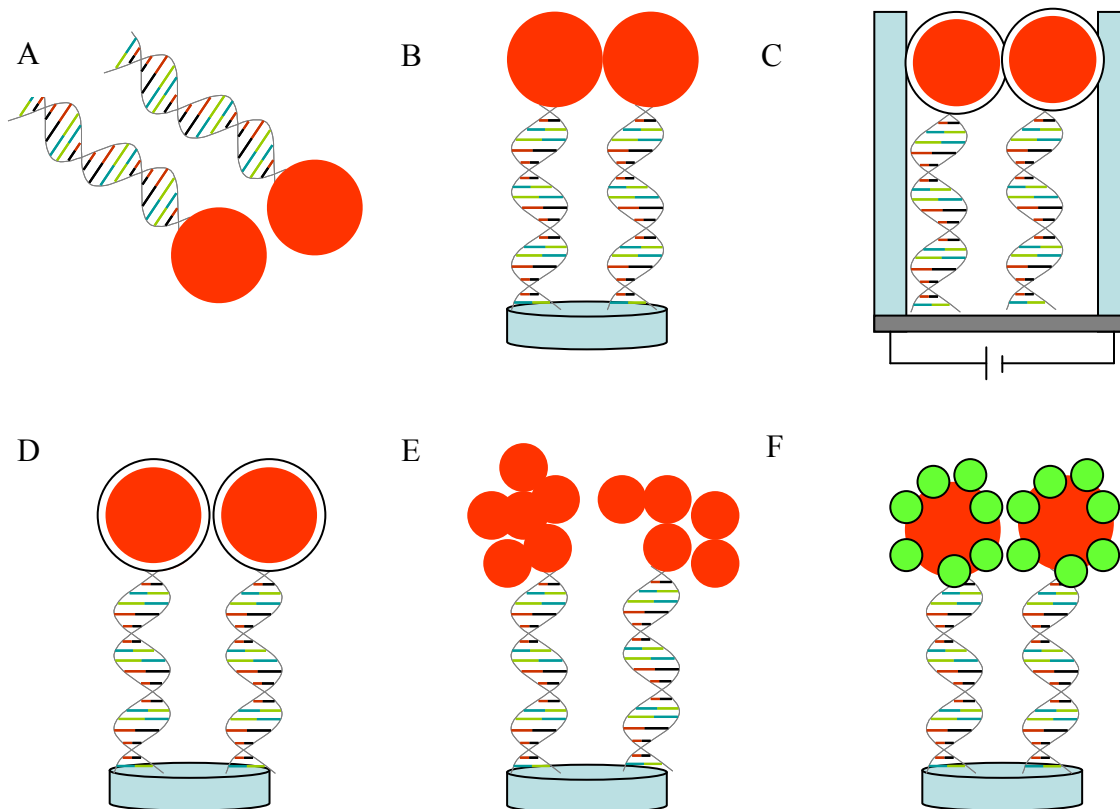


Figure 2.1. The different strategies used for the integration of gold nanoparticles (AuNPs) into DNA-sensing systems: (A) previously dissolving AuNPs by using HBr/Br₂ mixture followed by Au(III)-ion detection; (B) direct detection of AuNPs anchored onto the surface of the genosensor; (C) conductometric detection; (D) enhancement with Ag or Au followed by detection; (E) AuNPs as carriers of other AuNPs; and, (F) AuNPs as carriers of other electroactive labels (adapted from Castada, Alegret et al. 2007).

labels by detecting the gold ions released after dissolving them in acid; (B) direct detection of AuNPs anchored onto the surface of a conventional genosensor (based on stripping voltammetry); (C) silver enhancement using a conductometric technique; (D) enhancement of AuNPs anchored to conventional genosensor surface by using silver or gold; (E) AuNPs as carriers of other nanoparticles; and, (F) using AuNPs as carriers for other electroactive labels .

Table 2.1 summarizes some of the results obtained by using different strategies. Although clear improvements have been demonstrated by the same authors upon comparing their results (with and without enhancement) it is not so clear the improvement when comparing different

Table 2.1. Electrochemical genosensors using AuNPs as label. GE: gold electrode; DPV: differential pulse voltammetry; ASV: anodic stripping voltammetry; SPMBE: sandwich-type screen-printed microband electrode; PSA: potentiometric stripping analysis; SPEs: screen-printed electrodes; M-GECE: magnetic graphite-epoxy composite electrode, GCE: glassy carbon electrode (Castada, Alegret et al. 2007).

AnNPs size	Electrode	Detection Technique	Detection mode	Enhancement	Detection limits
1.4 nm	M-GECE	DPV	Direct	None	12 nM
20 nm	SPMBE	ASV	HBr/Br ₂	None	5 pM
5 nm	SPEs	PSA	HBr/Br ₂	None	5 ng
5 nm	SPE	PSA	Direct	Silver	1.2 fmol
10 nm	M-GECE	DPV	Direct	None	33 pmol
5 ± 1.3 nm	PGE	DPV	Direct	None	0.78 fmol
16.3 nm	Chitosan-modified GCE	DPV	-	Silver	50 pM
15 nm	SPMBE	ASV	HBr/Br ₂	Gold	600 aM

laboratories.

In this study, the good biological compatibility and high surface-to-volume ratio of AuNPs were employed for biosensor design. AuNPs also were measured electrochemically as an indicator of hybridization.

Magnetic Nanoparticle or beads (MNPs)

The biosensor detection is generally divided into two steps. The first is the capture, in which the microbial species or group of interest, such as antigen and target DNA, is removed, tagged or amplified to differentiate it from the remaining material in the sample. This step is typically responsible for the selectivity of the approach. The second step is the detection, in which the captured, tagged or amplified material is counted or measured quantitatively. The detector typically acts as a transducer, translating the biological, physical, or chemical alteration into a measurable electronic signal.

The current biggest technical challenges to the implementation of pathogen detection are the sample processing and detection sensitivity. There are two possible approaches to overcoming inadequate sensitivity: use the most advanced detectors available and more sensitive detector technology, or preconcentration, which can enhance sensitivity several fold by increasing the number of targets per unit volume at a relatively modest cost. As nanobiotechnology progresses, sensors to detect pathogens or their constituents become smaller and more sensitive. Owing to the nature of these nanoscale sensors, the sample size from which the detection is being made is typically several microliter or smaller. Therefore, the main challenge for scientists developing detection methods for pathogens is in the sample preparation now. Although the sample preparation requirements will vary from one food product to another, research into this step is required to bridge the emerging field of nano-biosensors with the food industry. The sample preparation will not only depend on the food matrix, but on the pathogen as well. Pathogenic viruses, bacteria and parasites might all exist within the same food product. For now, automation using more traditional detection methods is increasing in popularity, and the same will be true for less expensive and yet more powerful sensors of the future that are integrated with sample preparation.

Since more detection technologies are based on measuring sample volumes less than 1 ml, preconcentration may be necessary to achieve acceptable sensitivity. Several available modes of preconcentration are being used, including filtration, size-fractionation, centrifugation and magnetic separation or combinations of these methods. Magnetic nanoparticles (MNPs) or magnetic beads (MBs) are frequently used for concentration, separation, purification and

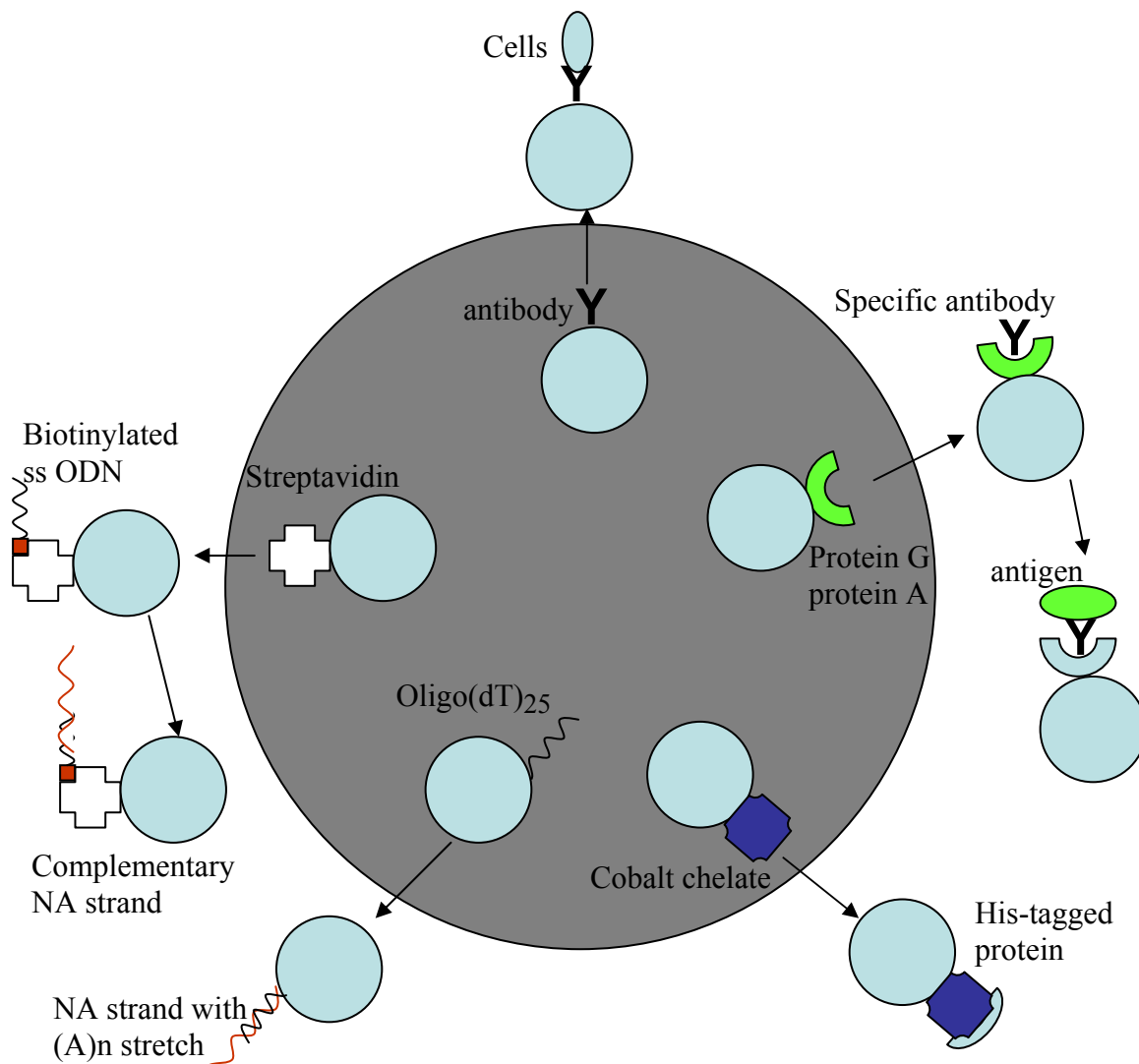


Figure 2.2. Magnetic beads (MBs) as versatile tools for bioassays. Beads modified with various recognition elements (examples of commercially available MBs shown on the gray background) can be used for specific bioaffinity capture of different molecules. For example, beads bearing covalently attached oligo(dT)₂₅ chains can bind nucleic acid involving (A)_n stretches, including natural eukaryotic mRNAs or tDNAs tagged with (A)_n adaptors. Streptavidin-coated beads are suitable for capturing any biotinylated molecules, including single strand or double strand nucleic acids, aptamers, peptides, proteins, etc. Antibodies can be attached to the beads either via a direct covalent linkage, or via specific antibody binding proteins such as protein A or protein G (beads functionalized with the latter proteins can be further modified with various antibodies on demand). Other affinity ligands attached to MBs are suitable for specific capture of tagged recombinant proteins (such as metal-affinity cobalt chelate for histidine tags). Biomolecules captured at the MB surface can serve as a biorecognition layer for interaction with other molecules. For example, a biotinylated single strand oligonucleotide (ssODN) immobilized at streptavidin-coated beads features a hybridization probe for complementary sequence, the dsDNA can represent a target for a DNA-binding protein, antibody can bind a specific antigen

(including antigens exposed at surfaces of whole cells), immobilized protein (e.g., via antibody, his-tag or biotin–streptavidin linkage) can interact with a specific nucleic acid or another protein, etc. (adapted from Palecek and Fojta 2007).

identification of molecules and specific cells. They are versatile tools in the separation of nucleic acids, proteins and other biomacromolecules, their complexes and cells. Figure 2.2 shows a schematic of magnetic beads as versatile tools for bioassays (Palecek and Fojta 2007).

Magnetic methods rely on efficient separation of paramagnetic or ferromagnetic particles from biological or chemical media. Superparamagnetic particles become magnetic under a strong magnetic field but retain no residual magnetism in the absence of magnetic field. These particles do not interact with each other when removed from the magnetic field. The diameter of the particles is usually between 0.5 and 10 μm . MNPs with hydrophilic surfaces are particularly convenient for DNA oligonucleotides, providing reproducible magnetic separation. MNPs can be prepared in various ways. Usually particles susceptible to magnetism, such as iron oxide, are coated with biological or synthetic polymers.

A number of companies offer MNPs and kits optimally adjusted for the desired application. Magnetic separators enabling automated handling of the beads are commercially available (Berensmeier 2006). With the use of such systems a rapid diagnosis of infections (Satoh, Iwata et al. 2003; Lee, Lien et al. 2008), and extraction of DNA and RNA from various media (Hourfar, Michelsen et al. 2005) is possible. New magnetic particles with improved properties, suitable for diagnostics in microbiology, cell isolation and other purposes were developed. Recently a list of 12 companies and their products was published (Berensmeier 2006), and it can be expected that materials with more specific binding properties and better separation will soon be developed. The scale-up procedures for the purification of large volumes of biological agents and

miniaturization for sensors and lab-on-a-chip techniques can be foreseen. In this study, magnetic particles were coated with DNA probe (pDNA) for sample separation and preconcentration.

Nanoparticle tracers (NTs)

Inorganic-colloid (quantum dots) nanoparticle tracers (NTs) are widely tagged to biological molecules for proteomic function based-medical studies in post-genomic era (Bruchez, Moronne et al. 1998), because NTs are dimensionally similar to biomolecules and a variety of bioconjugates are ideally suited as optical or molecular imaging (Chan and Nie 1998). Quantum confinement effects give rise to unique optical and electronic properties in quantum dots (QDs), giving them numerous advantages over current fluorophores, such as organic dyes, fluorescent proteins and lanthanide chelates. Properties that particularly influence fluorophore behavior, and therefore applicability to different situations, include the width of the excitation spectrum, the width of the emission spectrum, photostability, and the decay lifetime. So most current efforts for multiplex assays have focused on multi-color fluorescent detection in connection with different QDs. QDs have been used for the simultaneous fluorescent immunoassay of four toxins (Goldman, Clapp et al. 2004). Goldman et al. (2004) used QDs functionalized with antibodies to perform multiplexed fluoroimmunoassays for simultaneous detection of various toxins. This sensor could be used for environmental purposes for concurrently recognizing pathogens like cholera toxin in water. The fluorescence resonance energy transfer analysis (FRET) principle in QDs was also applied to a maltose biosensor (Medintz and Deschamps 2006). The sensing mechanism was the application of semiconductor QDs conjugated to a maltose binding protein covalently bound to a FRET acceptor dye. In absence of maltose, the dye occupied the protein binding sites. Energy transference from the QDs to the dyes quenched the QD fluorescence. When maltose was present, it replaced the dye leading to recovery of the fluorescence.

Compared to previous results using organic fluorophores, QDs gave an increased luminescence of 52% over 47 h after incubation with a collagenase (Medintz and Deschamps 2006).

Though current optical sensing approaches using QDs are effective for high-density arrays, they are often in the laboratory, require complicated equipment and special training, and complicated by the requirement of an elaborate excitation and detection scheme and by the broad emission bands so that they are hard to be miniaturized and portable. While electrochemical systems for biomedical diagnostics can be miniaturized and integrated into systems, including parts for signal processing, to provide great deal of advantages over optical detection schemes. They are not as susceptible to turbidity interference as optical-based detection, and typically have very low detection limits. So they are ideally suited for meeting the portability requirements of on-field detection of pathogens. QDs used for the electrochemical hybridization detection of multiple DNA targets was reported (Liu, Wang et al. 2004). Different inorganic quantum dots (QDs), namely nanoparticles tracers, (ZnS, CdS, and PbS) tagged to DNA or antibody for biological molecules detection are reported (Liu, Wang et al. 2004). The biosensor could detect multiplex proteins in a mixture containing 100 ng/mL β 2-microglobulin, IgG, BSA, and CRP in connection with ZnS-, CdS-, PbS-, and CuS-labeled antibodies, respectively. Baseline-resolved peaks of nearly similar sensitivity and favorable signal-to-noise characteristics were observed for the four proteins. Their metal components yielded well resolved highly sensitive stripping voltammetric signals for the corresponding targets (Liu, Wang et al. 2004). Nanoparticle tracers also were used to detect DNA hybridization based on the use of different nanoparticle tracer tags (Wang, Liu et al. 2003). This approach could be multiplexed and scaled by incorporating additional quantum-dot tracers (including bimetallic ones), by using microtiter plate platforms

(with each microwell carrying out multiple measurements), and through particle-based libraries for electrical barcoding in the future.

2.2 Electrochemical DNA sensor

Successful recognition of a specific sequence of DNA requires a highly specific recognition layer. DNA biosensors exploit the ability of a single strand of DNA (ssDNA) to recognize and hybridize with a complementary ssDNA in the recognition interface. The strand of DNA, which does the detection, the DNA probe, is immobilized onto the surface of the signal transducer (see Figure 2.3). Exposure of the recognition surface to a sample containing single strands of the DNA of interest, the target DNA, will result in hybridization where transduction can proceed.

In a DNA biosensor, the probe will most frequently consist of an oligonucleotide of about 15 to 50 bases long. To a large extent the selectivity, sensitivity and reproducibility of a DNA recognition interface will depend on the immobilization of the DNA probe (pDNA). When hybridization occurs, the probe and target strands must be free to coil around each other. Immobilization of the probe strand onto a transducer surface will inevitably cause a decrease in configurational freedom. Therefore minimization of the decrease in this freedom is required to achieve efficient hybridization. Single point attachment of the probe strand at either the 5' or 3' end of a pDNA is one strategy to maintaining efficient hybridization. Alkanethiols are molecules with an alkyl chain, (C-C)_n chain, as the back bone, a tail group, and a SH head group. They are used on noble metal substrates because of the strong affinity of sulfur for these metals and form a self assembled monolayer (SAM) on it. In this study, thiolated DNA probes (pDNA) and barcode DNA (bDNA) were coated on AuNPs homogeneously to improve the hybridization efficiency of pDNA and tDNA.

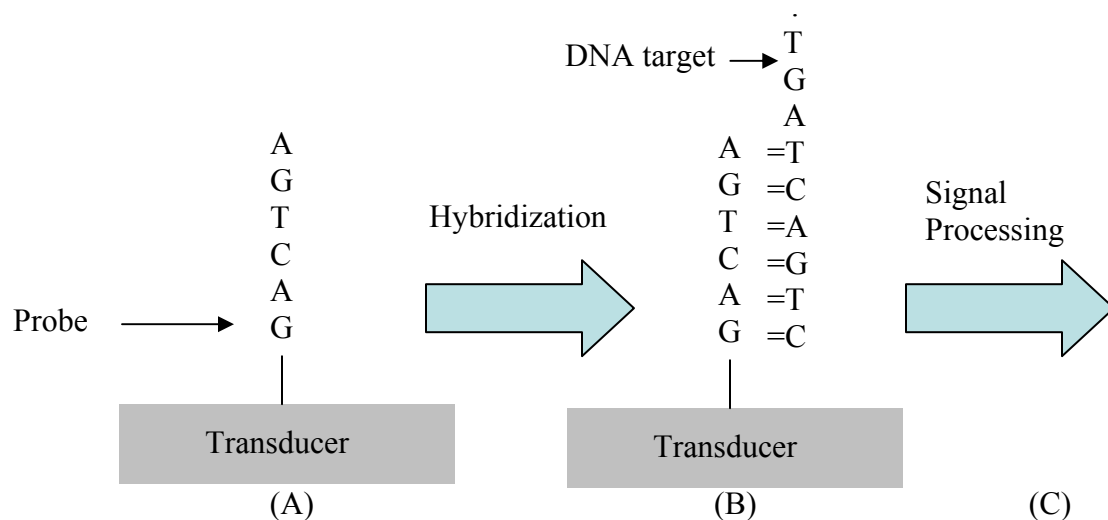


Figure 2.3. Schematic of an electrochemical DNA biosensor. (A) DNA probe immobilization; (B) hybridization between DNA probe and target DNA on the transducer; (C) signal processing by a biosensor system.

The basic categories of electrochemical detection of DNA include direct reduction/oxidation of DNA (Karadeniz, Gulmez et al. 2003; Ozkan-Ariksoysal, Tezcanli et al. 2008), indirect oxidation of tDNA through the use of electrochemical mediators (Yang and Thorp 2001), DNA-specific redox indicator detection (Miroslav Fojta 2003), DNA-mediated charge transport electrochemistry (Steel, Herne et al. 1998; Jackson and Hill 2001), and nanoparticle-based electrochemical amplification (Sun, Zhong et al. 2008). Table 2.2 shows comparison of platforms for DNA electrochemical sensing (Drummond, Hill et al. 2003).

Due to high background current, the direct detection of guanine (G) or adenine (A) on a DNA sequence is still not sensitive and not ideal for multiplex detection. Methods to oxidize tDNA indirectly through the use of electrochemical mediators have also been explored (Yang and Thorp 2001). An especially attractive approach uses polypyridyl complexes of Ru^{2+} and Os^{2+} to mediate the electrochemical oxidation of guanine. DNA-specific redox indicator detection is an analogy to fluorescence-based methods.

Table 2.2 Comparison of Platforms for DNA electrochemical sensing (Drummond, Hill et al. 2003).

Type of sensor	Advantages	Disadvantages
Direct DNA electrochemistry	Highly sensitive (femtomoles of target); requires no labeling step; amenable to range of electrode	High background signals; can not be multiplexed; destroy the sample
Indirect DNA electrochemistry	Highly sensitive (attomoles of target); usually requires no labeling step; multiple-target detection at same electrode	Probe substrate can be difficult to prepare; destroys the sample
DNA-specific redox indicator detection	Moderate to high sensitivity (femtomoles of target); well suited to multiple-target detection; samples remain unaltered	Chemical labeling step required unless “sandwich” method used; sequence variations can be problematic
Nanoparticle-based electrochemistry amplification	Extremely sensitive (femtomole to zeptomole range); well suited to multiple-target detection with different nanoparticles	Many development steps in assay; reliability and robustness of surface structure problematic; sample usually destroyed
DNA-mediated charge transport	Highly sensitive (femtomole range) and simple assay; requires no labeling; uniquely well suited for mismatch detection; sequence independent; amenable to multiplexing; applicable to DNA-protein sensing step	Biochemical preparation of target sample required

The reporting pDNAs are labeled with redox-active molecules. Appearance of the characteristic electrochemical response of the redox reporter therefore shows the hybridization event. Detection limits on the order of 10^{10} molecules have been reported (Miroslav Fojta 2003). DNA-mediated charge transport electrochemistry uses a redox active reporter molecule, such as intercalator, to bind the double helix of DNA noncovalently and facilitate the charge transport through DNA structure. It is uniquely suited to sense changes in DNA damage, mistakes, and mismatches.

Currently many applications of DNA sensing involve extremely small numbers of target analytes, with correspondingly few hybridization events. Many nanomaterials were deposited

onto traditional electrodes to improve the biosensor sensitivity. Multiwalled carbon nanotubes (MWNT) are receiving more and more attention interests in biosensor research. A MWNT nanoelectrode arrays embedded in a silicon dioxide (SiO_2) matrix for DNA detection was reported (Jessica Koehne 2003). The inherent guanine bases in the DNA amplicon target of 300 bases serve as signal moieties with the aid of tris(2,2'-bipyridine) ruthenium (II) ($\text{Ru}(\text{bpy})_3^{2+}$), providing an amplified anodic current associated with the oxidation of guanine groups at the nanoelectrode surface. The reduced size and density of the nanoelectrode array provided by MWNTs dramatically improves the sensitivity of electrochemical detection. In addition, the abundant guanine bases in tDNA produce a large signal. Less than 1000 target amplicons can be detected on a microspot, approaching the sensitivity limit of conventional laser-based fluorescence techniques. This method also eliminates the labeling requirement and makes the measurements much simpler (Jessica Koehne 2003). It was reported that lead selenide nanoparticle/chitosan composite films were prepared on the carbon paste electrode (CPE) for the detection of CaMV35S promoter genes in some transgenic plants (Xie, Jiao et al. 2008). The result showed the detection range from 5.0×10^{-11} to 5.0×10^{-6} M and the detection limit of 1.6×10^{-11} M. using this DNA electrochemical sensor.

Analyte amplification has also been accomplished in an innovative way indirectly using electrochemical detection of nanoparticles. Semi-conducting nanoparticle tracers (NPs) are good oligonucleotide labeling markers for DNA biosensors. For example, an electrochemical coding technology for the simultaneous detection of multiple DNA targets based on nanoparticle tracers with different redox potentials was reported (Wang, Liu et al. 2003). Such encoding nanoparticles thus offer a voltammetric signature with distinct electrical hybridization signals for

the corresponding DNA targets. The new electrochemical coding bioassay relies on the use of different inorganic-colloid (quantum dots) nanoparticle tracers, whose metal components yield well resolved highly sensitive stripping voltammetric signals for the corresponding targets. Three encoding nanoparticles (zinc sulfide, cadmium sulfide, and lead sulfide) have thus been used to differentiate the signals of three DNA targets in connection with a sandwich hybridization assay and stripping voltammetry of the corresponding heavy metals.

Figure 2.3 shows the schematic of multi-target DNA detection using different inorganic colloid nanoparticle tracers. The new multi-target electrical detection scheme incorporated the high sensitivity and selectivity advantages of nanoparticle-based electrical assays. This approach could be multiplexed and scaled by incorporating additional nanoparticle tracers, by using microtiter plate platforms (with each microwell carrying out multiple measurements), and

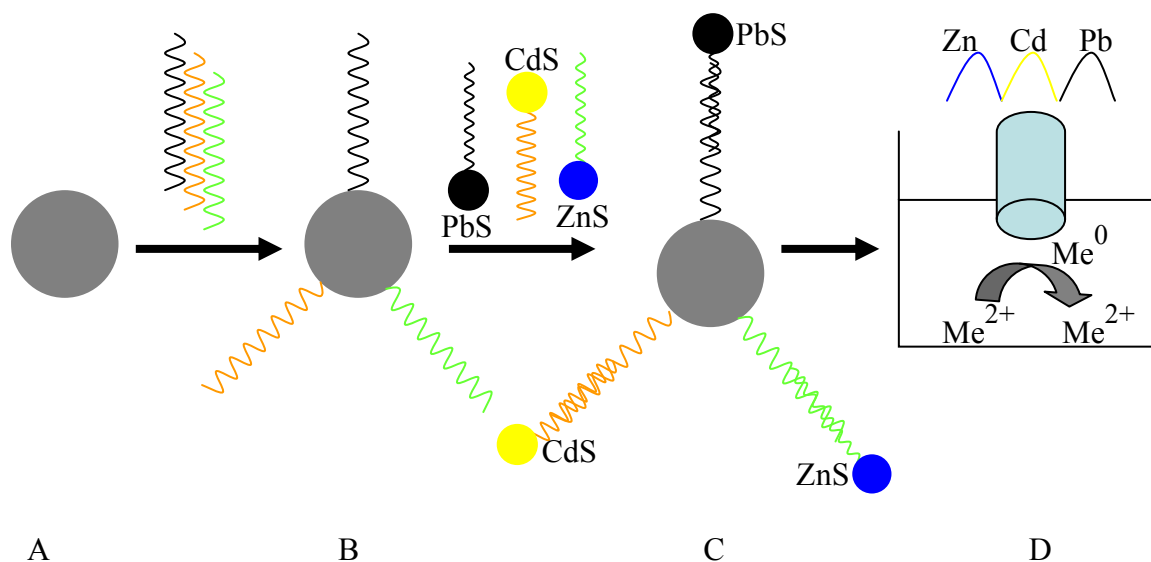


Figure 2.4. Multi-target electrical DNA detection protocol based on different inorganic colloid nanoparticle tracers. (A) Introduction of probe-modified magnetic beads. (B) Hybridization with the DNA targets. (C) Second hybridization with the QD-labeled probes. (D) Dissolution of QDs and electrochemical detection (adapted from Wang, Liu et al. 2003).

through particle-based libraries for electrical barcoding in the future. In addition, surface modification of electrodes the immobilization of pDNA was not necessary. It will save a lot of time of electrode preparation and prolong the shelf life of electrodes greatly.

2.3 Bio-barcode Assay

Most of the current DNA sensors need PCR amplification before applying the samples because of relatively low sensitivity. However, PCR is often criticized for its complex, expensive, time-consuming, and labor-intensive procedure. It limits the widespread application of DNA sensor.

The bio-barcode DNA assay is a promising new amplification and detection technique that makes use of short oligonucleotides as target identification strands and surrogate amplification units in both protein and nucleic acid detection (Hill and Mirkin 2006). The technique uses many advantageous properties of oligonucleotide-functionalized AuNPs including ease of fabrication, greater oligonucleotide binding capabilities, stability under a variety of conditions, catalytic ability, and optical properties (Demers, Ostblom et al. 2002; Lytton-Jean and Mirkin 2005). The large ratio between thiolated single-strand oligonucleotide barcodes DNA (bDNA) and pDNA on AuNPs provides significant amplification. It has been shown to have extraordinarily PCR-like sensitivity. Under controlled conditions, the assay has shown attomolar (10^{-18}) sensitivity for a variety of protein targets (Nam, Thaxton et al. 2003) and zeptomolar (10^{-21}) sensitivity for a variety of target genes (Nam, Stoeva et al. 2004). The bio-barcode DNA assay utilizes oligonucleotide-modified gold nanoparticles (AuNPs) for signal amplification and magnetic nanoparticles (MNPs) for easy and clean separation from the sample. Figure 2.5 shows a schematic of bio-barcode DNA assay. After immobilization of oligonucleotides on the surface of

nanoparticles, both nanoparticles can bind with the target DNA (tDNA) to form a sandwich structure, due to the specificity of DNA probe (pDNA). Figure 2.5A shows the tDNA sample hybridizing with the second pDNA

(2pDNA) on the MNPs, forming a MNP-2pDNA/tDNA complex (middle picture). Then AuNPs coated with the first pDNA (1pDNA) and bDNA are added to form a sandwich structure consisting of MNP-2pDNA/tDNA/1pDNA-AuNP-bDNA (picture on the right). After hybridization is complete, the sandwich structure is separated magnetically from unreacted pDNA-AuNP-bDNA. Finally the bDNA is released from the surface of AuNPs (Figure 2.5B). Based on different labels, the barcode strands can be identified on a microarray via scanometric

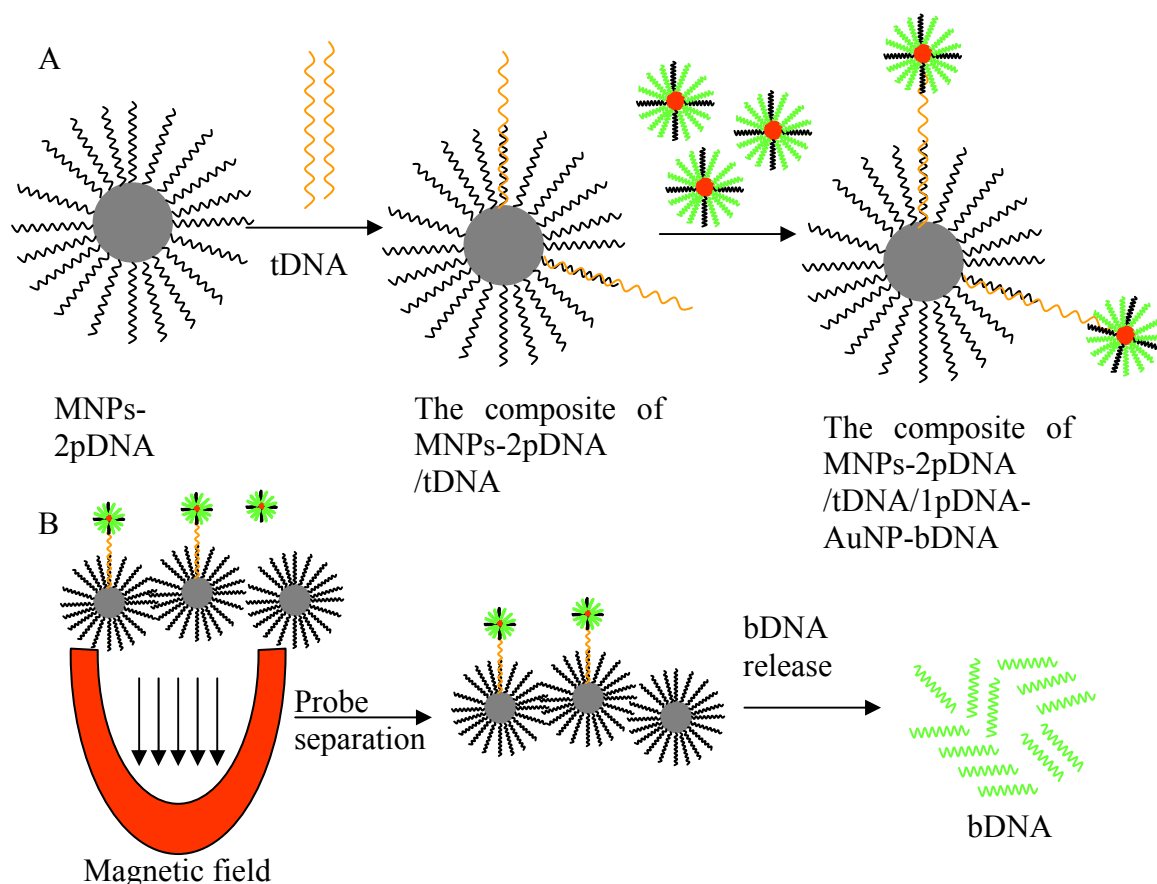


Figure 2.5. Schematic of bio-barcode DNA assay. (A) formation of MNP-2pDNA/tDNA/1pDNA-AuNP-bDNA sandwich structure; (B) probe separation and bDNA release.

detection (Taton, Mirkin et al. 2000; Stoeva, Lee et al. 2006), on-chip detection (Goluch, Nam et al. 2006), fluorescence (Oh, Nam et al. 2006), or Raman active dye (Cao, Jin et al. 2002) if the barcodes carry with them a detectable marker.

2.4 Screen-printed Carbon Electrode

Solid electrodes based on carbon materials are commonly used in electrochemical analysis due to their broad potential window, low background current, rich surface chemistry, low cost, chemical inertness, and suitability for various sensing and detection applications (Kissinger and Heineman 1996). The screen-printing microfabrication technology is nowadays well established for the mass production of thick film electrodes. This process implies the sequential deposition of layers of different conductive (carbon) or non-conductive inks on a variety of inert substrates. The screen-printed carbon electrode (SPCE) is made of electrochemically active graphite particles. A binder is added to enhance the affinity of the ink to the substrate in terms of adhesion properties and mechanical strength. Solvents are used to improve the viscosity of the ink for the printing process. Compared with conventional electrodes, the SPCE has several advantages, such as simplicity, convenience, low cost and the avoidance of contamination between samples (Susmel, Guilbault et al. 2003; Miscoria, Desbrieres et al. 2006). It represents a promising route for mass production of inexpensive, reproducible and disposable electrochemical sensors for the determination of trace levels of important compounds. There has been a lot of published work on the detection of metals with screen-printed carbon electrodes using stripping analysis techniques (Desmond, Lane et al. 1998; Kadara and Tothill 2004; Hwang, Han et al. 2008). Biosensors based on screen-printed carbon electrode (SPCE) have been extensively used for detection of glucose (Guan, Li et al. 2005; Xu, Li et al. 2005), cholesterol (Carrara, Shumyantseva et al. 2008), antigens (Kim, Seo et al. 2006) and DNA (Ruffien, Dequaire et al. 2003; Hernandez-

Santos, Diaz-Gonzalez et al. 2004). However, these electrochemical detection systems with electrochemical sensors need additional auxiliary and reference electrodes and a relatively large volume of electrolyte solution. This limits potential applications of electrochemical sensors for portable detection, especially for samples with a very small volume requirement such as body fluids. A SPCE integrated with an auxiliary/reference electrode was used in this study. Its volume requirement was 100 μ l. The potential application for portable detection is promising.

The SPCE can be enhanced with mercury or bismuth. The mercury-film electrode (MFE) and hanging mercury drop electrode (HMDE) are commonly used in the development of stripping voltammetry. However, because of the toxicity of mercury, future regulations and occupational health considerations may severely restrict its use as an electrode material. Bismuth is an environmentally friendly element, with low toxicity and a widespread pharmaceutical use (Rodilla, Miles et al. 1998). The bismuth electrodes can be prepared by simultaneous deposition of bismuth and the target heavy metals, in a manner analogous to in situ plated mercury film electrodes. Such electrodes display well-defined, sharp and highly reproducible stripping peaks for low (ppb) concentrations of lead, cadmium, or zinc over a low background current. Such use of "mercury-free" electrodes is particularly attractive for the development of multiplex metal sensors (Wang, Lu et al. 2000). In this study, a disposable integrated SPCE chip enhanced by bismuth was used for the multiplex detection of NT ions in 100 μ L of sample solution, which were released from bio-barcode assays.

2.5 Square wave anodic stripping voltammetry

Square wave anodic stripping voltammetry (SWASV) is a powerful tool for measuring trace metal ions. It can be viewed as combining the best aspects of square wave voltammetry (SWV)

and anodic stripping voltammetry (ASV). The technique includes the background suppression and sensitivity of differential pulse voltammetry, and the diagnostic value of anodic stripping voltammetry (Bard and Faulkner 2000). In square wave voltammetry, a square wave is superimposed on the potential staircase sweep. Oxidation or reduction of species is registered as a peak or trough in the current signal at the potential at which the species begins to be oxidized or reduced. Figure 2.6 shows waveform and measurement scheme for square wave voltammetry (Bard and Faulkner 2000).

The current is measured at the end of each potential change, right before the next, so that the contribution to the current signal from the capacitive charging current is minimized. The differential current is then plotted as a function of potential, and the reduction or oxidation of species is measured as a peak or trough. Due to the lesser contribution of capacitive charging

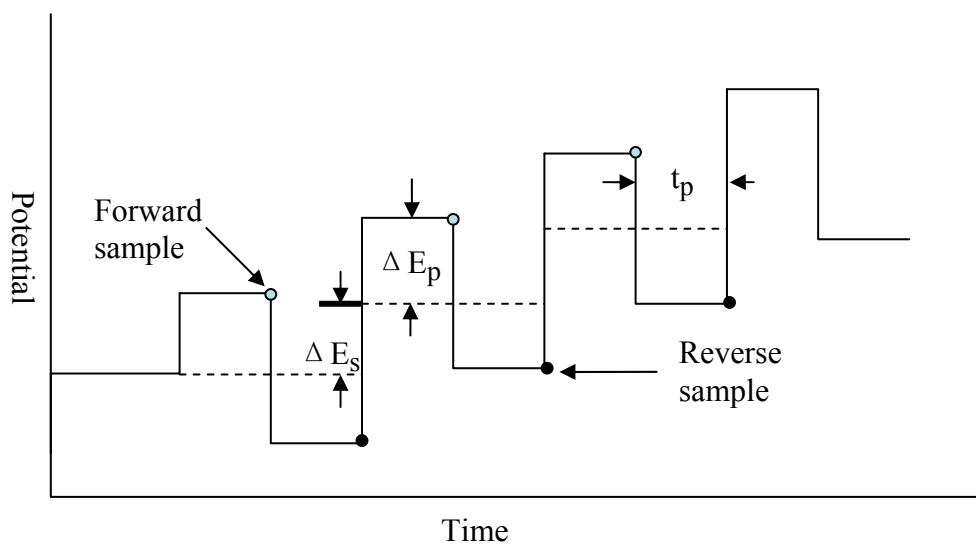


Figure 2.6. Waveform and measurement scheme for square wave voltammetry. Shown in bold is the actual potential waveform applied to the working electrode. The light intervening lines indicate the underlying staircase onto which the square wave can be regarded as having been superimposed. In each cycle, a forward current sample is taken at the time indicated by the solid dot, and a reverse current sample is taken at the time marked by the shaded dot (adapted from Bard and Faulkner 2000).

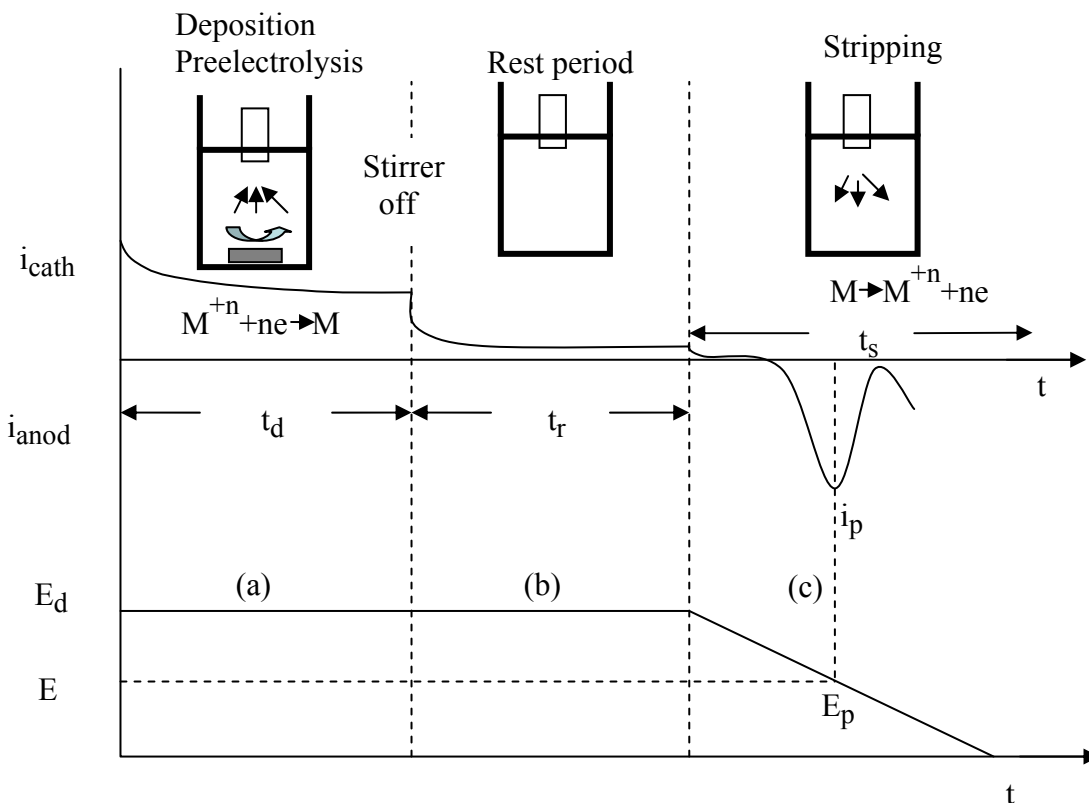


Figure 2.7. Principle of anodic stripping. Values shown are typical ones used; potentials and E_p are typical of Pb^{2+} analysis, (a) Preelectrolysis at E_d ; stirred solution, (b) Rest period; stirrer off. (c) Anodic scan ($\nu = 10\text{-}100$ mV/s) (adapted from Bard and Faulkner 2000).

current the detection limits for SWV are on the order of nanomolar concentrations (Bard and Faulkner 2000).

Besides the advanced measurement procedure of SWV that generates an extremely favorable signal-to-background ratio, the remarkable sensitivity of SWASV technique is also attributed to the combination of an effective pre-concentration step of anodic stripping techniques. Figure 2.7 shows the principle of anodic stripping. The analyte of interest is electroplated on the working electrode during a deposition step, and oxidized from the electrode during the stripping step. The current is measured during the stripping step. The oxidation of species is registered as a peak in the current signal at the potential at which the species begins to be oxidized. The stripping step can be either linear, staircase, square wave, or pulse (Bard and Faulkner 2000).

SWASV is a powerful electroanalytical technique for trace metal measurements. Because of its effective “built-in” preconcentration (deposition) step, this technique offers remarkably low (picomolar) detection limits. Four to six metals could be measured simultaneously in various matrixes at concentration levels down to 10^{-10} M, utilizing relatively inexpensive and portable instrumentation (Wang 2003).

Recent activity has led to highly sensitive nanoparticle-based stripping electrical bioassays based on capturing various colloidal metal and inorganic-crystal nanoparticle tags. Three metal sulfide nanoparticle tracers (zinc sulfide, cadmium sulfide, and lead sulfide) have been used to differentiate the signals of three DNA targets in connection with a sandwich hybridization assay and stripping voltammetry of the corresponding heavy metals (Wang, Liu et al. 2003). This electrochemical coding bioassay relied on the use of different inorganic-colloid nanoparticle tracers (quantum dots) as electrochemical indicators, whose metal components yielded well resolved highly sensitive stripping voltammetric signals for the corresponding targets. The new strategy thus combined a novel multi-target bio-detection with an inherently amplified signal and the high selectivity attribute of magnetic assays.

CHAPTER 3: MATERIALS AND METHODS

3.1 Reagents and Materials

Hydrogen tetrochloroaurate (III) trihydrate and sodium citrate dehydrate were used for the synthesis of gold nanoparticles. Sodium sulfide, 3-mercaptopropionic acid, lead nitrate and cadmium chloride were used for the synthesis of lead sulfide (PbS) and cadmium sulfide (CdS) NTs. 1,4-Dithio-DL-threitol (DTT) was used for the cleavage of oxidized thiolated oligonucleotides. 1-Ethyl-3-(3-dimethylaminopropyl) carbodiimide Hydrochloride (EDC) and N-hydroxysuccinimide (NHS) were used for the conjugation of carboxylic group on NTs and amine group on bio-barcoded AuNPs. Amine terminated MNPs were used for sample separation. All reagents were purchased from Sigma (St. Louis, MO). To validate and characterize SPCE chips, potassium ferricyanide, potassium chloride, lead chloride and cadmium chloride were purchased from Sigma (St. Louis, MO, USA). Bismuth standard stock solution (1000 mg/L, atomic absorption standard solution) was obtained from Fisher Scientific (Hanover Park, IL, USA). DNA isolation was performed using the QiaAmp DNA Mini Kit (Qiagen Inc., Valencia). Nap-5 column (GE Healthcare, Piscataway, NJ) was used to purify the DNA product from DTT solution. Sulfo-succinimidyl 4-N-maleimidomethyl cyclohexane-1-carboxylate (sulfo-SMCC; Pierce, WI) was used as a cross-linker between thiolated DNA probe (pDNA) and amine-coated MNPs. Sulfo-NHS acetate (Pierce, WI) was used to block unreacted sulfo-SMCC. Bismuth standard stock solution (1000 mg/L, atomic absorption standard solution) was obtained from Fisher Scientific (Hanover Park, IL, USA). All solutions were prepared in deionized water (~ 18 M Ω cm).

3.2 Facilities and Equipment

Target DNA (tDNA) was amplified by a thermocycler (Mastercycler Personal, Eppendorf). Gel electrophoresis (Runone System) was used to confirm the PCR product. After purification of the PCR product, a spectrophotometer (SmartSpec 3000, Bio-Rad Laboratories) was used to measure the concentration of pDNA in solution and tDNA in the sample. In the characterization experiments of AuNPs, a UV-Vis-NIR Scanning Spectrophotometer (UV-3101PC, Shimadzu) was used to determine the absorbance of AuNPs. A transmission electron microscope (TEM, JEOL100 CXII) was used to image and characterize the NTs and AuNPs. All magnetic separation was done using a magnetic separator (FlexiMag, SpheroTech). A centrifuge (Micro12, Fisher Scientific) was used to separate and purify the nanoparticles. An incubator (HS-101, Amerex Instrument Inc.) was used for the hybridization reaction. A fluorescent multi-label counter (Victor 3, PerkinElmer) was used for measuring the fluorescent signal. Electrochemical measurement was performed with a potentiostat/galvanostat (263A, Princeton Applied Research, MA) that is connected to a personal computer. The electrochemical software operating system (PowerSuite, Princeton Applied Research, MA) was used for electrochemical measurement and data analysis. The integrated SPCE chips were purchased from Gwent Inc. England. Figure 1 shows a schematic of the integrated SPCE chip, which is composed of two electrodes: carbon electrode (working electrode), and silver/silver chloride electrode (auxiliary and reference electrode). The working area is limited by a meshed well. The volume capacity of the electrochemical cell is 100 μ L.

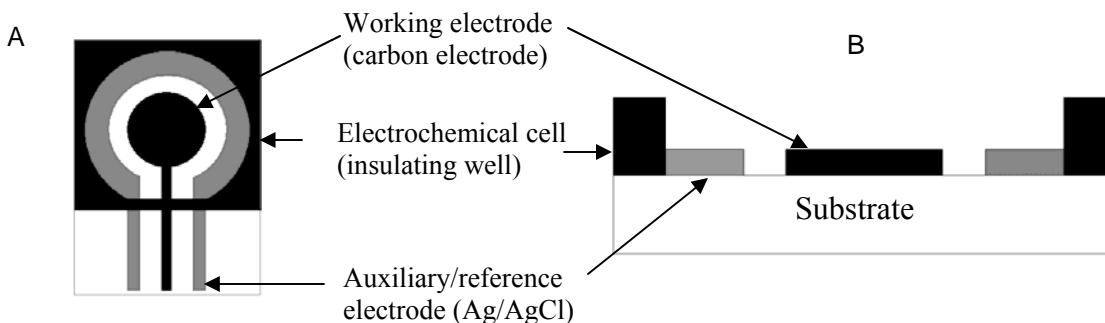


Figure 3.1. Schematic of screen-printed carbon electrode: A) top view, B) cross-section view. It is composed of working electrode (carbon electrode) and auxiliary/reference electrode (Ag/AgCl) in an insulating well.

3.3 Synthesis of Nanoparticles

Gold nanoparticles were synthesized by a chemical reduction method (Hill and Mirkin, 2006). Hydrogen tetrochloroaurate (III) trihydrate aqueous solution (1 mM, 50 mL) was prepared in a flask. The gold solution was heated while stirring on a hotplate. Once it refluxed vigorously, the solution was slowly titrated with 5 mL of 38.8 mM sodium citrate. The solution turned from yellow to clear, to black, to purple and finally deep red. The UV–VIS absorption spectrum of the AuNPs solution was measured by a UV-Vis-NIR Scanning Spectrophotometer (UV-3101PC, Shimadzu Inc.).

Nanoparticle tracers (PbS and CdS) were prepared according to the literature (Zhu, Zhang et al. 2004; Ding, Zhang et al. 2009) by using 3-mercaptopoacetic acid as a stabilizer. Briefly, 3-mercaptopoacetic acid (9.22 μL) was added to 50 mL of 0.4 mM $\text{Pb}(\text{NO}_3)_2$ solution; pH was adjusted to 7 with 0.5 M NaOH. The solution was bubbled with nitrogen for 30 min, then 1.34 mM Na_2S was dropwise added to the mixture. The reaction was carried out for 24 h under bubbled nitrogen, and then gradually a brown colloid was formed. For CdS nanoparticles, 2 μL of 3-mercaptopoacetic acid was added to 100 mL of 1 mM CdCl_2 solution; pH was adjusted to 11 using 0.5 M NaOH. The solution was bubbled with nitrogen for 30 min, then 50 mL of 1.34 mM

Na₂S was dropwise added. The reaction was carried out for 24 h under bubbled nitrogen, and a yellowish colloid was gradually formed. Both NTs were characterized using TEM.

3.4 Bacteria Culture, DNA isolation, PCR and DNA Probes

A clinical strain of *Salmonella* Enteritidis (strain S-64) and *Bacillus anthracis* Sterne strain was used in this study. The pathogen was grown following standard microbiological cultures. After enrichment, the cells were enumerated by spiral plating appropriately diluted cultures on agar. DNA isolation was performed from 1 mL of culture using the QiaAmp DNA Mini Kit (Qiagen, Valencia, CA).

The insertion element (*Iel*) gene (accession number Z83734) is chosen as the target of *Salmonella* Enteritidis because the sequence's specificity has been well studied in the literatures (Wang and Yeh 2002; Song, Ahn et al. 2005). The *pagA* gene (accession number M22589) from *Bacillus anthracis* Sterne strain will be used as the second target gene because *Bacillus anthracis* virulent strain and *Bacillus anthracis* Sterne strain have this genotypic similarity (Song, Ahn et al. 2005).

Primers and pDNAs for the insertion element (*Iel*) gene of *Salmonella* Enteritidis were as follows. The single stranded forward and reverse primers were *Iel*L-5'-CTAACAGGCGCATACGATCTGACA-3' and *Iel*R-5'-TACGCATAGCGATCT CCTTCGTT G-3'. The following thiolated oligonucleotides were used to conjugate with the nanoparticles: The first pDNA (1pDNA) on AuNPs: 5'-AATATGCTGCCTACTGCCCTACGCTT-SH-3'; the second pDNA (2pDNA) on MNPs: 5'-SH- TTTATGTAGTCCTGTATCTTCGCCGT-3' (Wang and Yeh 2002); bDNA on AuNPs: 5'-TTATTCGTAGCTAAAA AAAAAA-SH-3'(Hill and Mirkin 2006).

The primers and pDNAs of the *pagA* gene (accession number = M22589) from *Bacillus anthracis* Sterne strain were as follows: *pagAL*: 5'-AAAATGGAAGAGTGAGGGTG-3'; *pagAR*: 5'-CCGCCTTTCTACCAGATTTA-3'; 1pDNA: 5'-SH-GGAAGAGTGAGGGTGGATACAGGCT-3'; 2pDNA: 5'-AGATTTAAATCTGGTAGAAAGGCGG-SH-3' (Song, Ahn et al. 2005; Hill and Mirkin 2006).

TEX 613 ($\lambda_{\text{excitation}} = 596 \text{ nm}$, $\lambda_{\text{emission}} = 613 \text{ nm}$) was used to label the bDNA and 6 - Carboxyfluorescein (6-FAM; $\lambda_{\text{excitation}} = 495 \text{ nm}$, $\lambda_{\text{emission}} = 520 \text{ nm}$) was used to label the 2pDNA on MNPs. Both TEX 613 and 6-FAM were used to evaluate the conjugation efficiency. All oligonucleotides were synthesized by the Integrated DNA Technologies Inc. (Coralville, IA).

The PCR products were identified by gel electrophoresis and a UV transilluminator after purification. After PCR amplification, the PCR product was purified by PCR purification kits (QIAquick; QIAGEN, Valencia, CA) and diluted serially with distilled water. PCR product concentration and quality were measured with a Bio-Rad SmartSpec 3000 spectrophotometer. The serially diluted PCR products of tDNA were used as DNA samples for the experiments.

3.5 Functionalization of Nanoparticles

To ensure full reactivity, thiol-modified oligonucleotides should be reduced immediately before use. Otherwise, the thiol group on the oligonucleotides could not form a self-assembled monolayer on the surface of AuNPs due to loss of active thiol group. DTT solution (0.1 M) was prepared in the disulfide cleavage buffer (170 mM PBS buffer, pH=8.0). The thiolated oligonucleotide was suspended in 100 μL DTT solution and the solution was allowed to stand at room temperature for 2 hours. Nap-5 columns were then used for purifying the reduced thiolated oligonucleotides. The procedure was followed according to the manufacture's manual. After

purification, a UV-visible spectrophotometer was used to determine the DNA concentration. The AuNPs synthesized previously (1mL), the purified thiolated bDNA (5 nmol), and the purified thiolated 1pDNA (0.05 nmol) were then mixed together. Thiolated DNA would form a self-assembled monolayer on the surface of AuNPs. Figure 3.2 shows a schematic of the AuNPs functionalization. After a serial salt addition (Hill and Mirkin, 2006), the particles were stabilized for long-time storage at room temperature.

For the MNPs, the polyamine-functionalized iron oxide particles (1 mg) were reacted with 300 μ g of sulfo-SMCC bifunctional linker for 2 h in 1 mL coupling buffer (0.1M PBS buffer, 0.2M NaCl, pH = 7.2). The supernatant was removed after magnetic separation and the MNP-cross-linker conjugate were rinsed with the coupling buffer 3 times. The reduced thiolated 2pDNA (1 nmol) was added into 1 mL coupling buffer containing sulfo-SMCC-modified MNPs and reacted for 8 h.

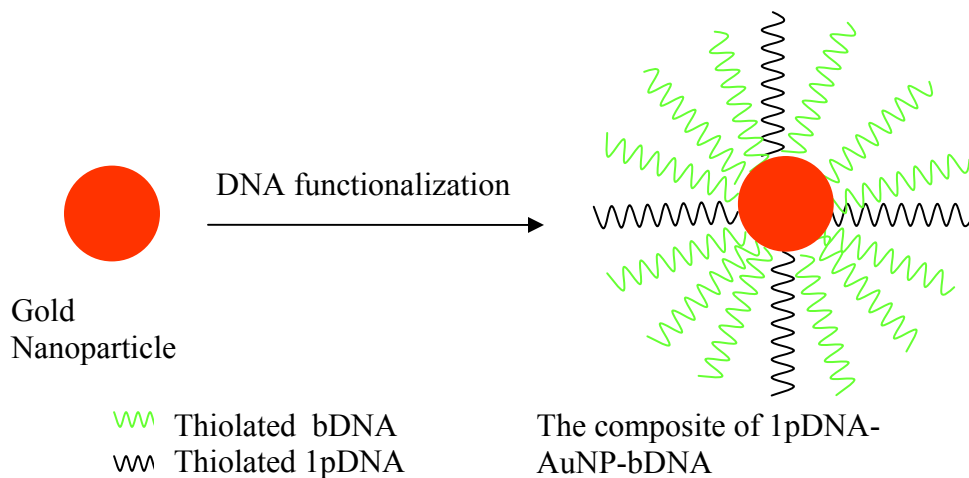


Figure 3.2. Schematic of the functionalization of AuNPs. A mixture of thiolated oligonucleotides (bDNA:1pDNA=100:1) form a self assembled monolayer on the surface of gold nanoparticles.

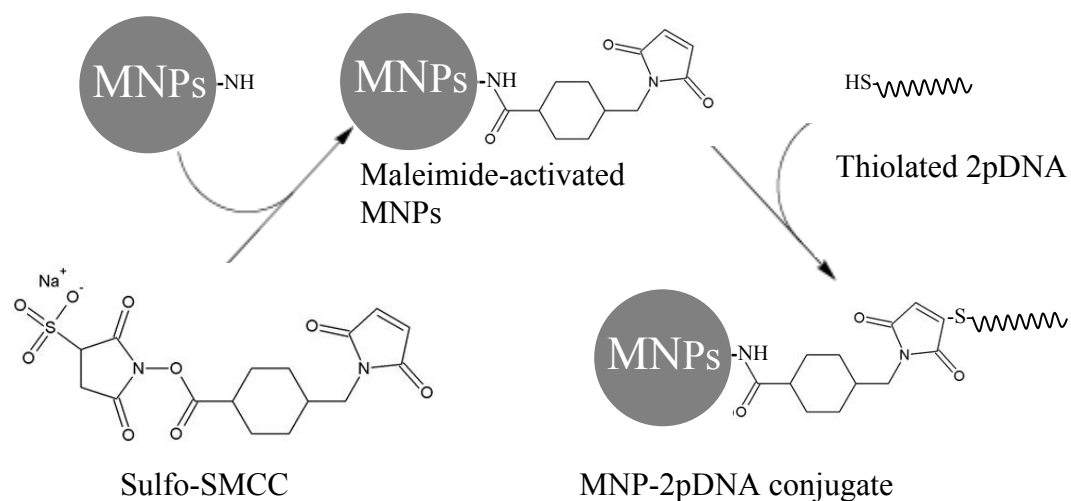


Figure 3.3. Schematic of the functionalization of MNPs. (1) formation of maleimide-activated MNPs; (2) formation of MNP-2pDNA conjugate.

Figure 3.3 shows the schematic of the MNP-pDNA conjugation. After conjugation, the pDNA-immobilized MNPs were rinsed with the coupling buffer 3 times. The unreacted pDNA in the supernatant was collected for the evaluation of conjugation efficiency. The functionalized MNPs were then suspended in 35 mL of 10 mM sulfo-NHS acetate. The solution was incubated and shaken at room temperature to block the unreacted sulfo-SMCC on the surface of MNPs. After passivation, the particles were centrifuged at 1100 g for 1 min and washed with passivation buffer (0.2M Tris, pH=8.5) and then with a storage buffer (10 mM PBS buffer, 0.2M NaCl, pH=7.4).

Fluorescein-labeled 2pDNA and bDNA were used to evaluate the conjugation efficiency. To separate the conjugates from unreacted oligonucleotides, different separation procedures were taken. After centrifuging at 12,000 g for 20 min, the fluorescence signal of the supernatant solution of 1pDNA/AuNPs/bDNA-TEX 613 was measured. The supernatant solution of MNPs/Sulfo-SMCC/2pDNA-6-FAM was measured after magnetic separation. The same

separation procedure was applied to their respective controls. Figure 3.4 shows the evaluation of conjugation efficiency: MNP- pDNA and AuNP-bDNA.

To conjugate NTs with bDNA on AuNPs, N-hydroxysuccinimide (NHS) and 1-Ethyl-3-[3-dimethylaminopropyl] carbodiimide Hydrochloride (EDC) were used to link the carboxylic group on NTs and amine group on bDNA. EDC (5 mg) was added to 25 μ L NTs, then 50 μ L of 9% NHS in dimethyl sulfoxide were added. Hydrochloride (775 μ L, pH 5) was added immediately. The reaction was carried out on a vortex mixer at room temperature for 20 min. To keep the optimal pH value of the reaction, 5 μ L of phosphate buffer (1 M NaCO₃, pH 8) was added. The solution was shaken for 8 hours at room temperature and the conjugation solution was washed with water at 12,000 g 3 times before usage.

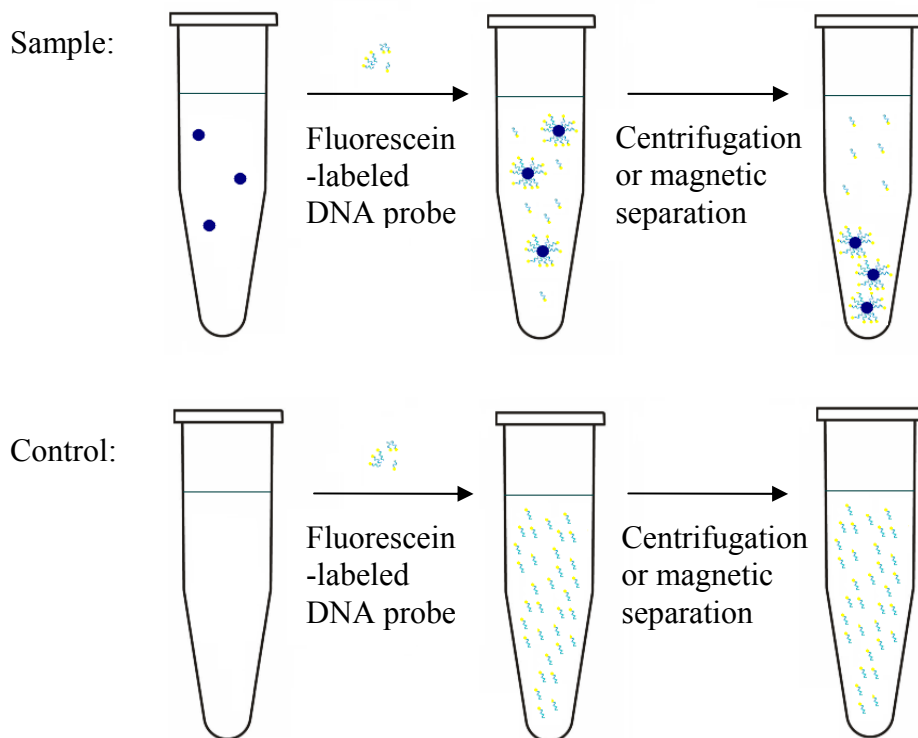


Figure 3.4 Evaluation of conjugation efficiency: MNP- pDNA and AuNP-bDNA.

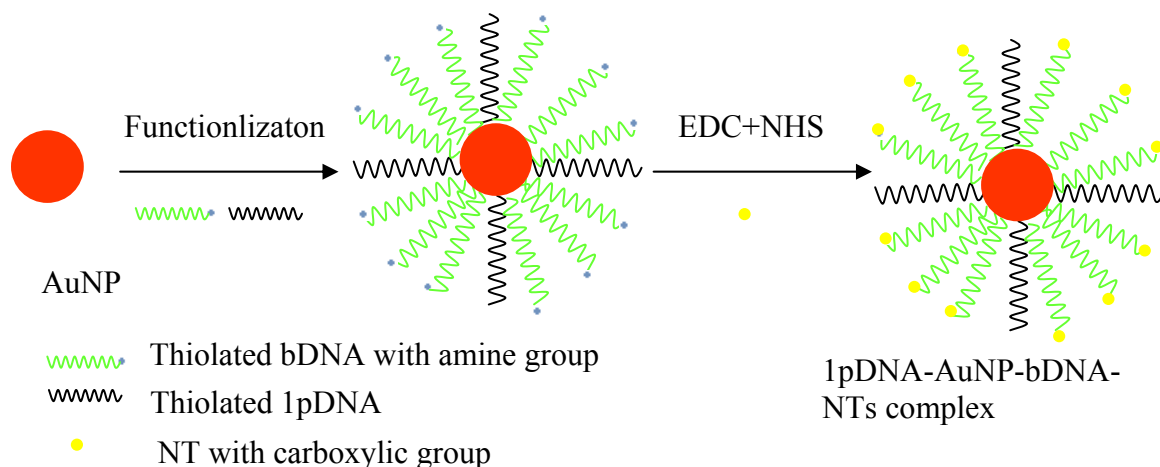


Figure 3.5. Schematic of conjugation of bio-barcoded AuNP with NTs. (1) functionalization of gold nanoparticles with thiolated bDNA and thiolated 1pDNA; (2) formation of the 1pDNA-AuNP-bDNA-NTs complex by cross-linking amine group on bDNA and carboxylic group on NTs through 1-Ethyl-3-[3-dimethylaminopropyl] carbodiimide Hydrochloride (EDC) and N-hydroxysuccinimide (NHS).

Figure 3.5 shows the schematic of the nanoparticle conjugations. After conjugation, the two functionalized 1pDNA-AuNP-bDNA-NTs for *pagA* gene and *Iel* gene were mixed in 1:1 ratio. The two 2pDNA-coated MNPs were mixed in 1:1 ratio also, for the following multiple detection. The nanoparticles then were ready for the bio-barcode assay.

3.6 Confirmation of DNA Hybridization

A solution containing tDNA in a PCR tube was put in the thermocycler at 95°C for 10 min to separate the dsDNA into ssDNA. Serially diluted DNA samples (40 μL) were mixed with 0.8 mg MNPs in 200 μL assay buffer (10mM PBS buffer, 0.15M NaCl, 0.1%SDS, pH=7.4). The hybridization reaction was maintained at a temperature of 45°C for 45 min in an incubator. After hybridization, the MNPs with DNA target were washed twice with the assay buffer, then resuspended in 200 μL of assay buffer. The functionalized AuNPs (100 μL) were centrifuged at 12,000 g for 20 min and the unreacted thiolated oligonucleotides in the supernatant were

removed. Finally the purified AuNPs complex was resuspended in 500 μL of assay buffer. The AuNPs complex (40 μL) was then added into 200 μL solution containing MNPs with DNA target. The hybridization was incubated at 45 $^{\circ}\text{C}$ for 2 h with shaking.

After the sandwich structure (MNP- 2pDNA / Target DNA / 1pDNA-AuNP-bDNA) was formed, the assay was put on the magnetic separator for 3 min and then the supernatant was removed. Unreacted solution components (DNA and AuNPs) were washed away 5 times with 500 μL of assay buffer in order to effectively remove AuNPs that were not specifically bound to the MNPs through hybridization.

Fluorescent detection of bio-barcode assay

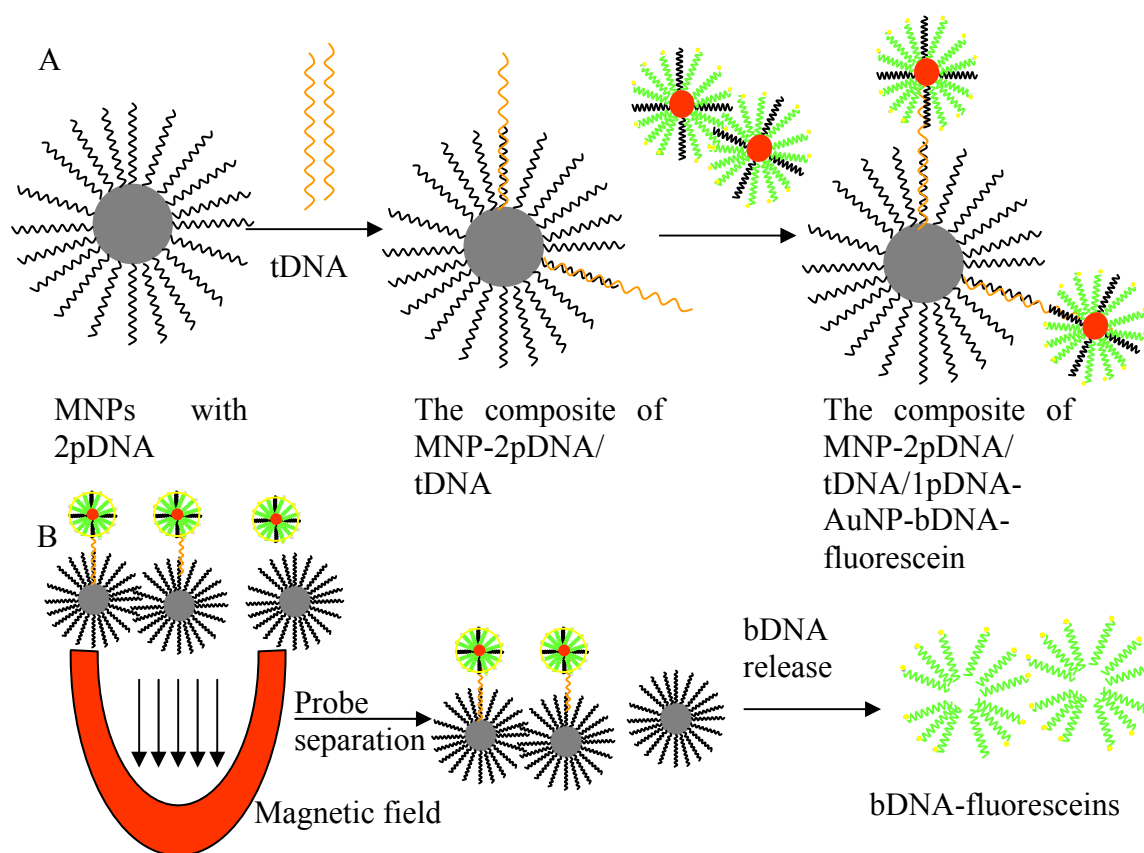


Figure 3.6. Schematic of the fluorescent bio-barcode assay: A) formation of MNP-2pDNA/tDNA/1pDNA-AuNP-bDNA-fluorescein; B) bDNA-fluorescein separation and release.

The MNP-target-AuNP complex was resuspended in 200 μL of 0.5M DTT solution. To release the bDNA from the surface of AuNPs, the complex was incubated at 50°C for 15 min, and then 45 min at 25°C under vortex. After magnetic separation and centrifugation, the released bDNA was ready for fluorescent measurement. Figure 3.6 shows a schematic of the fluorescent bio-barcode assay.

Gold Nanoparticle-based Electrochemical Biosensor Detection

The MNP-target-AuNP sandwich complexes were measured by differential pulse voltammetry (DPV) on SPCE under the optimum accumulation time. The potential was scanned from 1.25V to 0.0V with a step potential of 10 mV, modulation amplitude of 50 mV, and scan rate of 33.5 mV/s (Pumera, Aldavert et al. 2005). Figure 3.7 shows the schematic of the electrochemical detection of AuNPs. Following oxidative gold metal dissolution in an acidic solution, the released Au^{3+} ions were reduced on SPCE and indirectly quantified by differential pulse voltammetry (DPV). A potentiostat/galvanostat

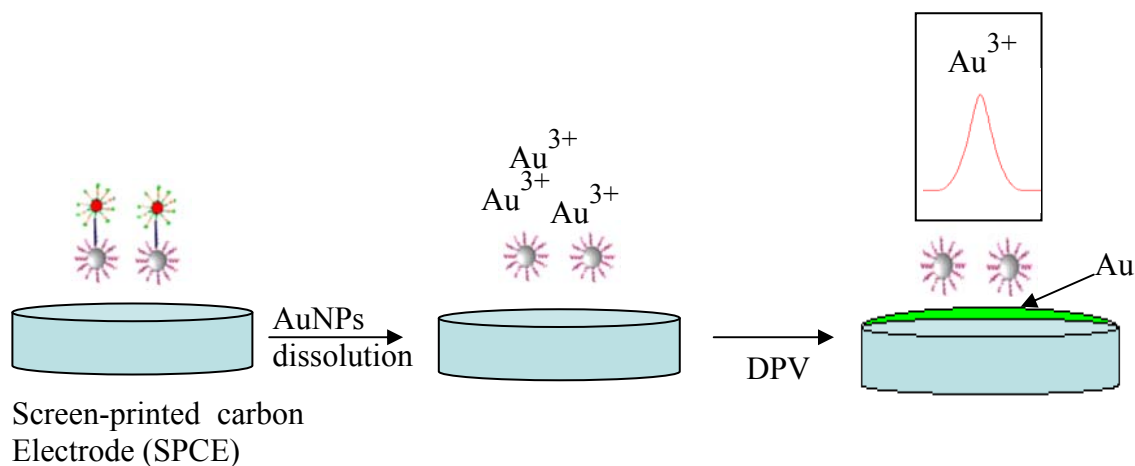


Figure 3.7. Schematics of electrochemical measurement of AuNPs. It is composed of 2 steps: AuNP dissolution on the SPCE and DPV measurement of Au^{3+} .

with PowerSuite software (Princeton Applied Research, TN) was used for electrochemical measurement and data analysis.

3.7 Electrochemical Validation and Optimization of the Biosensor

Cyclic voltammetry was performed using a potentiostat/galvanostat (263A, Princeton Applied Research, MA) in the presence of dissolved oxygen. The screen-printed electrode was connected to the potentiostat/galvanostat with a specially adapted electrical edge connector. The scanning potential was between -0.4 V and 0.6 V at a scan rate of 50 mV/s.

Stripping voltammetric measurements were performed with an in situ deposition of the bismuth film and target metals in the presence of dissolved oxygen. Studies were carried out by dropping a 100 μ L of sample solution in the well. Each electrochemical measurement was carried out in triplicate. A deposition potential of -1.2 V vs. Ag/AgCl was applied to the carbon working electrode without solution stirring. After deposition, the voltammogram was recorded by applying a positive-going square-wave voltammetric potential scan (with a frequency of 20 Hz, amplitude of 25 mV, and potential step of 5 mV). The scan was from -1.2 V to 0.0 V. To evaluate the reusability of electrochemical sensors, a conditioning step at +0.3 V without solution stirring was used to remove the target metals and bismuth prior to the next cycle. Bare SPCE sensors without in situ bismuth film coating were employed for comparison, with measurement procedures similar to those employed with the bismuth film-coated electrodes (with the exception of using bismuth (III)). All experiments were carried out at room temperature.

3.8 Electrochemical analysis

Stripping voltammetric measurements were performed with an in situ deposition of the

bismuth film and NT ions in the presence of dissolved oxygen. Studies were carried out by dropping a 100 μL of the sample solution in the well. A deposition potential of -1.2 V vs. Ag/AgCl was applied to the carbon working electrode without stirring the solution. After deposition, the voltammogram was recorded by applying a positive-going square-wave voltammetric potential scan (with a frequency of 20 Hz, amplitude of 25 mV, and potential step of 5 mV). The scan was from -1.2 V to 0.0 V (Wang, Lu et al. 2000). Based on our previous optimization studies, 1 mg/L of bismuth and 10 min of deposition time were used for all SWASV measurements. All experiments were carried out at room temperature. Figure 3.8 shows the electrochemical test systems.

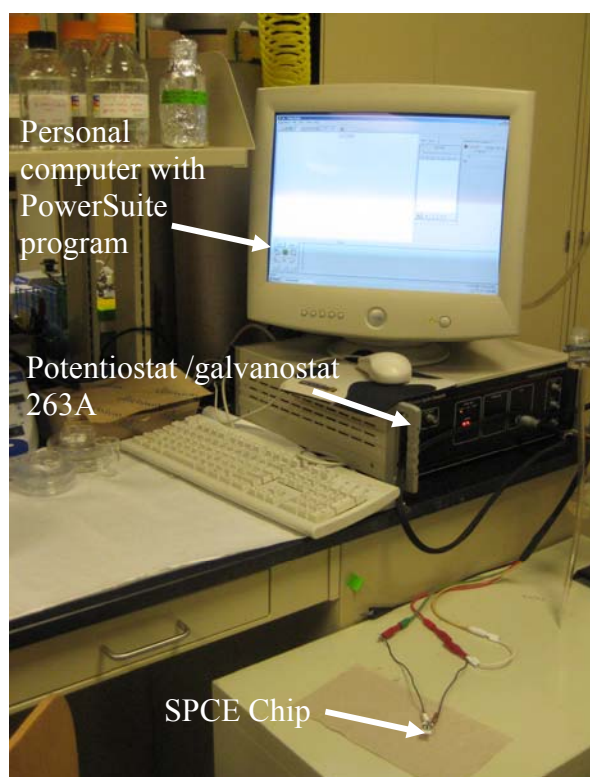


Figure 3.8. The composition of the electrochemical detection system: personal computer with PowerSuite program, potentiostat/galvanostat 263A, and a SPCE chip.

CHAPTER 4: RESULTS AND DISCUSSION

4.1 Characterization of Nanoparticles

The AuNP dimension and spectroscopic properties were characterized by using a transmission electron microscope (TEM) and a UV-Vis-NIR scanning spectrophotometer respectively. Figure 4.1A shows a transmission electron microscopy (TEM) image of our synthesized AuNPs with an average diameter of 15 nm. The dimension of AuNPs is homogenous. Figure 4.1B shows the absorption peak of the AuNPs at 519 nm wavelength. After one month storage in the room temperature, the AuNPs did not aggregate and their spectroscopic absorbance property was stable.

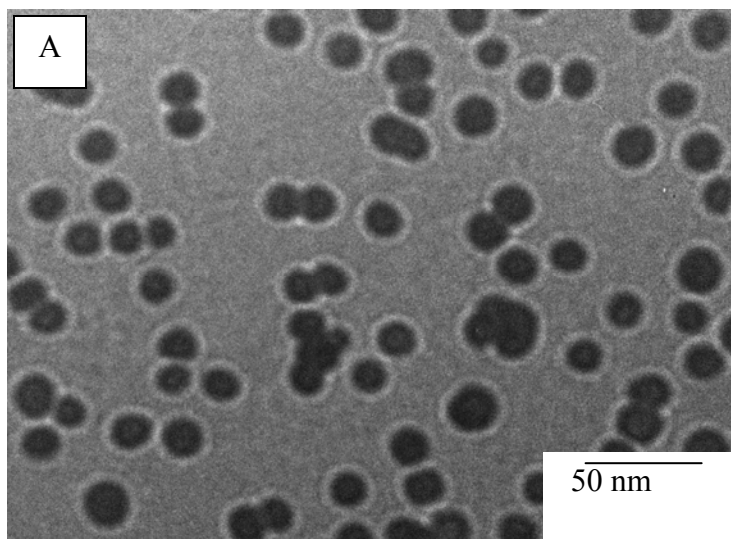


Figure 4.1 (cont'd)

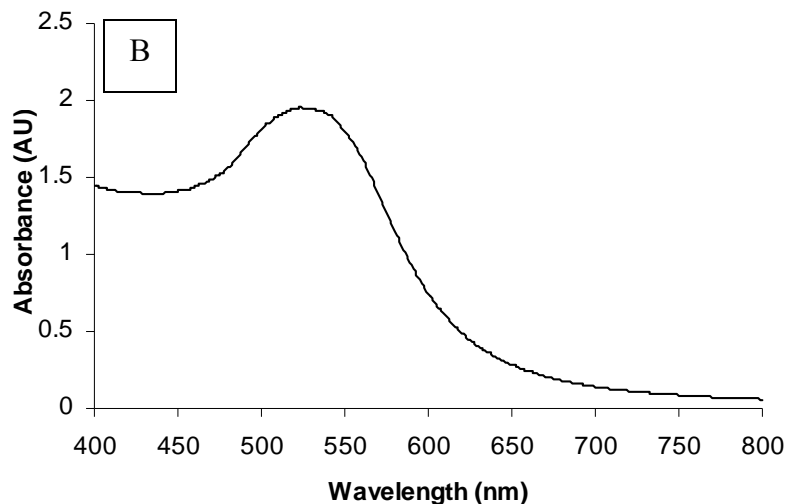


Figure 4.1. Characterization of AuNPs: A) TEM image of AuNPs, showing an average of 15 nm in diameter; B) Absorbance spectrum of AuNPs at 519 nm.

Figure 4.2 shows a TEM image of our synthesized CdS nanoparticles with an average diameter of 7 nm, and PbS nanoparticles with an average diameter of 3 nm. After one month of storage at 4°C, the CdS and PbS NTs were stable and did not aggregate.

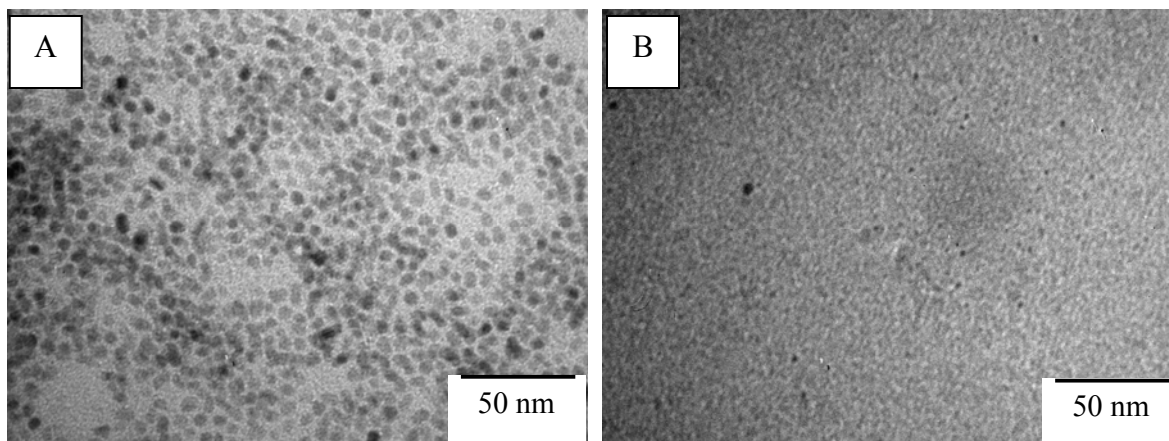


Figure 4.2. TEM images of NTs: A) CdS, showing an average diameter of 7 nm; B) PbS, showing an average diameter of 3 nm.

4.2 Functionalization of Nanoparticles

The 6-FAM labeled 2pDNA was used for confirming the functionalization of MNPs. Two controls were taken for evaluation of the conjugation efficiency. One was only the 6-FAM pDNA, and the other was 6-FAM pDNA and MNPs without sulfo-SMCC cross-linker. If the conjugation is efficient, less unconjugated 6-FAM labeled pDNAs will be left in the supernatant solution after magnetic separation.

Table 4.1 shows that the 6-FAM labeled bDNA has the highest fluorescence signal because there are no MNPs in the solution. Magnetic separation has no effect on it. Without sulfo-SMCC as a cross-linker in solution, the pDNA is not conjugated to the MNPs, hence the magnetic separation will not remove the 6-FAM labeled pDNA. However, some of the pDNA in solution could be washed out during magnetic separation; hence a decrease in fluorescence signal is observed. After adding sulfo-SMCC into the conjugation reaction, the conjugation efficiency improved greatly and the fluorescence signal decreased markedly. The result shows sulfo-SMCC worked as an efficient cross-linker to conjugate the thiolated oligonucleotides and amine-coated MNPs. Because the synthesized AuNPs have a peak absorbance at 519 nm, in order to avoid its interference with the excitation wavelength (520 nm) of 6-FAM, another fluorescent dye (TEX 613) was used to confirm the functionalization of AuNPs. The unconjugated TEX 613 labeled

Table 4.1. Fluorescence signal of supernatant solution for evaluation of conjugation efficiency between MNPs and 2pDNA.

	MNPs + Sulfo-SMCC + 6-FAM DNA	MNPs + 6-FAM DNA (Control 2)	6-FAM DNA (Control 1)
Fluorescence (0.1s) (Counts)	72735	293003	368146
Standard deviation	248.7	821.9	1942.1

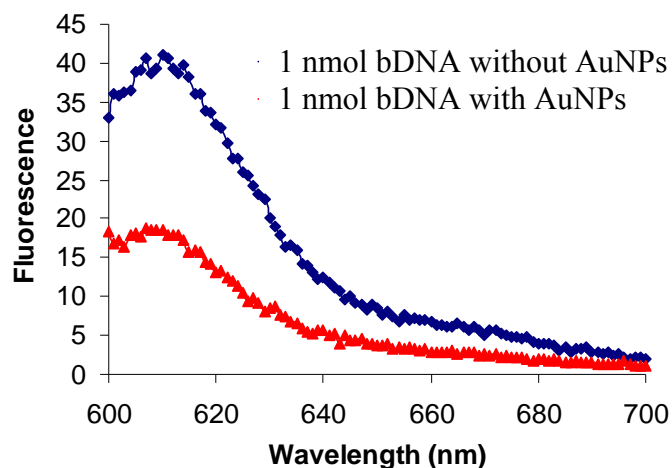


Figure 4.3. Fluorescence signal of supernatant solution for evaluation of conjugation efficiency between AuNPs and bDNA.

bDNA was left in the supernatant solution after centrifugation at 12,000 g for 20 min. The control was the TEX 613 labeled bDNA in the same buffer solution without AuNPs.

Figure 4.3 shows that almost half of the thiolated bDNA has been immobilized on the surface of AuNPs. The bio-barcoded AuNPs were found to be stable in solution in terms of non-aggregation. This phenomenon is probably because the negatively charged bDNA repels each other. Hence no aggregation occurs even at long storage time. The solution of bio-barcoded AuNPs retained its deep red color under room temperature for over a month, demonstrating stability of conjugation. On the contrary, the AuNPs in the solution without pDNA aggregated to larger particles and precipitated finally under the same buffer condition.

Confirmation of the functionalization of MNPs and AuNPs was accomplished in our previous publication (Zhang, Carr et al. 2009). 1-Ethyl-3-[3-dimethylaminopropyl] carbodiimide Hydrochloride (EDC) and N-hydroxysuccinimide (NHS) were used to crosslink the carboxylic group on NTs and the amine group on bio-barcoded AuNPs.

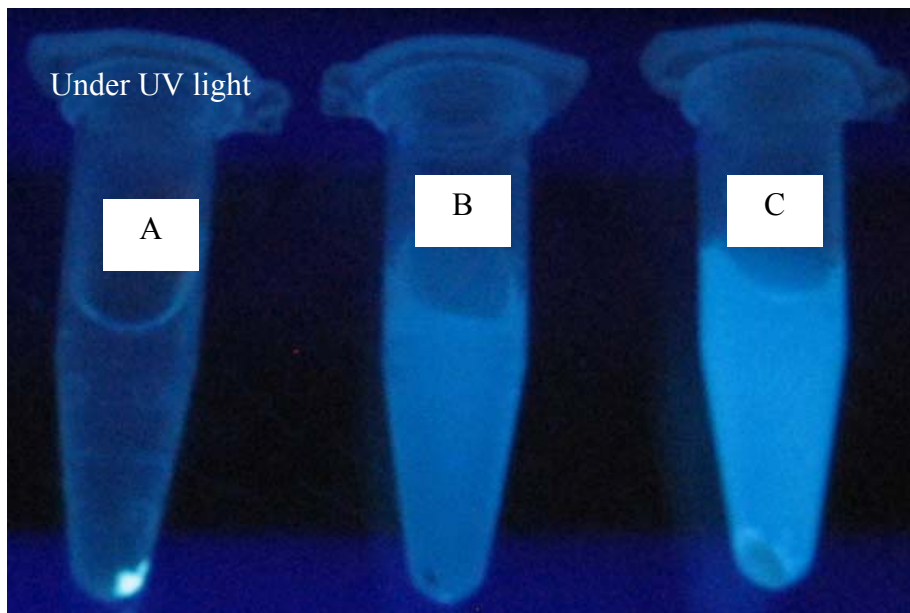
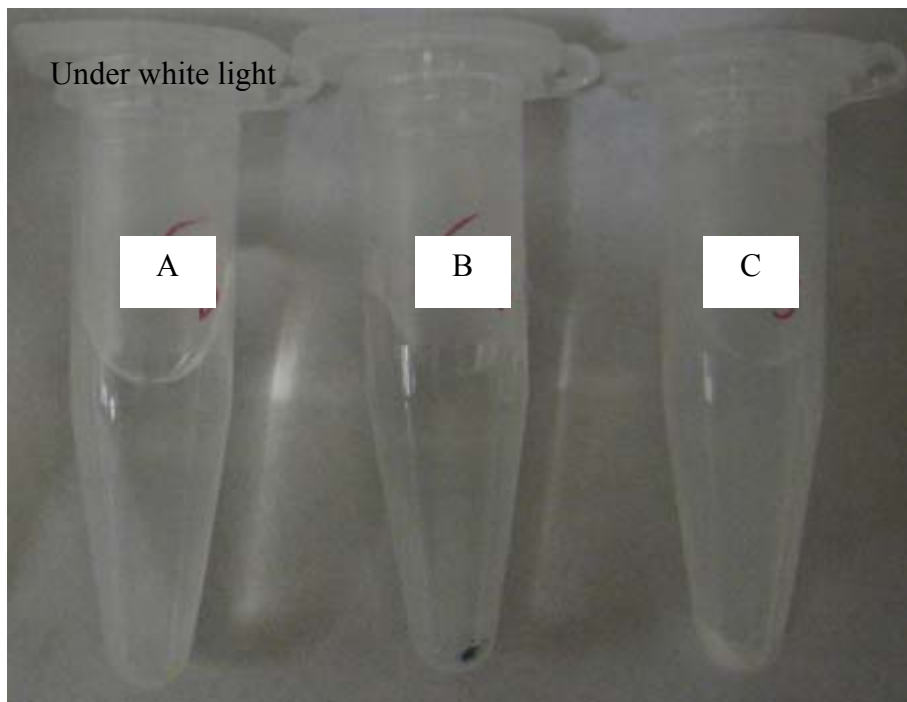


Figure 4.4. Confirmation of conjugation of NTs and AuNPs. Three test tubes labeled A, B, C are under white light and UV light after centrifugation at 12,000 g for 30 min. (Tube A: bio-barcode AuNPs, NTs, EDC, and NHS; tube B: bio-barcode AuNPs and NTs; tube C: NTs only).

Figure 4.4 shows 3 test tubes labeled A, B, C after centrifugation at 12,000 g for 30 min. Tube A contains bio-barcode AuNPs, NTs, EDC and NHS. Tube B and C are two controls.

Tube B has no cross linker while tube C only contains CdS NTs. There is a pellet that shows yellowish fluorescence under UV light in tube A. After the centrifugation, the conjugated particles become larger and are easier to be precipitated. Most of the NTs are conjugated with AuNPs and are precipitated in the bottom and show the fluorescence signal under UV light. In tube B, there is a red pellet under white light in the bottom, while the solution shows yellowish fluorescence under UV light. It shows that without cross linkers, the NTs and bio-barcoded AuNPs can not be conjugated. The AuNPs are larger and can be precipitated at 12,000 g so that we can see the red pellet under white light, while the NTs are smaller and still suspend in solution, showing the fluorescence in the solution under UV light. Tube C shows that centrifugation does not precipitate the NTs. The results show that conjugation of NTs and bio-barcoded AuNPs has been successful.

4.3 Fluorescent Detection Using Bio-barcode Assay

Figure 4.5 shows that the fluorescence signal of released bDNA has an exponential growth relationship with different concentrations of tDNA. At a concentration of 10 $\mu\text{g/mL}$ tDNA, the fluorescence signal has an average count of 5711. The signal linearly increases with increasing concentration of tDNA.

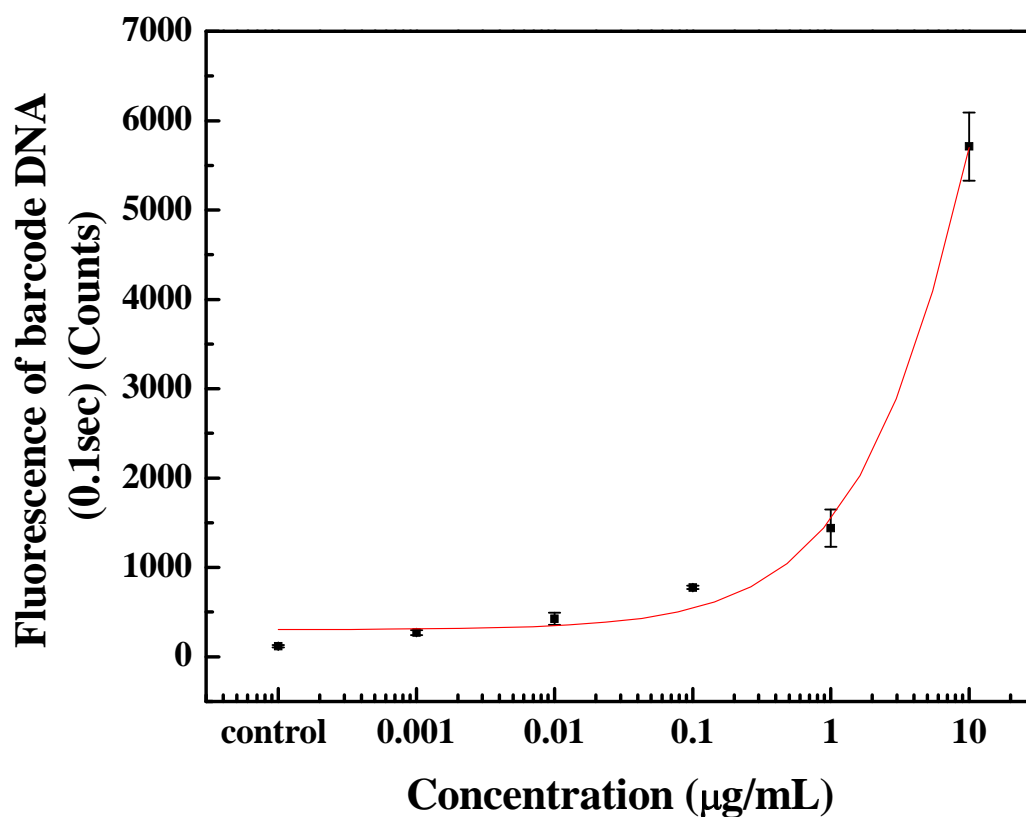


Figure 4.5. The fluorescence signal of released bDNA with different concentrations of tDNA.

Table 4.2. The relationship between tDNA and the fluorescence signal of released bDNA

Sample Concentration (µg/mL)	10	1	0.1	0.01	0.001	0
Fluorescence reading (counts)	5711	1440	777	426	270	117
3 * Standard Deviation (±)	380.88	209.16	18.52	67.26	28.84	12.01

Table 4.2 shows the mean and variance of the signal. The results show that the assay can detect as low as 1 ng/mL tDNA (or 2.15×10^{-16} mol).

4.4 Electrochemical Validation and Characterization of SPCE Chips

Cyclic voltammetry of ferricyanide on SPCE chips

Cyclic voltammetry (CV) was performed as the initial electroanalytical technique for the electrochemical characterization of the sensor surface due to its versatility and relative ease in measurement. A well characterized redox couple (ferrocyanide/ ferricyanide) was used to explore the electrochemical nature of the electrode surface. Figure 4.6 shows a cyclic voltammogram obtained on the electrochemical sensor covered by 100 μL unstirred solution of 5 mM ferricyanide. The ratio of the peak anodic current to the peak cathodic current was 0.95. The peak separation was much larger than the predicted value of the reversible voltammetric response and increased with scan rate. The results suggest that voltammetric response on the electrochemical sensor can be classed as irreversible.

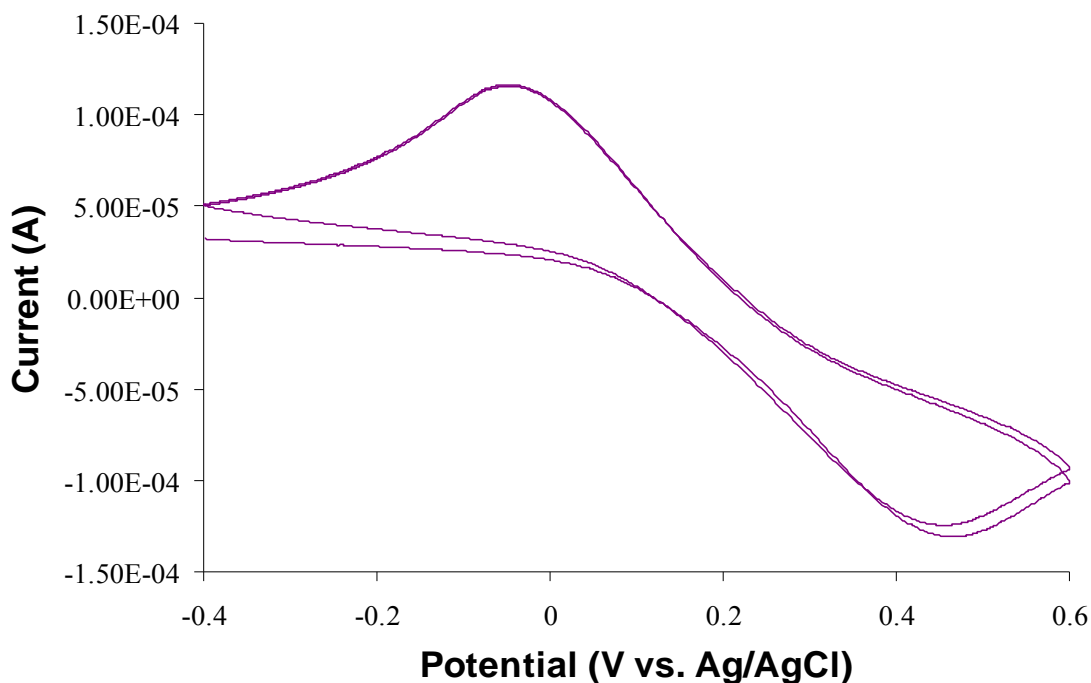


Figure 4.6. Cyclic voltammogram of bare SPCE sensor in a 5mM $\text{K}_3\text{Fe}(\text{CN})_6$ solution with 1M KCl. Scan rate is 50mV/s.

Reusability test

To avoid the interference from the residue of target metals and/or bismuth during the test of reusability, various cleaning time (10s, 30s, 1 min) was applied after each SWASV measurement. After 30 sec of cleaning, there was no oxidative signal of lead(II) and bismuth on the stripping voltammogram. The result showed that 30 sec was enough to oxidize and remove all bismuth and metal ions from the surface of the electrochemical sensor. Five milligrams per liter of lead(II) solution was then used to evaluate the reusability of the bismuth film-coated SPCE sensor and bare SPCE sensor.

Figure 4.7 shows that the bismuth film coating improves peak current height of SWASV of lead(II), compared to the bare SPCE sensor. When both electrodes were reused, the peak current of lead(II) decreased gradually.

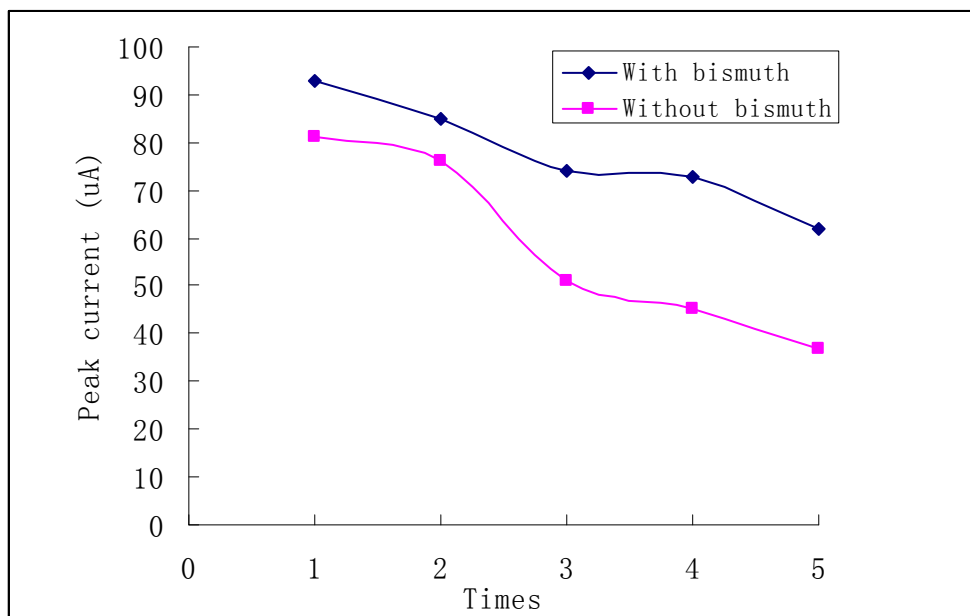


Figure 4.7. The repeatability test of 1 mg/L of bismuth film-coated SPCE sensor and bare SPCE sensor. Deposition: -1.2 V for 10 min; SWASV scan from -1.2 V to 0.0 V, frequency 20 Hz, amplitude 25 mV, and potential step 5 mV, at room temperature and in nonstirred solution.

When they were used for 5 times, the signal from bismuth film-coated SPCE sensor was only 66.7% compared to the first measurement; the signal from the bare SPCE sensor was 45.7% of that at the first time. The results show that the electrochemical sensor, with or without bismuth film coating, is only good for one-time disposable use in SWASV measurement of heavy metal.

Optimization of deposition time

The following parameters were optimized in order to perform the simultaneous determination of lead(II) and cadmium(II) on electrochemical sensors: deposition potential, concentration of bismuth(III) co-deposited in situ with the target metals (lead and cadmium), and deposition time. Deposition potential was chosen as -1.2V because further reduction of the deposition potential (to -1.4 V) would result in diminished stripping peak heights, multiple stripping peaks, and increased background current due to the hydrogen evolution (Reeder and Heineman 1998). Therefore, deposition potential of -1.2V was used in all subsequent SWASV measurement.

For the co-deposition of bismuth (III) ions with the target metals, the electrochemical sensor worked as a substrate on which a metallic film of bismuth was formed. The deposition of the bismuth film depends on its ion concentration and deposition (preconcentration) time. Various concentrations of bismuth (III) were chosen for co-deposition onto the bare SPCE sensor with 5 mg/L of lead(II) at -1.2 V for 2 min of deposition time. Figure 4.8 shows the lead(II) reoxidation peak on electrochemical sensors under various concentrations of bismuth ion. The peak currents increased when the concentrations of bismuth ion increased from 0.1 mg/L to 1 mg/L, because more bismuth was available for co-deposition with lead(II) and improved the stripping signal of lead(II). When the concentration of bismuth was increased to 10 mg/L, beyond the

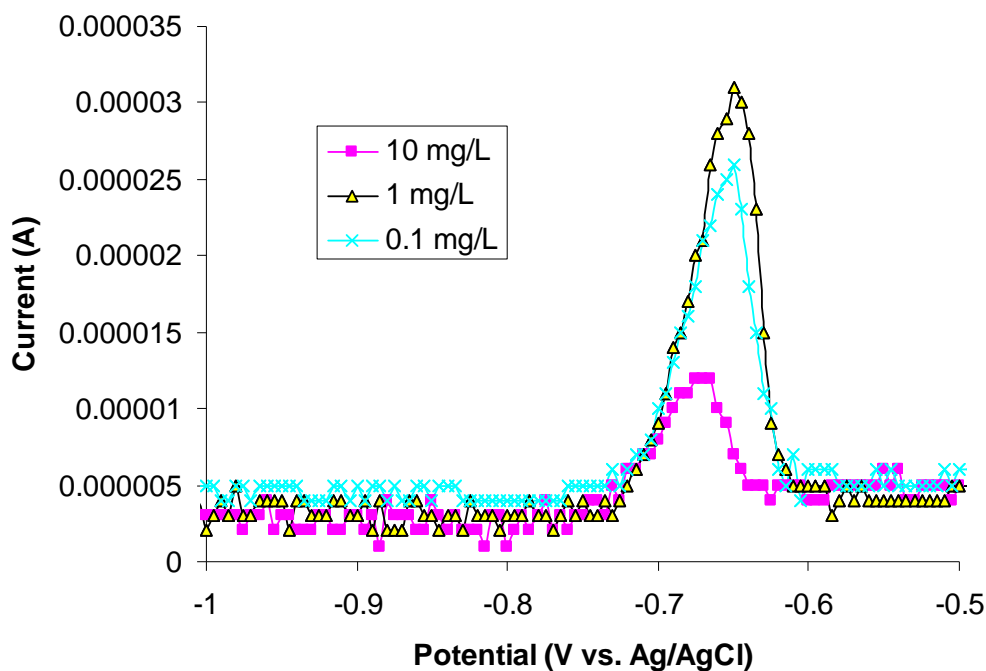


Figure 4.8. Stripping voltammogram of 5 mg/L of lead(II) with various concentrations of bismuth on electrochemical sensor after 2 min deposition at -1.2 V. SWASV scan from -1.2 V to 0.0 V, frequency 20 Hz, amplitude 25 mV, and potential step 5 mV, at room temperature and in nonstirred solution.

solubility of bismuth in 0.1 M acetate buffer (pH 4.5), precipitation interfered with the co-deposition and lowered the stripping signal of lead(II). So the 1 mg/L of bismuth was used for subsequent SWASV measurements.

The longer the deposition step, the larger is the amount of analyte available on the electrode during the stripping analysis. Increasing the deposition time resulted in increased signal (height of peak current) for both the lead(II) and bismuth stripping waves due to the increased amount of lead ion and bismuth ion reduced on the electrode surface. Kadara and Tothill reported that the diffusion of ions was accelerated under stirring condition and deposition times between 60 and 90 s were sufficient to obtain well defined stripping peaks for lead(II) at this solution concentration (Kadara and Tothill 2004). However, in order to detect a 100 μ L sample on an

electrochemical sensor, stirring the solution is not practical so that extra deposition time is needed.

Figure 4.9 shows that the peak currents of lead(II) increased rapidly with deposition time in the interval from 1 to 45 min. The signal from 10 min deposition is roughly twice compared to the 1 min deposition. For longer deposition time above 10 min, the peak current response of all electrodes decreased gradually and the wave of lead(II) reoxidation became wider. This result is potentially due to a change in reference electrode potential and the formation of intermetallic compounds after excessive deposition. So 10 min of deposition time was used in the subsequent experiments.

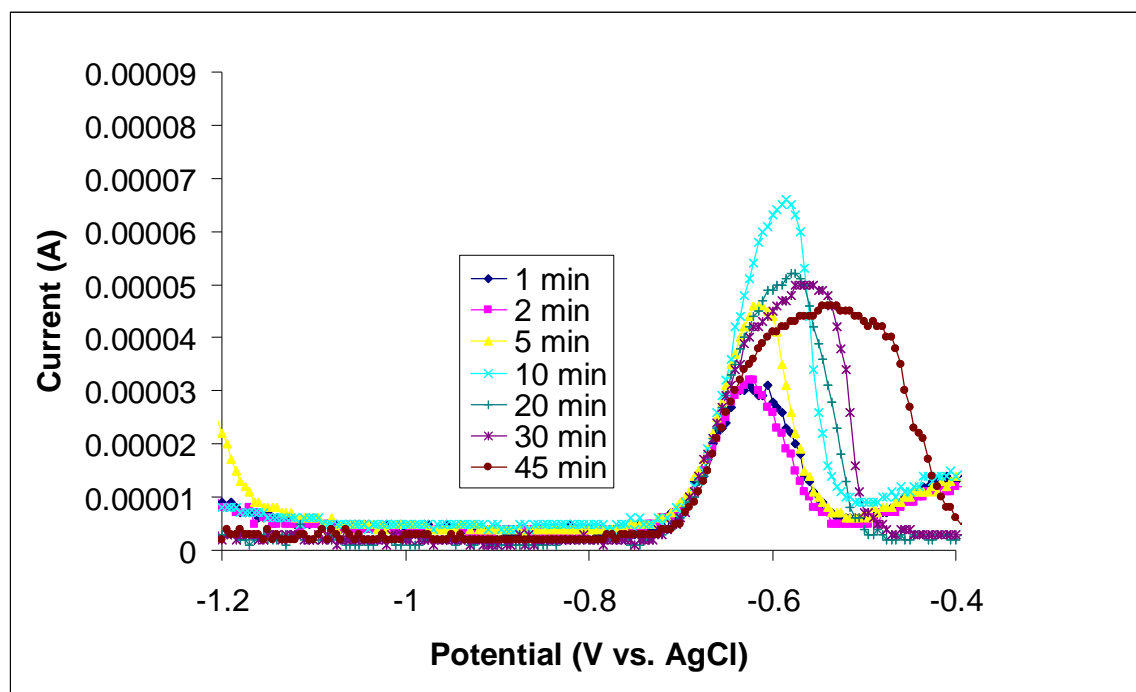


Figure 4.9. Stripping voltammogram on bismuth film-coated SPCE sensors with various deposition times. Deposition at -1.2 V; SWASV scan from -1.2 V to 0.0 V, frequency 20 Hz, amplitude 25 mV, and potential step 5 mV, at room temperature and in nonstirred solution.

SWASV measurement of lead and cadmium

Because the unimpeded diffusion to the bismuth-solution interface is available during the reoxidation step, theoretically, sharper and better defined stripping peaks are expected on bismuth film-coated SPCE sensors compared to bare SPCE sensors. However, both bismuth film-coated SPCE sensors and bare SPCE sensors generated sharp and well-defined stripping peaks in this study. Figure 4.10 shows well-defined sharp peaks over a flat baseline on bismuth film-coated SPCE sensors, following 10 min of deposition. Peak currents of various lead(II) concentrations (0.5 mg/L, 2 mg/L and 5 mg/L) are 36 μA , 51 μA , and 75 μA , respectively. Peak currents of various cadmium(II) concentrations (0.5 mg/L, 2 mg/L and 5 mg/L) are 37 μA , 48 μA , and 74 μA , respectively. Bismuth shows a peak current around 39 μA at -0.26 V vs. Ag/AgCl.

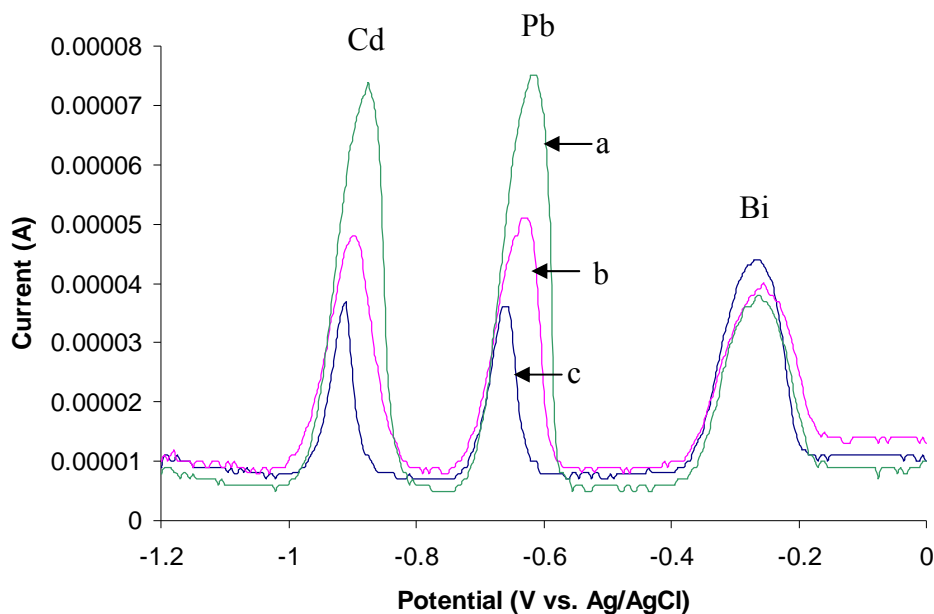


Figure 4.10. Stripping voltammogram of a mixture of lead(II) and cadmium(II) on bismuth film-coated SPCE sensors (a: 5 mg/L lead(II) and 5 mg/L cadmium(II); b: 2 mg/L lead(II) and 2 mg/L cadmium(II); c: 0.5 mg/L lead(II) and 0.5 mg/L cadmium(II)). Deposition: -1.2 V for 10 min; SWASV scan from -1.2 V to 0.0 V, frequency 20 Hz, amplitude 25 mV, and potential step 5 mV, with 1mg/mL bismuth, at room temperature and in nonstirred solution.

Figure 4.11 shows the stripping voltammograms for lead(II) and cadmium(II) obtained on bare SPCE sensors. Peak currents of various lead(II) concentrations (0.5 mg/L, 2 mg/L and 5 mg/L) were 20 μ A, 40 μ A, and 67 μ A, respectively. Peak currents of various cadmium(II) concentrations (0.5 mg/L, 2 mg/L and 5 mg/L) were 15 μ A, 30 μ A, and 40 μ A, respectively. When the concentration of lead(II) and cadmium(II) was 0.1 mg/L, there was no current peak in stripping voltammogram on both bare SPCE sensors and bismuth film-coated SPCE sensors (data not shown). The background noise was around 7 μ A for both metal ions on bismuth film-coated and bare SPCE sensors.

Figure 4.12 shows that the stripping performance for the same concentration of lead(II) on bare SPCE sensors exhibited a roughly comparable peak to that obtained on bismuth film-coated

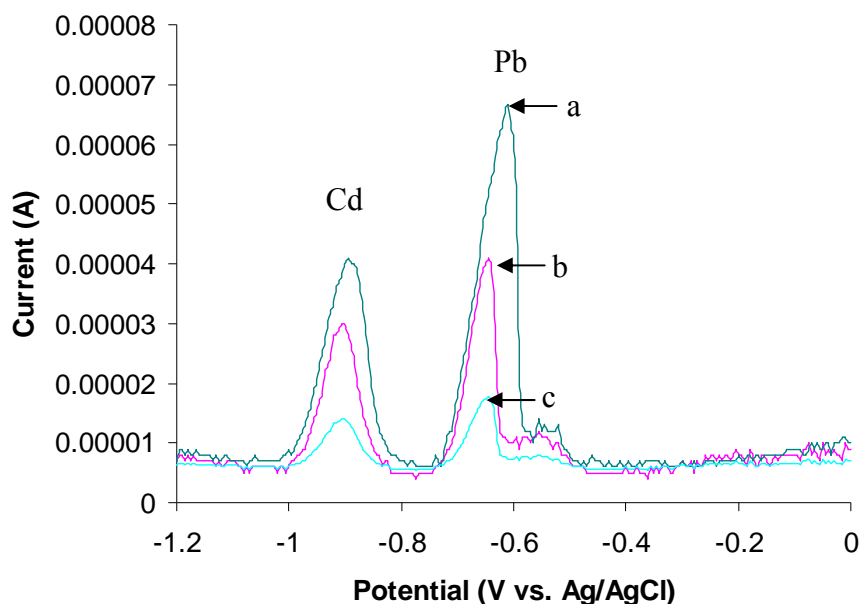


Figure 4.11. Stripping voltammogram of a mixture of lead(II) and cadmium(II) on bare SPCE sensors. (a: 5 mg/L lead(II) and 5 mg/L cadmium(II); b: 2 mg/L lead(II) and 2 mg/L cadmium(II); c: 0.5 mg/L lead(II) and 0.5 mg/L cadmium(II)). Deposition: -1.2 V for 10 min; SWASV scan from -1.2 V to 0.0 V, frequency 20 Hz, amplitude 25 mV, and potential step 5 mV, with 1mg/mL bismuth, at room temperature and in nonstirred solution.

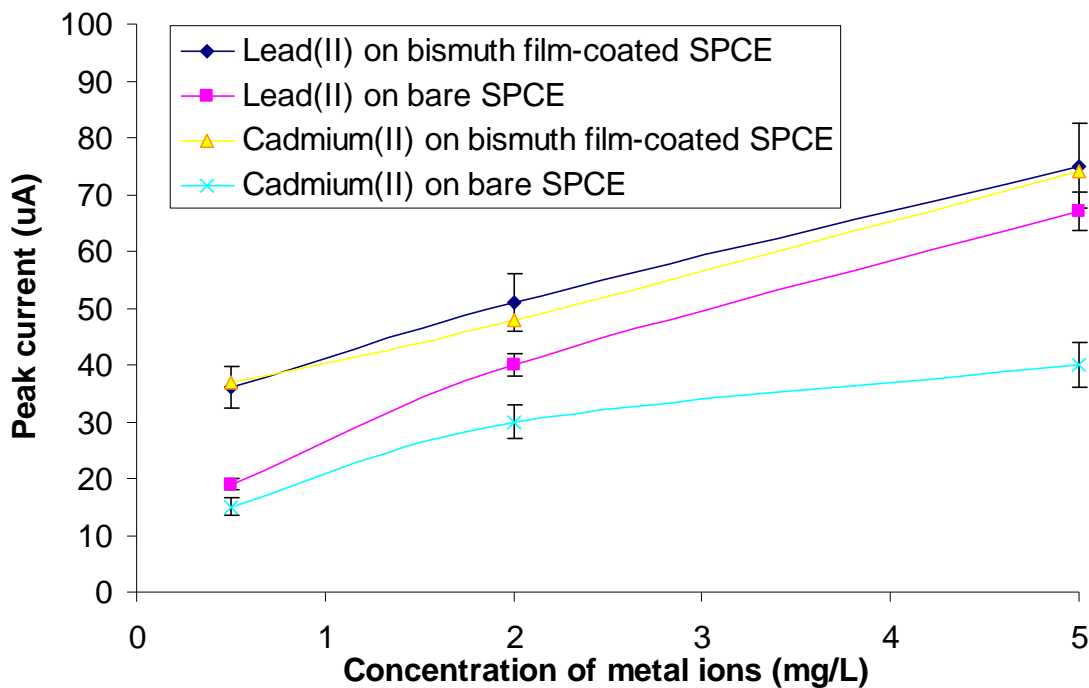


Figure 4.12. The peak currents of stripping voltammogram with different concentrations of lead(II) and cadmium(II).

SPCE sensors. However, the stripping performance for the same concentration of cadmium(II) on bare SPCE sensors exhibited a much lower peak to that of bismuth film-coated SPCE sensors. When the signal/noise was greater than 3, we concluded that the detection limits of cadmium(II) were 0.5 mg/L on bismuth film-coated SPCE sensors and 2 mg/L on bare SPCE sensors in 100 μ L of sample solution. The detection limits of lead(II) were 0.5 mg/L on bismuth film-coated SPCE sensors and 0.5 mg/L on bare SPCE sensors in 100 μ L of sample solution. Cadmium(II) detection benefited from the addition of bismuth.

4.5 Detection of AuNPs on SPCE Chips

CV of unmodified AuNPs on SPCE

Compared with conventional electrodes, screen-printed carbon electrodes have several advantages, such as simplicity, convenience, low cost and the avoidance of contamination between samples (Susmel, Guilbault et al. 2003; Miscoria, Desbrieres et al. 2006). Biosensors based on screen-printed carbon electrode (SPCE) have been extensively used for the detection of glucose (Guan, Li et al. 2005; Xu, Li et al. 2005), cholesterol (Carrara, Shumyantseva et al. 2008), antigens (Kim, Seo et al. 2006) and DNA (Ruffien, Dequaire et al. 2003; Hernandez-Santos, Diaz-Gonzalez et al. 2004).

Oligonucleotide-functionalized AuNPs were used as signal indicators in this study because of their ease of fabrication, greater oligonucleotide binding capabilities, stability under a variety of

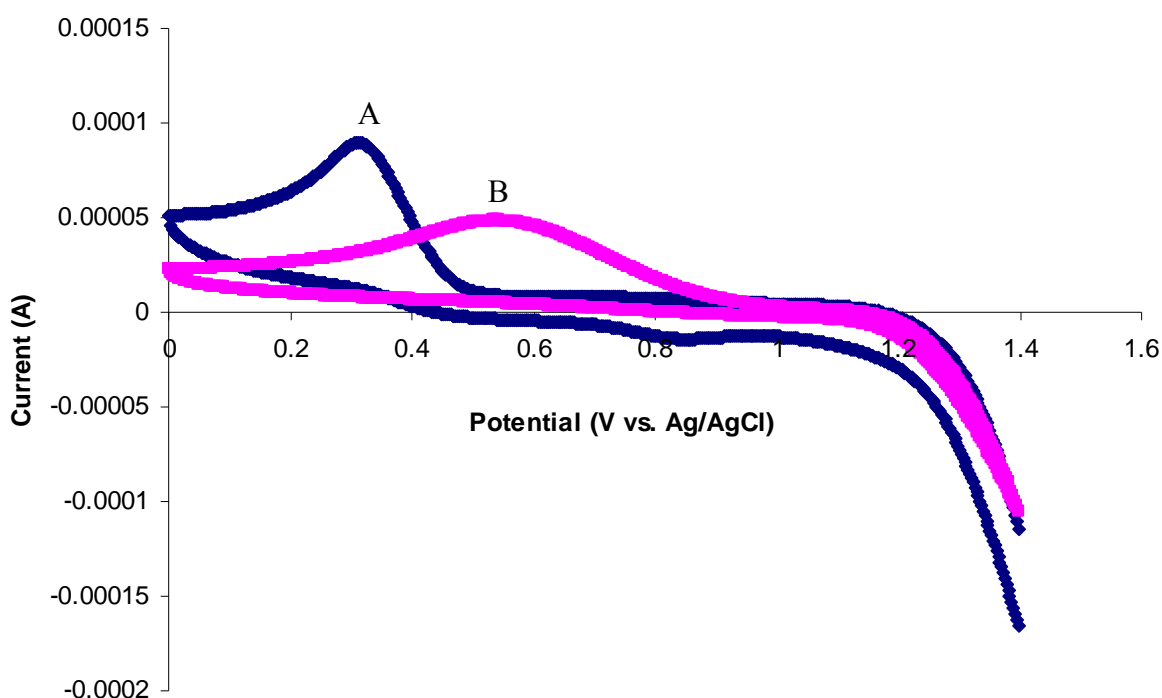


Figure 4.13. Cyclic voltammogram of unmodified AuNPs (1.17×10^{-8} M) on SPCE. : (A) AuNPs in 0.1M HCl; (B) 0.1 M HCl. CV scan from 1.4V to 0.0, scan rate 100 mV/s after 1.25 V electrooxidation for 2 min.

conditions, and good electrochemical properties (Demers, Ostblom et al. 2002; Lytton-Jean and Mirkin 2005).

Figure 4.13B shows that when there is no AuNPs, the carbon electrode is oxidized when performing oxidative procedure at 1.25V for 2 min. The carbon electrode can produce a reduction peak at 0.58 V. When the AuNPs exist in the solution, the AuNPs are oxidized instead of the carbon electrode under 1.25V for 2 min. The curve (Figure 4.13A) shows that there is a reduction peak of Au^{3+} at 0.35 V. Meanwhile, the background signal at 0.58 V from the carbon electrode is suppressed greatly by AuNPs. The possible reason is that the surface of SPCE is covered by a self-assembled layer of AuNPs due to physical adsorption. The SPCE is protected by AuNPs and this prevents the electrooxidation process from proceeding on the carbon electrode surface.

Optimization of detection of probe modified-AuNPs

The accumulation time is the time from dropping the sample on the SPCE to the beginning of electrochemical detection. It is an important factor for the electrochemical measurement of AuNPs because more AuNPs would be adsorbed on the SPCE surface when the accumulation time is longer. The electrooxidation process would generate more Au^{3+} ions in the solution, which could be translated to a higher DPV signal and thus improve the biosensor sensitivity.

The sample solution was dried after 20 min at room temperature. The drying allowed most of the AuNPs to adsorb physically on the SPCE surface. Then 100 μL of 0.1M HCl was added again for DPV measurement. Figure 4.14 shows the DPV current for 0, 10, 20 min of accumulation times. Figure 4.14A has 20 min of accumulation time which allows for more AuNPs to be reduced or oxidized, leading to a comparatively high signal. With 10 min and 0 min accumulation times, peak current are at 0.86 mA and 0.36 mA, respectively. They are only 72%

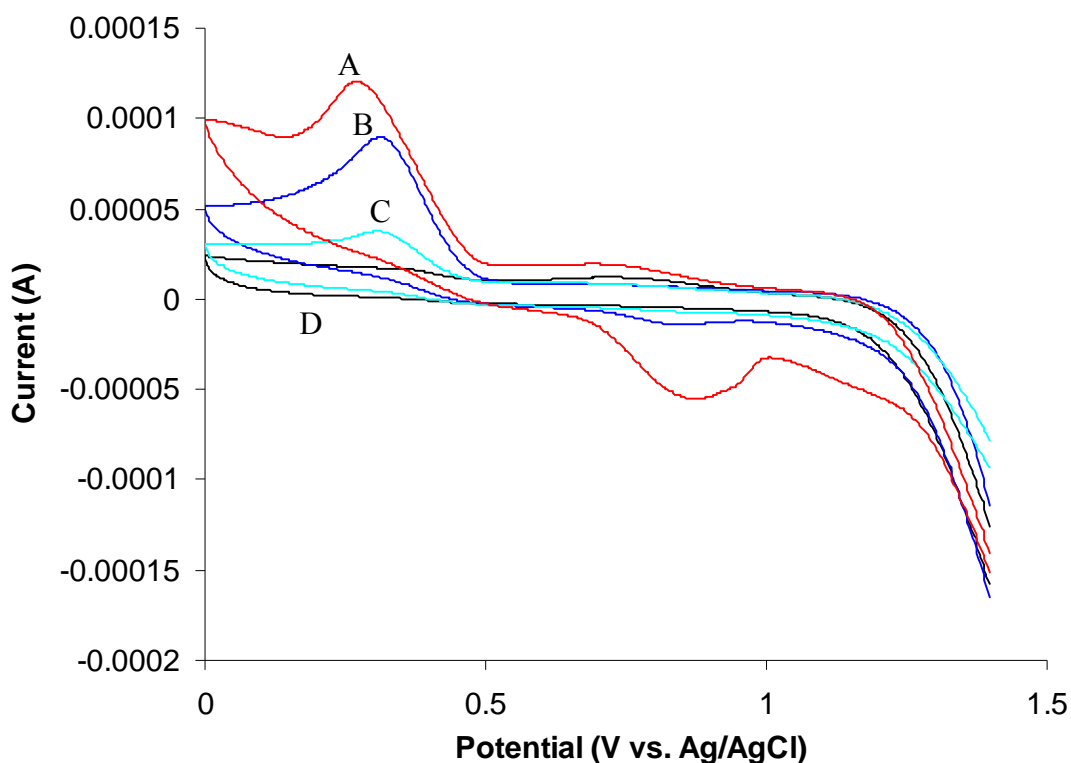


Figure 4.14. Cyclic voltammogram of probe-modified AuNPs in 0.1 M HCl on SPCE: (A) accumulation for 20 min; (B) accumulation for 10 min; (C) no accumulation; (D) control, no AuNPs and no accumulation. Conditions: electrooxidation potential, +1.25 V; electrooxidation time, 2 min, CV scan from +1.4 V to 0 V, scan rate 100 mV/s, nonstirred solution.

and 30% of the reduction peak current at 1.21 mA for the 20 min accumulation time. Drying led to more AuNPs available on the surface of SPCEs, resulting in the higher sensitivity of SPCE biosensors. Accumulation time of 20 min was used for the succeeding DPV detection of the DNA sandwich complex.

DPV detection of DNA sandwich complex

Figure 4.15 shows the DPV response of the sandwich complex (MNP-2pDNA/tDNA/1pDNA-AuNPs) after hybridization for various tDNA concentrations (0.7-700

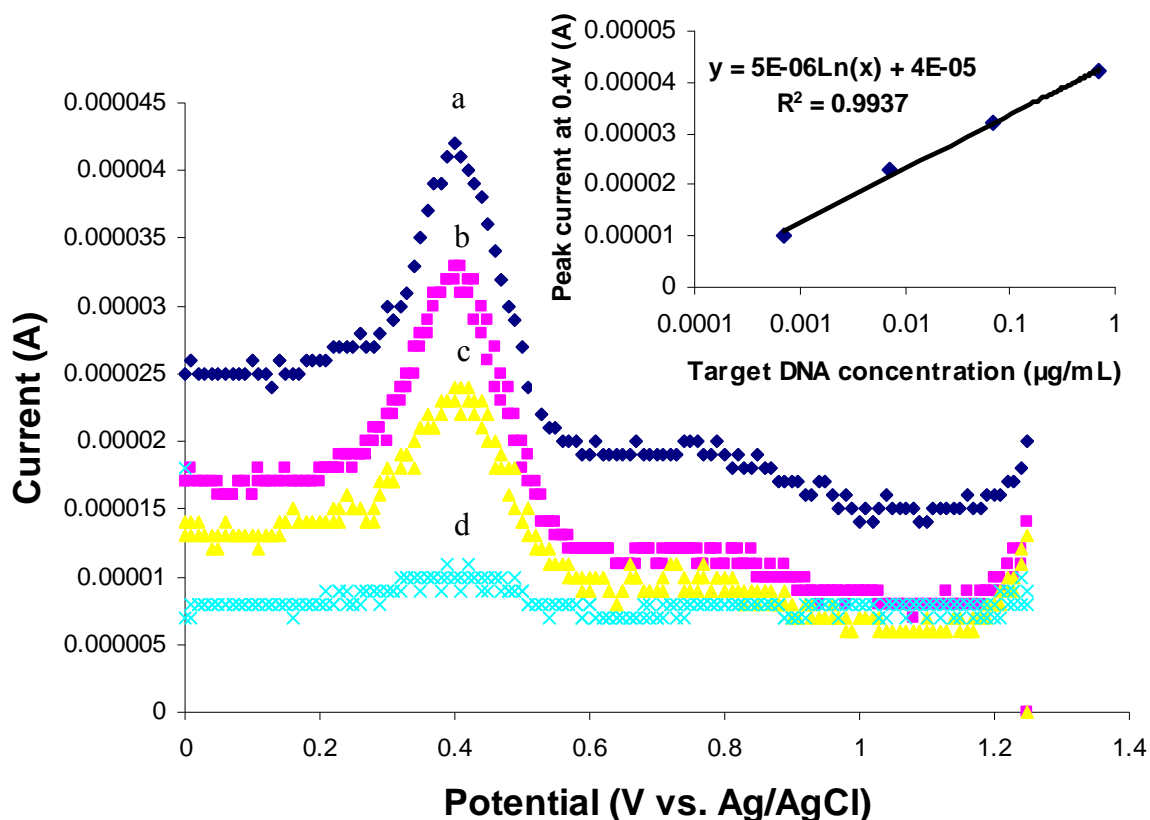


Figure 4.15. DPV hybridization response of different concentrations of DNA targets on SPCE (a: 700 ng/mL; b: 70 ng/mL; c: 7 ng/mL; d: 0.7 ng/mL) and the calibration plot between peak current and the tDNA concentration (inset). DPV scan from +1.25 V to 0 V, step potential 10 mV, modulation amplitude 50 mV, scan rate 50 mV/s, and nonstirred solution.

ng/mL). Following oxidative gold metal dissolution in the acidic solution, the Au^{3+} was reduced at the potential around 0.4V (vs. Ag/AgCl) on the SPCE. Inset shows that the peak current has a log-linear relationship with increasing concentrations of tDNA. The detection limit is 0.7 ng/mL of tDNA.

4.6 Biosensor Detection of Single Target DNA

Figure 4.16 is a schematic showing the bio-barcode assay. After immobilization of oligonucleotides on the surface of nanoparticles, both nanoparticles can bind with the tDNA to form a sandwich structure, due to the specificity of pDNA. Figure 4.16A shows the tDNA sample hybridizing with the pDNA on the MNPs, forming a MNP-2pDNA/tDNA complex (middle picture). Then bio-barcoded AuNPs are added to form a sandwich structure consisting of MNP-2pDNA/tDNA/1pDNA-AuNP-bDNA (picture on the right). After hybridization is complete, the NTs on the bDNA are released in 1M nitric acid and the metal ions are measured with SWAPV on the SPCE DNA sensor (Figure 4.16B).

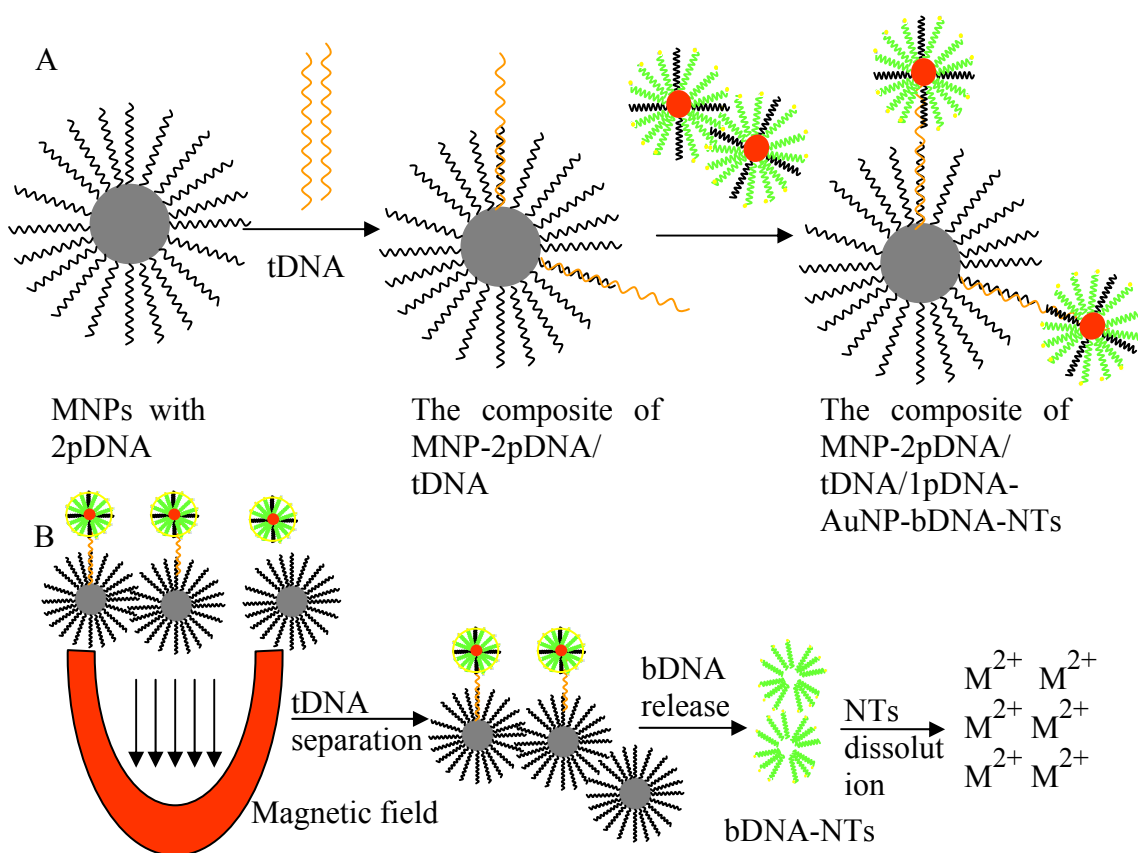


Figure 4.16. Schematic of the bio-barcode assay. (A) formation of MNP-2pDNA/tDNA/1pDNA-AuNP-bDNA-NTs sandwich structure; (B) tDNA separation and tracer dissolution.

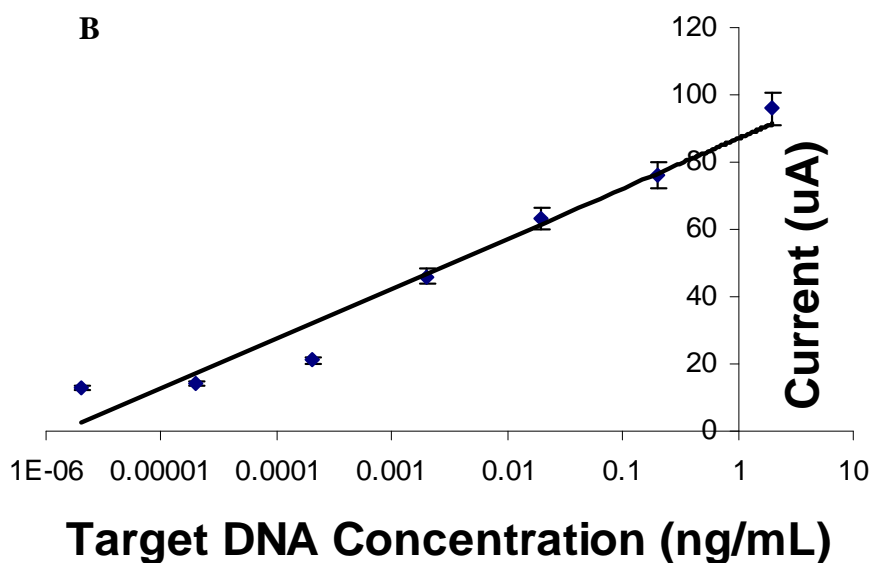
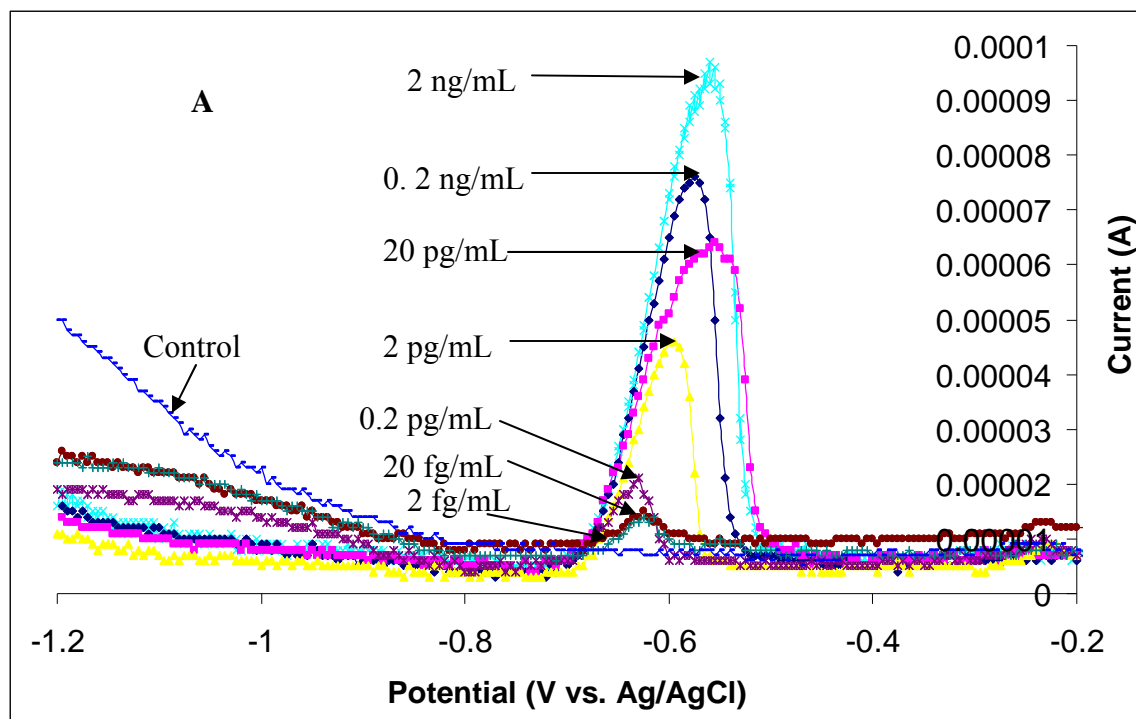


Figure 4.17. Single detection of various concentrations of *pagA* gene from *Bacillus anthracis* with the bio-barcode biosensor using PbS NTs. (A) stripping voltammogram of various concentrations of *pagA* gene from *Bacillus anthracis*; (B) the relationship of tDNA concentration and peak current. Conditions: deposition at -1.2 V for 10 min; SWASV scan from -1.2 V to 0.0 V, frequency 20 Hz, amplitude 25 mV, and potential step 5 mV, with 1mg/mL bismuth, at room temperature and in nonstirred solution.

Figure 4.17 shows the electrochemical signal of Pb^{2+} from *pagA* gene from *Bacillus anthracis* in single target detection. The peak currents of various tDNA concentrations (2 ng/mL, 0.2 ng/mL, 20 pg/mL, 2 pg/mL, 0.2 pg/mL, 0.02 pg/mL, 2 fg/mL, and 0.2 fg/mL) are 96 μA , 76 μA , 63 μA , 46 μA , 21 μA , 14 μA , and 13 μA respectively. The biosensor shows that the sensitivity of single detection of *pagA* gene from *Bacillus anthracis* is 0.2 pg/mL or 200 fg/mL.

4.7 Biosensor Detection of Multiplex Target DNA

Figure 4.18A is a schematic showing the multiple bio-barcode assay. After immobilization of oligonucleotides on the surface of nanoparticles, both nanoparticles can bind with the tDNAs to form a sandwich structure due to the specificity of pDNA. First, the tDNA samples hybridize with the pDNA on the MNPs, forming a MNP-2pDNA/tDNA complex (middle picture). Then the 1pDNA-AuNP-bDNA-NTs complex is added to form a sandwich structure consisting of MNP-2pDNA/ tDNA/1pDNA-AuNP-bDNA-NTs. After hybridization is complete, the NTs on the bDNA are released in 1M nitric acid and the NT ions are measured by SWASV on the SPCE chip. Figure 4.18B shows that SWASV measurements are performed with an in situ deposition of the bismuth film and target metals (Pb and Cd) in the presence of dissolved oxygen using a potentiostat/galvanostat.

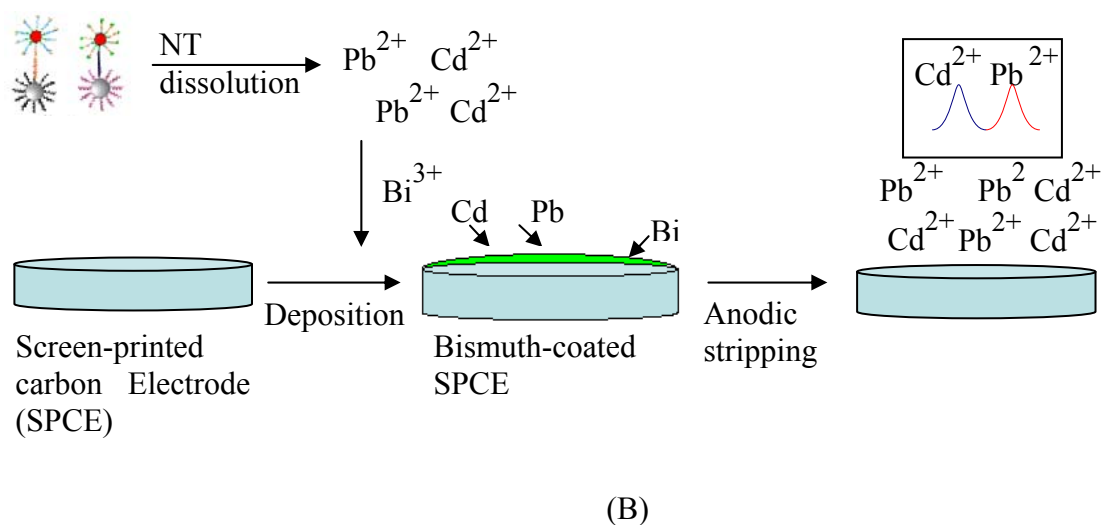
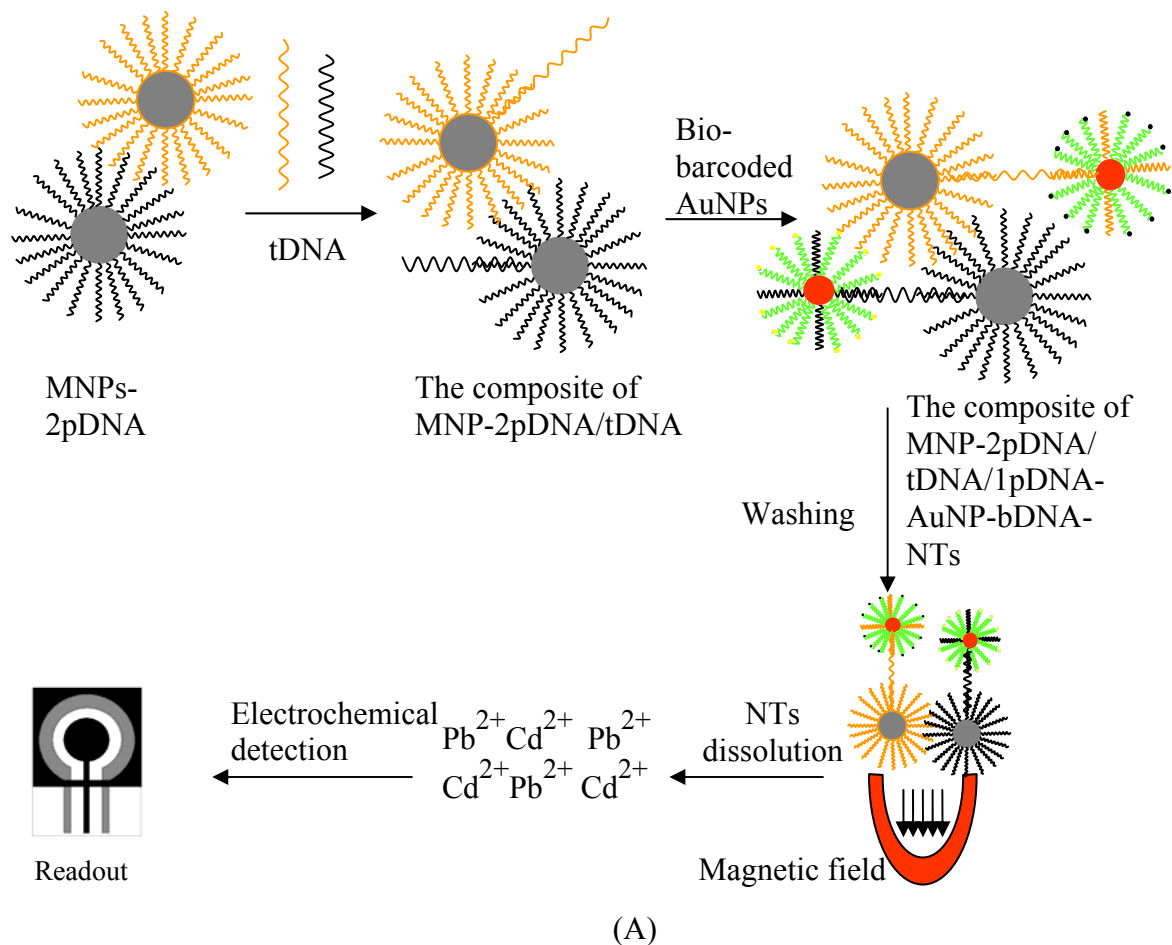


Figure 4.18. Schematic of the multiple bio-barcode biosensor: A) bio-barcode assay; B) SWASV measurement.

Figure 4.19 shows the electrochemical signal of released NT ions (Pb^{2+} and Cd^{2+}) and the specificity of the biosensor. When there is only 0.05 $\mu\text{g/mL}$ of *pagA* gene from *Bacillus anthracis*, the stripping voltammogram shows a current peak of 39 μA at -0.61 V from dissolved Pb^{2+} , and no peak at -0.87 V (Figure 4.19A). When there is only 0.05 $\mu\text{g/mL}$ of the insertion element (*Iel*) gene of *Salmonella* Enteritidis, the stripping voltammogram shows a current peak of 46 μA at -0.87 V from dissolved Cd^{2+} , and a small peak at -0.61 V (Figure 4.19B).

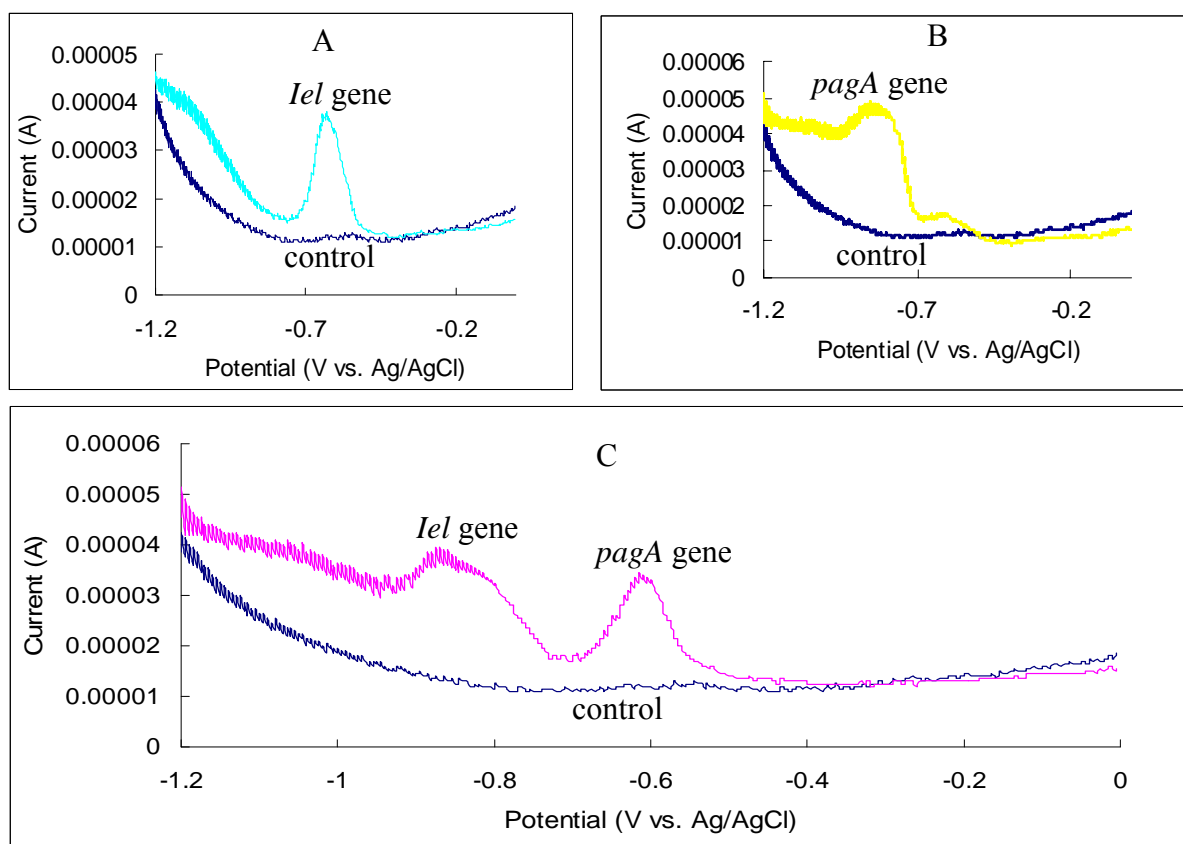


Figure 4.19. Specificity test of the multiple bio-barcode biosensor using distilled water as control. (A) control and 0.05 $\mu\text{g/mL}$ of the insertion element (*Iel*) gene of *Salmonella* Enteritidis; (B) control and 0.05 $\mu\text{g/mL}$ of *pagA* gene from *Bacillus anthracis*; (C) control and a mixture of 0.05 $\mu\text{g/mL}$ of the insertion element (*Iel*) gene and 0.05 $\mu\text{g/mL}$ of *pagA* gene. Conditions: deposition at -1.2 V for 10 min; SWASV scan from -1.2 V to 0.0 V, frequency 20 Hz, amplitude 25 mV, and potential step 5 mV, with 1mg/mL bismuth, at room temperature and in nonstirred solution.

The possible reason would be that the washing steps were not thorough and the unreacted PbS NTs generate the noise. When the sample contains no tDNA, there are no stripping signal at -0.61 V (Pb^{2+}) and -0.87 V (Cd^{2+}). When the sample contains 0.05 $\mu\text{g/mL}$ of the *pagA* gene from *Bacillus anthracis* and the insertion element (*Iel*) gene of *Salmonella* Enteritidis, the peak current at -0.61 V (vs. Ag/AgCl) is 35 μA and the peak current at -0.87 V (vs. Ag/AgCl) is 39 μA , respectively (Figure 4.19C). The results show that this bio-barcode DNA sensor has a good specificity. It can differentiate *pagA* gene from *Bacillus anthracis* (labeled with CdS) and *Iel* gene of *Salmonella* Enteritidis (labeled with PbS) when the concentration of tDNA is relatively high.

Figure 4.20 shows the sensitivity of the biosensor. For the detection of the *pagA* gene from *Bacillus anthracis*, the peak currents at -0.61 V (vs. Ag/AgCl) of various concentrations (50 ng/mL, 5 ng/mL, 500 pg/mL, and 50 pg/mL) are 38 μA , 34 μA , 29.5 μA , and 23 μA , respectively. For the detection of the insertion element (*Iel*) gene of *Salmonella* Enteritidis, the currents at -0.87 V at various tDNA concentrations (50 ng/mL, 5 ng/mL, 500 pg/mL, and 50 pg/mL) are 42.5 μA and 35 μA , 32 μA , and 27 μA , respectively. Figure 4.20B shows that the stripping signal of released Pb^{2+} and Cd^{2+} have a linear relationship with the logarithmic concentrations of tDNA. The signal increases with increasing logarithmic concentration of tDNA. The results show that the detection limit of this bio-barcode DNA sensor is as low as 50 pg/mL (lowest concentration tested) of tDNAs using CdS and PbS NTs.

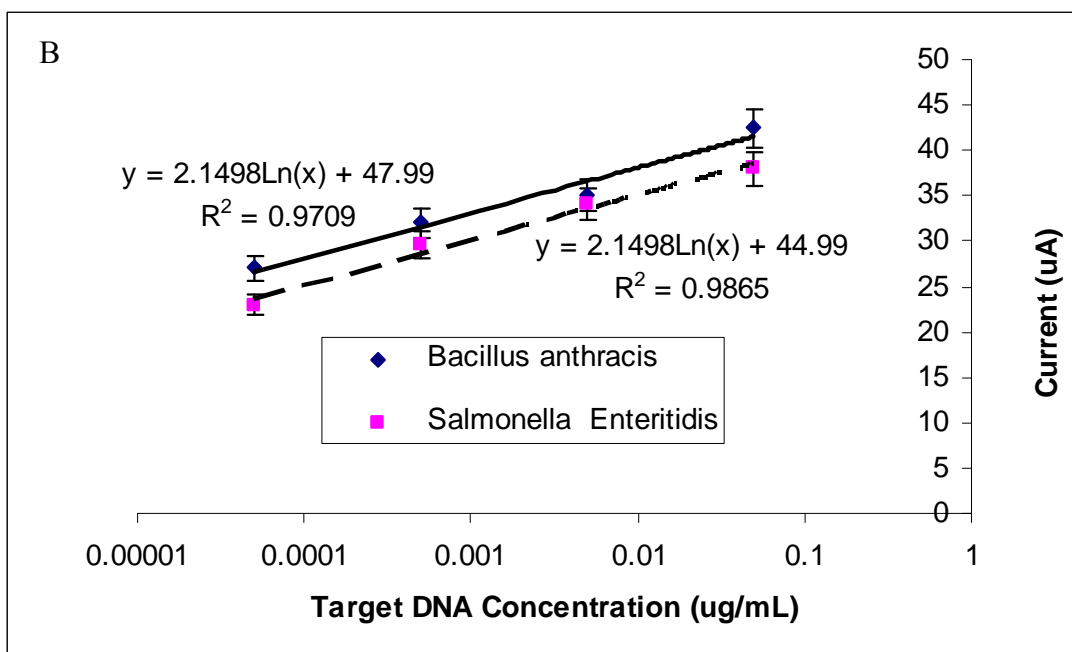
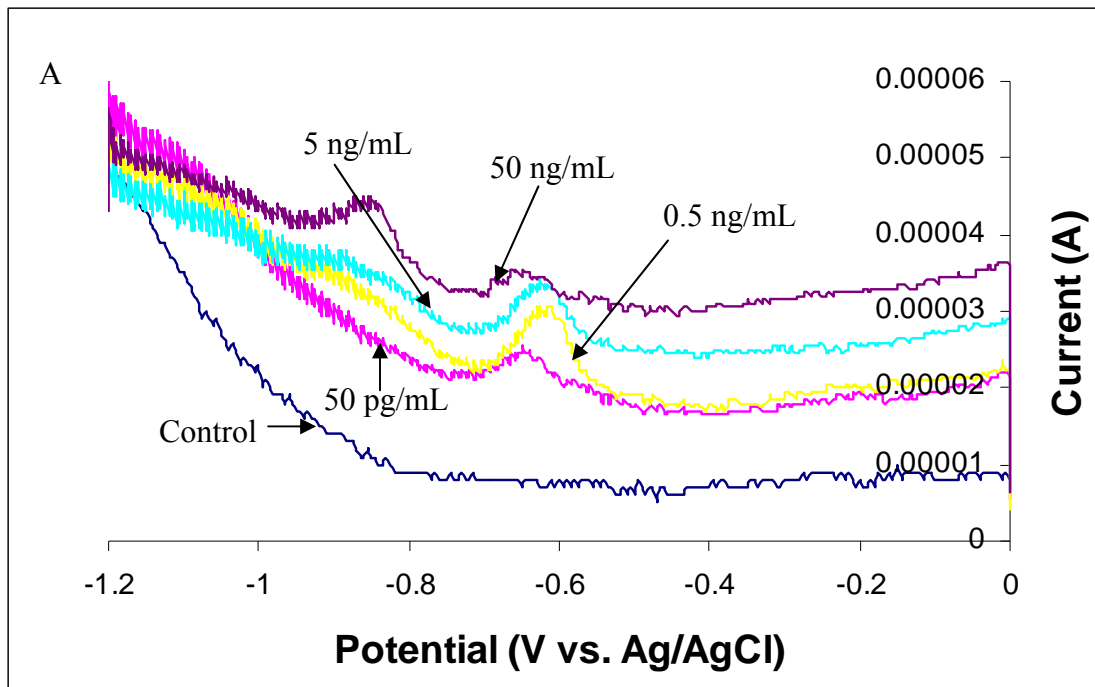


Figure 4.20. The stripping signal of released NT ions (Pb^{2+} and Cd^{2+}) with different concentrations of tDNAs: A) stripping voltammogram of various concentrations of tDNA; B) the calibration plot between peak current and the tDNA concentration. Conditions: deposition at -1.2 V for 10 min; SWASV scan from -1.2 V to 0.0 V, frequency 20 Hz, amplitude 25 mV, and potential step 5 mV, with 1mg/mL bismuth, at room temperature and in nonstirred solution

4.8 Conclusion and Summary

Conclusion

A highly amplified, nanoparticle-based, bio-barcode electrochemical biosensor for the multiple detection of *pagA* gene (accession number = M22589) from *Bacillus anthracis* and insertion element (*Iel*) gene (accession number = Z83734) from *Salmonella* Enteritidis was described in this research. The biosensor system was mainly composed of three nanoparticles: gold nanoparticles (AuNPs) for a carrier of signals, magnetic nanoparticles (MNPs) for clean separation and preconcentration, and nanoparticle tracers (NTs, such as PbS and CdS) for signal amplification. After mixing the nanoparticles with the tDNA, the sandwich structure (MNP-2pDNA / tDNA / 1pDNA-AuNP-bDNA-NTs) was formed. The released NT ions showed a non-overlapping stripping behavior by square wave anodic stripping voltammetry (SWASV) on screen-printed carbon electrode (SPCE) chips. The screen-printed carbon electrode (SPCE) was chosen because of its broad potential window, low background current, rich surface chemistry, low cost, chemical inertness, and suitability for the detection of trace levels of metal ions. SWASV has an extremely favorable signal-to-background ratio and remarkable sensitivity due to an effective pre-concentration step of anodic stripping techniques. Bio-barcode assay has been shown to have extraordinarily PCR-like sensitivity because the large ratio between thiolated single-strand oligonucleotide barcodes and pDNA on AuNPs provides significant amplification.

There were six specific aims of this study as follows:

1) Synthesize and characterize gold nanoparticles and nanoparticle tracers (PbS and CdS): The nanoparticles were synthesized successfully and characterized. The absorption peak of the AuNPs was at 519 nm wavelength. TEM shown the diameters of AuNPs, PbS NTs and CdS NTs were 15 nm, 3 nm, and 7 nm respectively. They were stable in room temperature for months.

2) Functionalize gold nanoparticles and magnetic nanoparticles, and conjugate bio-barcoded AuNPs with nanoparticle tracers: The conjugation reaction between the two nanoparticles and thiolated oligonucleotides, carboxylic group on NTs and amine group on bio-barcoded AuNPs were efficient.

3) Evaluate and optimize SPCE chips for NT ions detection: The cyclic voltammogram of ferricyanide showed that the voltammetric response of SPCE chips was irreversible. The electrochemical sensors were only good for one-time use. Due to the limitation of stirring, deposition potential of -1.2 V, 1 mg/L of bismuth and 10 min deposition time were applied to the all SWASV measurements.

4) Fluorescence detection of bio-barcode assay and gold nanoparticle detection to confirm hybridization: The fluorescence signal of released bDNA had an exponential relationship with tDNA concentration. The detection limit of this bio-barcoded DNA assay was 1 ng/mL (or 2.15×10^{-16} mol). After hybridization, the detection limit of the insertion element (*Iel*) gene of *Salmonella* Enteritidis was 0.7 ng/mL (or 1.5×10^{-16} mol) using AuNPs as an electrochemical indicator.

5) Evaluate biosensor sensitivity using a single purified PCR product from target organisms: The sensitivity of single detection of *pagA* gene from *Bacillus anthracis* using PbS NTs is as low as 0.2 pg/mL.

6) Design multiplex detection of multiple targets in the same samples and evaluate its sensitivity and specificity: The biosensor had a good specificity, and the detection limit of this multiplex bio-barcoded DNA sensor was 50 pg/mL using PbS or CdS NTs.

Limitation and Future Possibilities

The nanoparticle-based bio-barcoded DNA sensor faces several issues that need to be addressed before it can be adopted as an on-site biosensor. Though the detection system is easy to miniaturize, the current system is still large and heavy; Even though this detection system can reach the PCR-like sensitivity, DNA extraction from pathogens and restriction enzymes to cut the long gene sequence are still necessary. It will need battery-operated centrifuge.

To further improve the sensitivity of the biosensor, it is important to optimize the ratio of lpDNA to bDNA to maximize the amplification while maintaining the hybridization efficiency to the tDNA. A better understanding of the steric hindrance of nanoparticle tracers during hybridization is essential to improve the hybridization efficiency.

In the future, the SPCE chips can be incorporated into a pocket PC. The biosensor detection systems will be handheld, portable, cost-effective, have PCR-like sensitivity, can simultaneously detect multiplex pathogens. Figure 4.21 shows a schematic of the future ultrasensitive electrochemical biosensor.

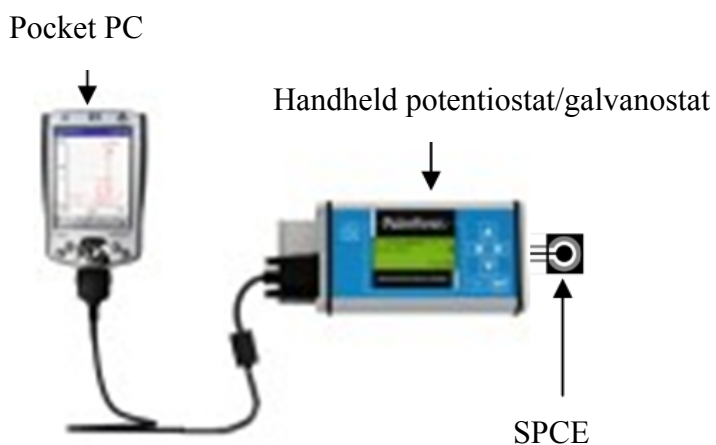


Figure 4.21. Schematic of ultra-sensitive portable electrochemical biosensor system.

APPENDICES

APPENDIX I

DNA Extraction Procedure (Cited from manufacturer's manual)

- 1) In the biosafety cabinet, pipette 1 ml of bacterial culture into a 1.5 ml micro centrifuge tube, and centrifuge for 5 min at 5000 x g (7500 rpm).
- 2) Remove 910 μ L supernatant, then add Buffer ATL 90 μ L (supplied in the QIAamp DNA Mini Kit), to a total volume of 180 μ L.
- 3) Add 20 μ L Proteinase K, mix by shaking, and take it out from biosafety cabinet. Incubate and shake in hybridization oven at 56°C until the tissue is completely lysed. Vortex occasionally during incubation to disperse the sample.
- 4) Briefly centrifuge the 1.5 ml microcentrifuge tube for 1 min to remove drops from the inside of the lid. Add 200 μ L Buffer AL to the sample, mix by pulse-vortexing for 15 s, and incubate in hybridization oven at 70°C for 10 min.
- 5) Briefly centrifuge the 1.5 ml microcentrifuge tube for 1 min to remove drops from inside the lid. Add 200 μ L ethanol (96–100%) to the sample, and mix by pulse-vortexing for 15 s.
- 6) After mixing, briefly centrifuge the 1.5 ml microcentrifuge tube to remove drops from inside the lid. Carefully apply the mixture (including the precipitate) to the QIAamp Spin Column (in a 2 ml collection tube) **without wetting the rim**. Close the cap, and centrifuge at 6000 x g (8000 rpm) for 1 min.
- 7) Place the QIAamp Spin Column in a clean 2 ml collection tube (provided), and discard the tube containing the filtrate.
- 8) Carefully open the QIAamp Spin Column and add 500 μ L Buffer AW1 **without wetting the rim**. Close the cap, and centrifuge at 6000 x g (8000 rpm) for 1 min.
- 9) Place the QIAamp Spin Column in a clean 2 ml collection tube (provided), and discard the collection tube containing the filtrate.
- 10) Carefully open the QIAamp Spin Column and add 500 μ L Buffer AW2 **without wetting the rim**. Close the cap and centrifuge at full speed (20,000 x g; 14,000 rpm) for 3 min.
- 11) Place the QIAamp Spin Column in a new 2 ml collection tube (not provided) and discard the collection tube containing the filtrate. Centrifuge at 20,000 x g (14,000 rpm) for 1 min.
- 12) Place the QIAamp Spin Column in a clean 1.5 ml microcentrifuge tube (not provided), and discard the collection tube containing the filtrate.

- 13) Carefully open the QIAamp Spin Column and add 200 μL Buffer AE or distilled water. Incubate at room temperature for 5 min, and then centrifuge at 6000 x g (8000 rpm) for 1 min.
- 14) The filtrate in the 1.5 mL is the extracted DNA sample. Its concentration and purification can be measured with SmartSpec 3000 Spectrophotomete.
- 15) It should be stored at -20°C

APPENDIX II

PCR Amplification (Cited from manufacturer's manual)

- 1) Thaw the PCR Master Mix at room temperature. Vortex the Master Mix and then spin it briefly in a microcentrifuge to collect the material in the bottom of the tube.
- 2) Prepare one of the following reaction mixes on ice:

Component	Volume	Final Conc.
PCR Master Mix, 2X	50 μ l	1X
Reverse primer, 10 μ M	1.0–10.0 μ l	0.1–1.0 μ M
Forward primer, 10 μ M	1.0–10.0 μ l	0.1–1.0 μ M
DNA template	1–5 μ l	<250ng
Nuclease-Free Water to	100 μ l	N.A.

- 3) Put the PCR tube into the thermocycler.
- 4) Choose the program name “SALMO” and start PCR amplification.

Denaturation : 94°C 5 min
 94°C 30 sec
Annealing: 59°C 30 sec
Extension: 72°C 45 sec
Cycle Number: 30
Final extension: 72°C 10 min
Refrigeration: 4°C

After PCR, run the electrophoresis gel or store under -20°C freezer.

APPENDIX III

Procedure of Bio-Barcode Assay (Adapted from Hill and Mirkin 2006)

1. 13 nm Gold nanoparticles preparation

- 1) Clean all glassware with pure water, rinse copiously with pure water and dry in oven at 100°C. Wash a large stir bar.
- 2) Blow out glassware with N₂ or air
- 3) Prepare 50 ml of 1mM hydrogen tetrochloroaurate (III) trihydrate with pure water (0.0197 g + 50 ml H₂O) in a 100 ml flask. Use plastic spatula.
- 4) Pour the gold solution into the flask and bring to a vigorous boil while stirring. Using a foil to cover the opening roughly.
- 5) While the gold solution is heating, prepare 5 ml of 38.8 mM sodium citrate dehydrate with pure water in the (0.057g sodium citrate + 5 ml H₂O)
- 6) Once the gold solution is refluxing vigorously, add all the sodium citrate solution and reseal the flask top with foil paper. The solution will turn from yellow to clear, to black, to purple and finally deep red.
- 7) After 15 min, turn heat off and allow the reaction to cool to room temperature.
- 8) The UV-vis absorption spectrum of AuNPs solution showed a strong surface plasma resonance at a wavelength of 519 nm.

2. Magnetic nanoparticle preparation

- 1) Melt the solid of 1,6-hexanediamine to liquid phase at 45C in a water bath for 2 hours
- 2) A solution of 1,6-hexanediamine (6.5 g), anhydrous sodium acetate (2.0 g) and FeCl₃·6H₂O (1.0 g) in Ethylene glycol (30 mL) was stirred vigorously at 50 °C to give a transparent solution.
- 3) This solution was then covered with an aluminum foil and transferred into an oven and reacted at 198 °C for 6 h.
- 4) Under ultrasonic conditions, the magnetite nanoparticles were then rinsed with ethanol and water for 15 min to effectively remove the solvent and unbound 1,6-hexanediamine, repeat the washing step 3 times respectively. During each rinsing step, the nanoparticles were separated from the supernatant by using magnet for 3 min.

- 5) The magnetite nanoparticles dried at 50 °C in the hybridization oven before characterization and application.
- 6) Store the MNPs in storage buffer (Na₂HPO₄ 8.0 mM, NaH₂PO₄ 2mM, NaCl 0.15M, Tween 20 0.05%, pH 7.4) under 4°C.

4. DNA functionalization on gold Nanoparticles (AuNPs)

- 1) Take out 5 nmol of thiolated barcode DNA and 0.05 nmol 1pDNA from freezer and mix them together.
- 2) Prepare 1 ml of 0.1 M DTT (0.0154g) solution in the disulfide cleavage buffer.
- 3) Add 100 µL of DTT solution to the barcode DNA, wrap in foil and let stand at room temperature for 2 hours. Vortex once half an hour.
- 4) Flushing a Nap-5 column with pure water. 3 column volumes of water must flush through before adding barcode DNA
- 5) Adding 100 µL of DNA to the column after all the water has run through
- 6) Once the 100 µL of DNA has flowed into the column, add 400 µL of pure water to the column and allow it to flow through uncollected.
- 7) Then add 950 µL of pure water to the column, and collect the flow through in 1.5 mL microcentrifuge tubes.
- 8) Use Nanodrop to determine the DNA concentration.
- 9) Add 1 ml of AuNPs (concentration: AU = 1 at 520 nm) in a 15 ml test tube.
- 10) Add the freshly reduced thiolated oligo to the AuNPs. Recode the volume.
- 11) Wrap in foil and place on shaker overnight at room temperature.
- 12) Add **195** µL of phosphate adjustment buffer. Calculation: $(1000\mu\text{L AuNP} + X \mu\text{L DNA}) / 10 = Y \mu\text{L}$
- 13) Add **21.5** µL of surfactant solution. Calculation: $(1000\mu\text{L AuNP} + X \mu\text{L DNA} + Y \mu\text{L phosphate adjustment buffer}) / 100 = Z \mu\text{L}$
- 14) Rewrap in foil and place on shaker for 30 min.

15) Add salting buffer at six times in 2 days. So every time just add **53.5** μL of salting buffer. Do the additions while shaking gently. Calculation: $(1000\mu\text{L AuNP} + X \mu\text{L DNA} + Y \mu\text{L phosphate adjustment buffer}) * 0.3 / 2 = \mathbf{S \mu\text{L}}$.

16) After the last salt addition, allow the particles to equilibrate overnight.

The particles can be store at room temperature for one month in this state.

5. DNA functionalization of magnetic nanoparticles (MNPs)

- 1) Sonicate MNPs stock solution (50mg/mL) for 30 min to disperse Nanoparticles evenly.
- 2) Take out 5 mg (100 μL) of the polyamine-functionalized MNPs from stock solution (50mg/mL). It will react with 0.5 mg of sulfosuccinimidyl 4-N-maleimidomethyl cyclohexane-1-carboxylate (Sulfo-SMCC) bifunctional linker in 10 mL coupling buffer.
- 3) Put the tubes into shaker for 1 hour at room temperature.
- 4) Put it on the magnet 3 min, remove the supernatant (unreacted Sulfo-SMCC) and rinsing it with the coupling buffer. Repeat the process 3 times. Finally take off all supernatant.
- 5) Take out 10 nmol of thiolated 2pDNA from freezer.
- 6) Prepare 1 ml of 0.1 M DTT (0.0154g) solution in the disulfide cleavage buffer.
- 7) Add 100 μL of DTT solution to 2pDNA, wrap in foil and let stand at room temperature for 2 hours. Vortex once half an hour.
- 8) Flushing a Nap-5 column with coupling buffer. 3 column volumes of coupling buffer must flush through before adding barcode DNA
- 9) Adding all DNA (suppose the volume now is X) to the column after all the coupling buffer has run through.
- 10) Once the X μL of DNA has flowed into the column, add 500-X μL of coupling buffer to the column and allow it to flow through uncollected.
- 11) Then add 950 μL coupling buffer to the column, and collect the flow through in 1.5 mL microcentrifuge tubes.
- 12) Use Nanodrop to determine the DNA concentration.
Attention: Coupling buffer as a blank.
- 13) Put the cleaved and purified thiolated oligonucleotide with sulfo-SMCC-modified MNPs in 1 ml coupling buffer for overnight (>8 h).

- 14) Put it on the magnet for 3 min, remove the supernatant and rinsing it with the coupling buffer. Repeat the process 3 times.
- 15) The particles were centrifuged (Eppendorf Centrifuge 5415D) (4,000 RPM; 1 min) and washed (3 x) with passivation buffer (2x) and then with a storage buffer (2 x) (10 mM sodium phosphate buffer pH 7.4 with 0.20 M NaCl).
- 16) Finally, the target binding DNA-modified MNPs were re-dispersed in 2 mL of 0.1 M PBS solution prior to use.

6. Hybridization of sandwich structure

- 1) Determine the number of samples to be tested, including one for the negative control (pure water).
- 2) Wash the MNPs twice with the assay buffer.
- 3) A solution (40 μ L per sample test) containing tDNA in PCR tube was put in the thermocycler at 95C for 10 min to separate the dsDNA to ssDNA, then put in freezer (-20C) immediately for 5 min to keep them separate.
- 4) Mix in 1.5 mL microcentrifuge tubes. 40 μ L DNA sample + 0.8 mg MNPs + X μ L assay buffer = 200 μ L
- 5) Shake the reactions at a temperature 45C for 45 min in the **rotating** hybridization oven. So that the MNPs do not settle.
- 6) During the incubation, centrifuge 200 μ L of AuNPs at 13000 g for 30 min. remove the supernatant and resuspend in 1 mL assay buffer. Repeat 3 times.
- 7) After final spin/wash, resuspend the AuNPs in assay buffer to generate 1 nM solution (AU=0.27). Calculation based on the Beer's law $A = \epsilon \cdot c \cdot l$. The molar absorptivity at 519 nm is $2.7 \cdot 10^8$ liter mole⁻¹ cm⁻¹ so that **1 AU = 3.7 nM**.
- 8) Wash the MNPs with target twice with the assay buffer on the magnetic separator, and finally resuspend in 200 μ L assay buffer.
- 9) Add 40 μ L of AuNPs probe recently washed.
- 10) Incubate at 45C for 1.5 h with in the **rotating** hybridization oven.

7. Releasing barcode DNA with dithiothreitol (DTT)

- 1) Prepare a 0.0771 g DTT solution in 1 mL assay buffer (0.5M). (Must be fresh every day)

- 2) Wash the MNP-target-AuNP complexes twice with the assay buffer on the magnetic separator, and finally suspend the MNP-target-AuNP complexes in 200 μ L 0.5M DTT buffer.
- 3) Incubate samples at 50°C for 15 min, and then 45 min at 25°C under **vortex** every 5 min.

8. Detection of Barcode DNA

A. conventional fluorophore detection methods (Fluorescence-based barcode DNA)

- 1) After barcode release, extract the MNPs down to the magnet for 3 min and transfer 150 μ L supernatant to clean 1.5 mL microcentrifuge tubes.
- 2) Spin the supernatants for 5 min at 13,000g to pellet the aggregated AuNPs
- 3) Prepare serial dilution of known concentrations in barcode release buffer to generate a calibration curve
- 4) Remove 100 μ L supernatant from gold pellet and place in a new micro-centrifuge tube.
- 5) Fill the microplate with the 100 μ L supernatant.
- 6) Follow the instrument manual, measure fluorescence and perform data analysis.

B. Electrochemical detection of barcode DNA

APPENDIX IV

Table 5. Buffer preparation.

Buffer	Na ₂ HPO ₄ (g)	NaH ₂ PO ₄ (g)	NaCl (g)	SDS (g)	Pure water (ml)	pH
Coupling buffer	4.392	2.291	5.884		500	7.2
Disulfide cleavage buffer	11.468	0.509			500	8.0
Storage buffer	0.570	0.118	5.884		500	7.4
Passivation buffer	10.119	0.449	4.383		500	8.0
Salting buffer	0.0562	0.0125	5.844		50	7.0
Phosphate adjustment buffer	0.562	0.125			50	7.0
Assay buffer	0.562	0.125	4.383	0.500	500	7.4
Surfactant solution				10.000	90	

Na ₂ HPO ₄	Disodium hydrogen phosphate
NaH ₂ PO ₄	Sodium dihydrogen phosphate
NaCl	Sodium chloride
SDS	Sodium dodecyl sulfate

APPENDIX V

Conjugation of carboxylic group on NTs with amine group on bio-barcoded AuNPs

1. Weigh out 5mg EDC into tube
2. Immediately add 25 μL of CdS-COOH or PbS-COOH to EDC
3. Immediately add 50 μL of NHS-DMSO solution (44mg of NHS in 500 μL DMSO)
4. Add 775 μL of pH5 water to make total volume 850 μL
5. Quick vortex, quick spin
6. Wrap in tin foil, react 20min at room temp
7. Adjust pH to 7.0 with NaCO_3 . (4 μL of 1M NaCO_3 pH8)
8. Add AuNP-barcode-NH₂ (61 μL)
9. Wrap in tin foil, tape to vortex at 800rpm for 1hr
10. Add 3 μL of 1M NaCO_3 pH8
11. Wrap in tin foil, tape to vortex at 800rpm overnight (or 1h)
12. Spin 15min at 12,000 g, wash 3x times with PBS buffer
13. Resuspend in 1000 μL of PBS buffer

BIBLIOGRAPHY

BIBLIOGRAPHY

- Alocilja, E. C. and S. M. Radke (2003). "Market analysis of biosensors for food safety." Biosensors and Bioelectronics **18**(5-6): 841-846.
- Bard, A. J. and L. R. Faulkner (2000). Electrochemical Methods: Fundamentals and Applications. New York, Wiley.
- Bard, A. J. and L. R. Faulkner (2001). ELECTROCHEMICAL METHODS: Fundamentals and Applications. New York, JOHN WILEY & SONS, INC.
- Berensmeier, S. (2006). "Magnetic particles for the separation and purification of nucleic acids." Applied Microbiological Biotechnology **73**(3): 495-504.
- Bruchez, M., Jr., M. Moronne, et al. (1998). "Semiconductor nanocrystals as fluorescent biological labels." Science **281**(5385): 2013-6.
- Cao, Y. C., R. Jin, et al. (2002). "Nanoparticles with Raman spectroscopic fingerprints for DNA and RNA detection." Science **297**(5586): 1536-40.
- Carrara, S., V. V. Shumyantseva, et al. (2008). "Screen-printed electrodes based on carbon nanotubes and cytochrome P450scc for highly sensitive cholesterol biosensors." Biosens Bioelectron **24**(1): 148-50.
- Castada, M., S. Alegret, et al. (2007). "Electrochemical Sensing of DNA Using Gold Nanoparticles." Electroanalysis **19**(7-8): 743-753.
- CDC (2005). Salmonella surveillance summary, 2004, US Department of Health and Human Services.
- CDC (2010). "Surveillance for Foodborne Disease Outbreaks --- United States, 2006." Annals of Emergency Medicine **55**(1): 47-49.
- Chan, W. C. and S. Nie (1998). "Quantum dot bioconjugates for ultrasensitive nonisotopic detection." Science **281**(5385): 2016-8.
- Demers, L. M., M. Ostblom, et al. (2002). "Thermal desorption behavior and binding properties of DNA bases and nucleosides on gold." J Am Chem Soc **124**(38): 11248-9.
- Desmond, D., B. Lane, et al. (1998). "Environmental monitoring system for trace metals using stripping voltammetry." Sensors and Actuators, B: Chemical **B48**(1-3 pt 4): 409-414.
- Ding, C., Q. Zhang, et al. (2009). "Electrochemical detection of DNA hybridization based on bio-bar code method." Biosensors and Bioelectronics **24**(10): 3140-3143.
- Drummond, T. G., M. G. Hill, et al. (2003). "Electrochemical DNA sensors." Nat Biotechnol **21**(10): 1192-9.

- Drummond, T. G., M. G. Hill, et al. (2003). "Electrochemical DNA sensors." Nat Biotech **21**(10): 1192-1199.
- Dubertret, B. (2005). "Quantum dots: DNA detectives." Nature Materials **4**(11): 797-798.
- Goldman, E. R., A. R. Clapp, et al. (2004). "Multiplexed toxin analysis using four colors of quantum dot fluororeagents." Anal Chem **76**(3): 684-8.
- Goluch, E. D., J. M. Nam, et al. (2006). "A bio-barcode assay for on-chip attomolar-sensitivity protein detection." Lab Chip **6**(10): 1293-9.
- Guan, W. J., Y. Li, et al. (2005). "Glucose biosensor based on multi-wall carbon nanotubes and screen printed carbon electrodes." Biosens Bioelectron **21**(3): 508-12.
- Guo, S. and S. Dong (2009). "Biomolecule-nanoparticle hybrids for electrochemical biosensors." TrAC Trends in Analytical Chemistry **28**(1): 96-109.
- Hernandez-Santos, D., M. Diaz-Gonzalez, et al. (2004). "Enzymatic genosensor on streptavidin-modified screen-printed carbon electrodes." Anal Chem **76**(23): 6887-93.
- Hill, H. D. and C. A. Mirkin (2006). "The bio-barcode assay for the detection of protein and nucleic acid targets using DTT-induced ligand exchange." Nat Protoc **1**(1): 324-36.
- Hourfar, M. K., U. Michelsen, et al. (2005). "High-Throughput Purification of Viral RNA Based on Novel Aqueous Chemistry for Nucleic Acid Isolation." Clin Chem **51**(7): 1217-1222.
- Huang, G. S., M. T. Wang, et al. (2006). "A versatile QCM matrix system for online and high-throughput bio-sensing." Analyst **131**(3): 382-7.
- Hughes, J. M. and J. L. Gerberding (2002). "Anthrax bioterrorism: lessons learned and future directions." Emerg Infect Dis **8**(10): 1013-4.
- Hwang, G. H., W. K. Han, et al. (2008). "Determination of trace metals by anodic stripping voltammetry using a bismuth-modified carbon nanotube electrode." Talanta **76**(2): 301-308.
- Jackson, N. M. and M. G. Hill (2001). "Electrochemistry at DNA-modified surfaces: new probes for charge transport through the double helix." Curr Opin Chem Biol **5**(2): 209-15.
- Jessica Koehne , H. C., Jun Li , Alan M Cassell , Qi Ye , Hou Tee Ng , Jie Han 1 and M Meyyappan (2003). "Ultrasensitive label-free DNA analysis using an electronic chip based on carbon nanotube nanoelectrode arrays " Nanotechnology **14**: 1239-1245.
- Jianrong, C., M. Yuqing, et al. (2004). "Nanotechnology and biosensors." Biotechnology Advances **22**(7): 505-518.

- Kadara, R. O. and I. E. Tothill (2004). "Stripping chronopotentiometric measurements of lead(II) and cadmium(II) in soils extracts and wastewaters using a bismuth film screen-printed electrode assembly." Analytical and Bioanalytical Chemistry **378**(3): 770-775.
- Kalogianni, D. P., T. Koraki, et al. (2006). "Nanoparticle-based DNA biosensor for visual detection of genetically modified organisms." Biosensors and Bioelectronics **21**(7): 1069-1076.
- Karadeniz, H., B. Gulmez, et al. (2003). "Disposable electrochemical biosensor for the detection of the interaction between DNA and lycorine based on guanine and adenine signals." J Pharm Biomed Anal **33**(2): 295-302.
- Karakus, E., S. Pekyardımcı, et al. (2006). "Potentiometric bienzymatic biosensor based on PVC membrane containing palmitic acid for determination of creatine." Process Biochemistry **41**(6): 1371-1377.
- Karslan, L., S. K. Kayahan, et al. (2009). "A new amperometric cholesterol biosensor based on poly(3,4-ethylenedioxyppyrrrole)." Sensors and Actuators B: Chemical **136**(2): 484-488.
- Khanna, V. K. (2008). "New-generation nano-engineered biosensors, enabling nanotechnologies and nanomaterials." Sensor Review **28**(1).
- Kim, J.-H., K.-S. Seo, et al. (2006). "Rapid diagnostic barcode system for codetection of multiple protein markers." IEEE Sensors Journal **6**(2): 248-252.
- Kim, Y.-H., J.-S. Park, et al. (2009). "An impedimetric biosensor for real-time monitoring of bacterial growth in a microbial fermentor." Sensors and Actuators B: Chemical **138**(1): 270-277.
- Kissinger, P. T. and W. R. Heineman (1996). Laboratory Techniques in Electroanalytical Chemistry. New York, Marcel Dekker.
- Lee, T. Y. and Y. B. Shim (2001). "Direct DNA hybridization detection based on the oligonucleotide-functionalized conductive polymer." Anal Chem **73**(22): 5629-32.
- Lee, W.-C., K.-Y. Lien, et al. (2008). "An integrated microfluidic system using magnetic beads for virus detection." Diagnostic Microbiology and Infectious Disease **60**(1): 51-58.
- Lin, J., W. Qu, et al. (2007). "Disposable biosensor based on enzyme immobilized on Au-chitosan-modified indium tin oxide electrode with flow injection amperometric analysis." Analytical Biochemistry **360**(2): 288-293.
- Liu, G., J. Wang, et al. (2004). "Electrochemical coding for multiplexed immunoassays of proteins." Analytical Chemistry **76**(23): 7126-7130.

- Lytton-Jean, A. K. R. and C. A. Mirkin (2005). "A Thermodynamic Investigation into the Binding Properties of DNA Functionalized Gold Nanoparticle Probes and Molecular Fluorophore Probes." J. Am. Chem. Soc. **127**(37): 12754-12755.
- Medintz, I. L. and J. R. Deschamps (2006). "Maltose-binding protein: a versatile platform for prototyping biosensing." Current Opinion in Biotechnology **17**(1): 17-27.
- Miroslav Fojta, L. H. S. B. P. K. M. M. R. K. (2003). "Two-Surface Strategy in Electrochemical DNA Hybridization Assays: Detection of Osmium-Labeled Target DNA at Carbon Electrodes." Electroanalysis **15**(5-6): 431-440.
- Miscoria, S. A., J. Desbrieres, et al. (2006). "Glucose biosensor based on the layer-by-layer self-assembling of glucose oxidase and chitosan derivatives on a thiolated gold surface." Anal Chim Acta **578**(2): 137-44.
- Nam, J. M., S. I. Stoeva, et al. (2004). "Bio-bar-code-based DNA detection with PCR-like sensitivity." J Am Chem Soc **126**(19): 5932-3.
- Nam, J. M., C. S. Thaxton, et al. (2003). "Nanoparticle-based bio-bar codes for the ultrasensitive detection of proteins." Science **301**(5641): 1884-6.
- Oh, B. K., J. M. Nam, et al. (2006). "A fluorophore-based bio-barcode amplification assay for proteins." Small **2**(1): 103-8.
- Ozkan-Ariksoysal, D., B. Tezcanli, et al. (2008). "Design of electrochemical biosensor systems for the detection of specific DNA sequences in PCR-amplified nucleic acids related to the catechol-O-methyltransferase Val108/158Met polymorphism based on intrinsic guanine signal." Anal Chem **80**(3): 588-96.
- Pal, S. and E. C. Alocilja (2009). "Electrically active polyaniline coated magnetic (EAPM) nanoparticle as novel transducer in biosensor for detection of Bacillus anthracis spores in food samples." Biosensors and Bioelectronics **24**(5): 1437-1444.
- Pal, S., E. C. Alocilja, et al. (2007). "Nanowire labeled direct-charge transfer biosensor for detecting Bacillus species." Biosensors and Bioelectronics **22**(9-10): 2329-2336.
- Palecek, E. and M. Fojta (2007). "Magnetic beads as versatile tools for electrochemical DNA and protein biosensing." Talanta **74**(3): 276-290.
- Pingarr, J. M., P. Yez-Sede, et al. (2008). "Gold nanoparticle-based electrochemical biosensors." Electrochimica Acta **53**(19): 5848-5866.
- Pu, K.-Y., S. Y.-H. Pan, et al. (2008). "Optimization of interactions between a cationic conjugated polymer and chromophore-labeled DNA for optical amplification of fluorescent sensors." Journal of Physical Chemistry B **112**(31): 9295-9300.

- Pumera, M., M. Aldavert, et al. (2005). "Direct voltammetric determination of gold nanoparticles using graphite-epoxy composite electrode." Electrochimica Acta **50**(18): 3702-3707.
- Reeder, G. S. and W. R. Heineman (1998). "Electrochemical characterization of a microfabricated thick-film carbon sensor for trace determination of lead." Sensors and Actuators, B: Chemical **B52**(1-2): 58-64.
- Ren, X., X. Meng, et al. (2005). "Using silver nanoparticle to enhance current response of biosensor." Biosensors and Bioelectronics **21**(3): 433-437.
- Ruffien, A., M. Dequaire, et al. (2003). "Covalent immobilization of oligonucleotides on p-aminophenyl-modified carbon screen-printed electrodes for viral DNA sensing." Chem Commun (Camb)(7): 912-3.
- Sassolas, A., B. D. Leca-Bouvier, et al. (2008). "DNA biosensors and microarrays." Chem Rev **108**(1): 109-39.
- Satoh, K., A. Iwata, et al. (2003). "Virus concentration using polyethyleneimine-conjugated magnetic beads for improving the sensitivity of nucleic acid amplification tests." Journal of Virological Methods **114**(1): 11-19.
- Song, L., S. Ahn, et al. (2005). "Detecting biological warfare agents." Emerg Infect Dis **11**(10): 1629-32.
- Steel, A. B., T. M. Herne, et al. (1998). "Electrochemical Quantitation of DNA Immobilized on Gold." Anal. Chem. **70**(22): 4670-4677.
- Stoeva, S. I., J. S. Lee, et al. (2006). "Multiplexed DNA detection with biobarcode nanoparticle probes." Angew Chem Int Ed Engl **45**(20): 3303-6.
- Sun, W., J. Zhong, et al. (2008). "Electrochemical biosensor for the detection of cauliflower mosaic virus 35 S gene sequences using lead sulfide nanoparticles as oligonucleotide labels." Analytical Biochemistry **377**(2): 115-119.
- Susmel, S., G. G. Guilbault, et al. (2003). "Demonstration of labelless detection of food pathogens using electrochemical redox probe and screen printed gold electrodes." Biosens Bioelectron **18**(7): 881-9.
- Tam, P. D., N. Van Hieu, et al. (2009). "DNA sensor development based on multi-wall carbon nanotubes for label-free influenza virus (type A) detection." Journal of Immunological Methods **350**(1-2): 118-124.
- Taton, T. A., C. A. Mirkin, et al. (2000). "Scanometric DNA array detection with nanoparticle probes." Science **289**(5485): 1757-60.

- Templin, M. F., D. Stoll, et al. (2002). "Protein microarray technology." Trends Biotechnol **20**(4): 160-6.
- Ting, B. P., J. Zhang, et al. (2009). "A DNA biosensor based on the detection of doxorubicin-conjugated Ag nanoparticle labels using solid-state voltammetry." Biosensors and Bioelectronics **25**(2): 282-287.
- Wang, J. (2002). "Portable electrochemical systems." TrAC Trends in Analytical Chemistry **21**(4): 226-232.
- Wang, J., G. Liu, et al. (2003). "Electrochemical coding technology for simultaneous detection of multiple DNA targets." J Am Chem Soc **125**(11): 3214-5.
- Wang, J., J. Lu, et al. (2000). "Bismuth-coated carbon electrodes for anodic stripping voltammetry." Anal Chem **72**(14): 3218-22.
- Wang, S. J. and D. B. Yeh (2002). "Designing of polymerase chain reaction primers for the detection of Salmonella enteritidis in foods and faecal samples." Lett Appl Microbiol **34**(6): 422-7.
- Weng, J., J. Zhang, et al. (2008). "Label-free DNA sensor by boron-doped diamond electrode using an ac impedimetric approach." Anal Chem **80**(18): 7075-83.
- Weyant R.S, E. J., J.W, Papovic T. Media . (2001). "Basic Laboratory protocols for presumptive identification of Bacillus anthracis." Centers for Disease Control and Prevention.
- Xie, J.-K., K. Jiao, et al. (2008). "DNA Electrochemical Sensor Based on PbSe Nanoparticle for the Sensitive Detection of CaMV35S Gene Sequence." Chinese Journal of Analytical Chemistry **36**(7): 874-878.
- Xu, H., G. Li, et al. (2005). "A glucose oxidase sensor based on screen-printed carbon electrodes modified by polypyrrole." Conf Proc IEEE Eng Med Biol Soc **2**: 1917-20.
- Yang, I. V. and H. H. Thorp (2001). "Modification of Indium Tin Oxide Electrodes with Repeat Polynucleotides: Electrochemical Detection of Trinucleotide Repeat Expansion." Anal. Chem. **73**(21): 5316-5322.
- Zhang, D. and E. C. Alocilja (2008). "Characterization of nanoporous silicon-based DNA biosensor for the detection of Salmonella enteritidis." IEEE Sensors Journal **8**(6): 775-780.
- Zhang, D., D. J. Carr, et al. (2009). "Fluorescent bio-barcode DNA assay for the detection of Salmonella enterica serovar Enteritidis." Biosensors and Bioelectronics **24**(5): 1377-1381.

Zhu, N., A. Zhang, et al. (2004). "Lead Sulfide Nanoparticle as Oligonucleotides Labels for Electrochemical Stripping Detection of DNA Hybridization." Electroanalysis **16**(7): 577-582.